Chapter 3

Contact Uncertainty Analysis

This Chapter analyzes the sources of uncertainty that affect a planar assembly task and their effect on the contact situations involving one or several basic contacts. The approach:

- makes the analysis in physical and configuration space, taking into account the dependence between the sources of uncertainty and considering possible complementary contact situations,
- presents a contact identification procedure which uses the nominal $\mathcal{C}'$-space,
- introduces a method to reduce uncertainty and to adapt the motion commands during the task execution,
- includes a force analysis.

3.1 Sources of uncertainty

Modelling and sensing uncertainties affect the task planning and execution. The nominal model of a task is the description of the nominal objects involved in the task, and the specification of their nominal initial and goal configurations. Modelling uncertainties include deviations of the shape and size of the objects and the uncertainty in their positioning. Sensing uncertainties deal with the uncertainty in the sensory information of configuration and force.

The manipulation and fusion of the sources of uncertainty affecting the geometry of the task has been done following different approaches like, for instance, verifying the assemblability by propagating tolerances [10, 67, 68], extending the degrees of freedom of the Configuration Space [33], mapping the real world uncertainty into the Configuration Space [5] or considering probabilities [35].

In this work uncertainties are propagated considering the worst case for each uncertainty source in order to cover all the real possible cases. For three degrees of freedom the different sources of uncertainty are classified below. Figure 3.1 illustrates the sources of uncertainty that affect the geometry of the task.

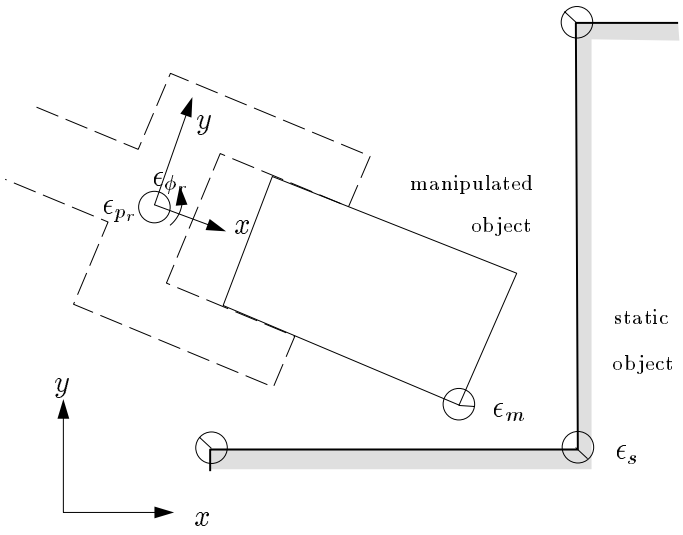

Figure 3.1: *Sources of uncertainty that affect the geometry of the task.*

3.1.1 Modelling uncertainty

a) Manufacturing tolerances of object shape and size.

There exist several approaches dealing with homogeneous specification of tolerances; typically they are based on the nominal object description [82, 9] and, in some cases, they also consider the assembly context [35, 56, 55, 19, 114].

In the proposed approach, each object vertex is constrained to be inside a circle of radius ϵ_t centered on its nominal position. Let (v_{x0}, v_{y0}) and (v_x, v_y) be the nominal and the actual vertex position in the object reference system, respectively. Then:

$$\|(v_x, v_y) - (v_{x0}, v_{y0})\| \leq \epsilon_t \tag{3.1}$$

ϵ_t will be expressed as ϵ_{t_s} and ϵ_{t_m} to distinguish between the tolerances of the static objects and those of the manipulated object. The effect of manufacturing tolerances is a possible change in the shape and size of the object that may allow a set of contact situations different from the nominal ones (i.e. the ones allowed by the nominal geometry). Those that can only appear due to the deviations from the nominal geometry will be called *complementary contact situations*. Figure 3.2 shows a complementary contact situation due to the effect of the manufacturing tolerances.

b) Imprecision in the positioning of the static objects.

It depends on how the objects are positioned in the work environment. A reasonable assumption is that the static objects are placed in the workspace by feeders in such a way that each object vertex lies inside a circle of radius ϵ_s centered on its nominal position. Let (a_{x0}, a_{y0}) and (a_x, a_y) be the nominal and the actual vertex position in the world reference system, respectively. Then:

$$\|(a_x, a_y) - (a_{x0}, a_{y0})\| \leq \epsilon_s \tag{3.2}$$

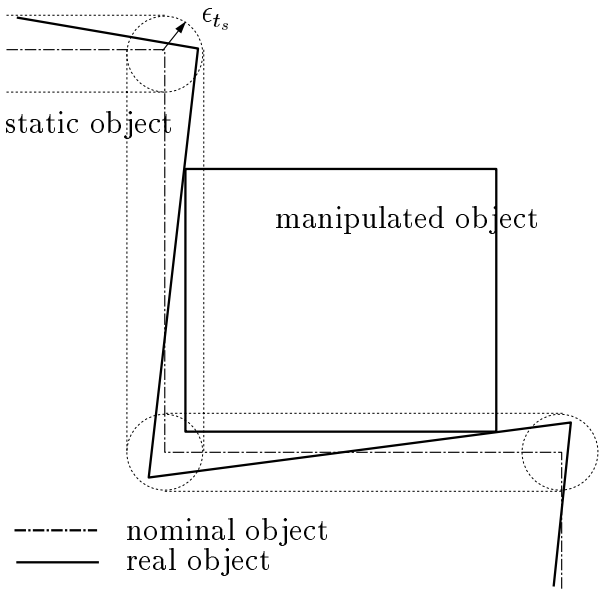

Figure 3.2: *Complementary contact situation due to the manufacturing tolerances of the static object (for clarity the manipulated object has been drawn without tolerances).*

ϵ_s depends on ϵ_{t_s} and on the feeder error but, since the positioning operation can reduce the uncertainty, it can be regarded as a source itself. When there is more than one static object in the work environment, the imprecision in the positioning of the objects can give rise to complementary contact situations as it is shown in Figure 3.3.

c) Imprecision in the positioning of the object in the robot gripper.

The position of the vertices of the manipulated object depends on the uncertainties from sources (a), (b), plus the imprecision in the position and orientation of the robot (source (d) in Section 3.1.2) and undesired slippings of the object in the gripper; nevertheless, since the grasping operation can reduce these uncertainties [79], it can be regarded as a source itself.

It is assumed that each object vertex lies inside a circle of radius ϵ_m centered on its nominal position. Let (h_{x0}, h_{y0}) and (h_x, h_y) be the nominal and the actual vertex position in the gripper reference system, respectively. Then:

$$\|(h_x, h_y) - (h_{x0}, h_{y0})\| \leq \epsilon_m \tag{3.3}$$

3.1.2 Sensing uncertainty

d) Imprecision in the position and orientation of the robot.

There are several works dealing with this source of uncertainty, the main topics tackled being the origin of the uncertainty [27, 61] and the resulting uncertainty at the robot end-effector considering the robot kinematics [8, 78].

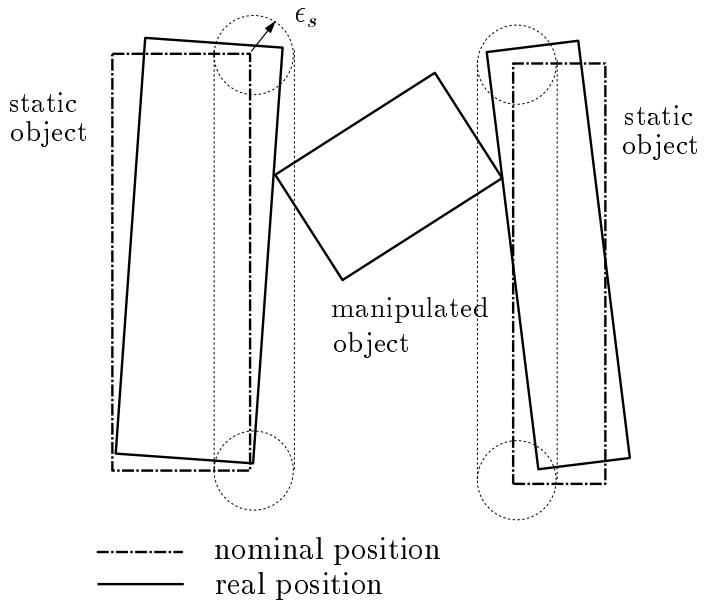

Figure 3.3: *Complementary contact situation due to the imprecision in the positioning of the static objects.*

In the proposed approach the worst case uncertainty at the robot end-effector is considered, since this is normally the way in which the robot manufacturers specify the robot precision. Let (x_o, y_o, ϕ_o) and (x_r, y_r, ϕ_r) be the observed and the actual configuration of the robot, i.e. the position and orientation of the gripper reference system with respect to the world reference system. The actual position is constrained to be inside a circle of radius ϵ_{p_r} centered at the observed position; and the actual orientation has a maximum deviation ϵ_{ϕ_r} with respect to the observed one:

$$\|(x_r, y_r) - (x_o, y_o)\| \leq \epsilon_{p_r} \tag{3.4}$$

$$|\phi_r - \phi_o| \leq \epsilon_{\phi_r} \tag{3.5}$$

Let ϕ_{o_m} and ϕ_{o_M} be defined as:

$$\phi_{o_m} = \phi_o - \epsilon_{\phi_r} \tag{3.6}$$

$$\phi_{o_M} = \phi_o + \epsilon_{\phi_r} \tag{3.7}$$

Then, equation (3.5) will be rewritten as:

$$\phi_r \in [\phi_{o_m}, \phi_{o_M}] \tag{3.8}$$

e) Imprecision of the force/torque sensor. Since typical force/torque sensors provide each component value with a specified resolution, its uncertainty can be modelled for three degrees of freedom considering that the components, f_x, f_y and f_q, of the generalized force $\vec{g}$ (Section 2.8) have independent maximum deviations ϵ_{f_x}, ϵ_{f_y} and ϵ_{f_q}, respectively. In the tridimensional force space this is equivalent to an uncertainty rectangular

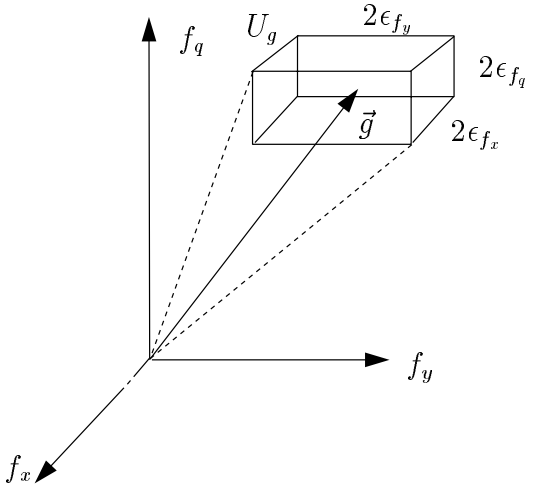

Figure 3.4: *Force uncertainty parallelepiped U_g.*

parallelepiped U_g centered in the observed generalized force $\vec{g}_o = [f_{xo} \;\; f_{yo} \;\; f_{qo}]^T$ and with sides having a length of $2\epsilon_{f_x}$, $2\epsilon_{f_y}$ and $2\epsilon_{f_q}$ (Figure 3.4):

$$\|f_x - f_{xo}\| \leq \epsilon_{f_x} \tag{3.9}$$
$$\|f_y - f_{yo}\| \leq \epsilon_{f_y} \tag{3.10}$$
$$\|f_q - f_{qo}\| \leq \epsilon_{f_q} \tag{3.11}$$

3.2 Analysis in physical space

This section studies how modelling and sensing uncertainties affect the position and orientation of the contact edge and the position of the contact vertex. Let ϵ_v and ϵ_{t_v} be the uncertainty in the position of the the contact vertex due to the imprecision in the positioning of the objects and to the manufacturing tolerances, respectively. Let ϵ_e and ϵ_{t_e} be defined in a similar way for the vertices of the contact edge. Then, for type-A basic contacts:

$$\begin{aligned} \epsilon_v &= \epsilon_s \\ \epsilon_{t_v} &= \epsilon_{t_s} \\ \epsilon_e &= \epsilon_m \\ \epsilon_{t_e} &= \epsilon_{t_m} \end{aligned} \tag{3.12}$$

And for type-B basic contacts:

$$\begin{aligned} \epsilon_v &= \epsilon_m \\ \epsilon_{t_v} &= \epsilon_{t_m} \\ \epsilon_e &= \epsilon_s \\ \epsilon_{t_e} &= \epsilon_{t_s} \end{aligned} \tag{3.13}$$

3.2.1 Modelling uncertainty on the contact edge

The contact edge, e, must satisfy two conditions, that constrain its position and orientation according to uncertainty:

Condition 1: The extremes of e must lie inside uncertainty circles of radius ϵ_e centered on the nominal position of the extremes of the nominal edge.

Condition 2: The length l of e must satisfy $l \in [l_0 - 2\epsilon_{t_e}, l_0 + 2\epsilon_{t_e}]$, l_0 being its nominal length.

Let β be the deviation in the orientation of e with respect to its nominal orientation. It is assumed that $|\beta| < \pi/2$.

Proposition 1: *The maximum value β_{max} of $|\beta|$ is:*

$$\beta_{max} = \begin{cases} \arcsin(\frac{\epsilon_e}{l_0/2}) & \text{if} \quad (l_0 - \sqrt{l_0^2 - 4\epsilon_e^2})/2 \leq \epsilon_{t_e} \leq \epsilon_e \\ 2\arcsin(\sqrt{\frac{\epsilon_e^2 - \epsilon_{t_e}^2}{l_0(l_0 - 2\epsilon_{t_e})}}) & \text{otherwise} \end{cases} \tag{3.14}$$

Proof: The maximum possible deviation in the orientation of e occurs when the edge is tangent to the uncertainty circles of its vertices (Figure 3.5a). Then, the length of the actual edge is $l = \sqrt{l_0^2 - 4\epsilon_e^2}$ and the maximum deviation is determined by the expression $\beta_{max} = \arcsin(\frac{\epsilon_e}{l_0/2})$. For a given ϵ_e, this maximum orientation is reachable only if the minimum possible length of the edge, $l_0 - 2\epsilon_{t_e}$, satisfies $l_0 - 2\epsilon_{t_e} \leq l$. This condition can be rewritten to show that this maximum orientation is reachable when the maximum deviation ϵ_{t_e} lies in the range $(l_0 - \sqrt{l_0^2 - 4\epsilon_e^2})/2 \leq \epsilon_{t_e} \leq \epsilon_e$.

When this is not satisfied, i.e. $0 \leq \epsilon_{t_e} \leq (l_0 - \sqrt{l_0^2 - 4\epsilon_e^2})/2$, the maximum deviation is reached for the minimum possible length of the edge, i.e. $l_0 - 2\epsilon_{t_e}$. The expression of the maximum deviation is obtained by using the cosinus theorem (Figure 3.5b):

$$\epsilon_e^2 = \left(\frac{l_0}{2}\right)^2 + \left(\frac{l_0 - 2\epsilon_{t_e}}{2}\right)^2 - 2\left(\frac{l_0}{2}\right)\left(\frac{l_0 - 2\epsilon_{t_e}}{2}\right)\cos\beta_{max} \tag{3.15}$$

and the trigonometric expression $\cos\beta = 1 - 2\sin^2\frac{\beta}{2}$. As a result:

$$\beta_{max} = 2\arcsin(\sqrt{\frac{\epsilon_e^2 - \epsilon_{t_e}^2}{l_0(l_0 - 2\epsilon_{t_e})}}) \tag{3.16}$$

If $\epsilon_{t_e} = 0$, like in Figure 3.5b, this expression becomes:

$$\beta_{max} = 2\arcsin(\epsilon_e/l_0) \tag{3.17}$$

$\diamond$

Corollary 1: For a given deviation β, the range of orientations of the manipulated object that may produce contact is $[\phi_m + \beta, \phi_M + \beta]$, being $[\phi_m, \phi_M]$ the nominal range of contact orientations.

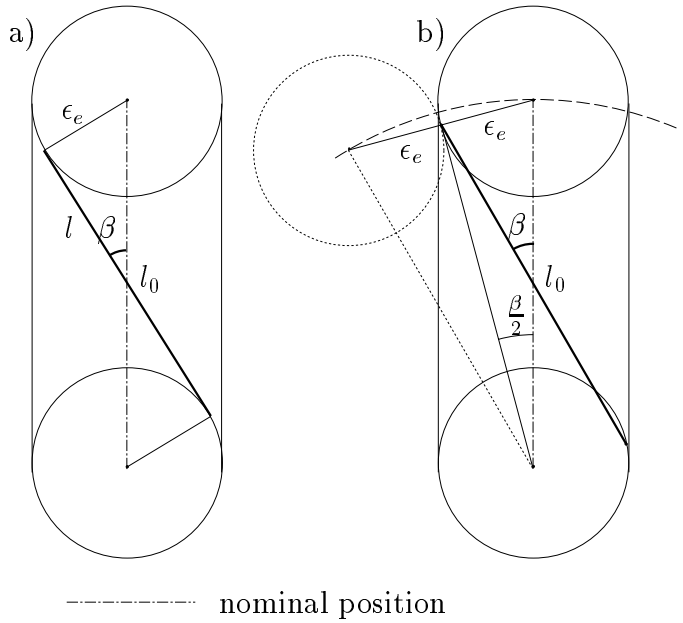

Figure 3.5: *The maximum deviation in the orientation of the contact edge.*

Let $V_a = (v_{ax}, v_{ay})$ and $V_b = (v_{bx}, v_{by})$ be the vertices of e such that V_a is first encountered when the border of the object is followed counterclockwise. Let ψ be the orientation of the outward normal of e and $v_{a_0} = (v_{ax_0}, v_{ay_0})$ and $v_{b_0} = (v_{bx_0}, v_{by_0})$ be the nominal positions of V_a and V_b, respectively. Let finally $\mathbf{C}(x, y, r)$ be a circle of radius r centered on (x, y).

Proposition 2: *The region* $\mathbf{R}(e, V_a, \beta)$ *where the vertex* V_a *of* e *lies for a given deviation* β *is:*

$$\mathbf{R}(e, V_a, \beta) = \mathbf{C}(v_{ax_0}, v_{ay_0}, \epsilon_e) \cap \bigcup_{\forall l \in [l_0 - 2\epsilon_{t_e}, l_0 + 2\epsilon_{t_e}]} \mathbf{C}(v_{bx_0} - l\sin(\psi+\beta),\ v_{by_0} + l\cos(\psi+\beta), \epsilon_e) \tag{3.18}$$

Proof: From condition 1 V_a satisfies:

$$V_a \in \mathbf{C}(v_{ax_0}, v_{ay_0}, \epsilon_e) \tag{3.19}$$

From condition 2 V_a satisfies:

$$V_a \in \bigcup_{\forall l \in [l_0 - 2\epsilon_{t_e}, l_0 + 2\epsilon_{t_e}]} \mathbf{C}(v_{bx_0} - l\sin(\psi+\beta), v_{by_0} + l\cos(\psi+\beta), \epsilon_e) \tag{3.20}$$

Then, $\mathbf{R}(e, V_a, \beta)$ is the intersection of the circle of equation (3.19) and the reunion of circles of equation (3.20). ◇

A similar reasoning can be done for vertex V_b. Region $\mathbf{R}(e, V_a, \beta)$ is illustrated in Figure 3.6 for two different values of ϵ_{t_e}.

Corollary 2.1: $\mathbf{R}(e, v, \beta_1) \subset \mathbf{R}(e, v, \beta_2)$ if $|\beta_1| > |\beta_2|$ and $\beta_1\beta_2 \geq 0$.

Corollary 2.2: The border of $\mathbf{R}(e, V_a, \beta)$ has two arcs a_1 and a_2 (Figure 3.6a) of the circles defined by (3.20) corresponding to the maximum and minimum possible lengths of e, respectively, if $2\epsilon_{t_e} < \epsilon_e$.

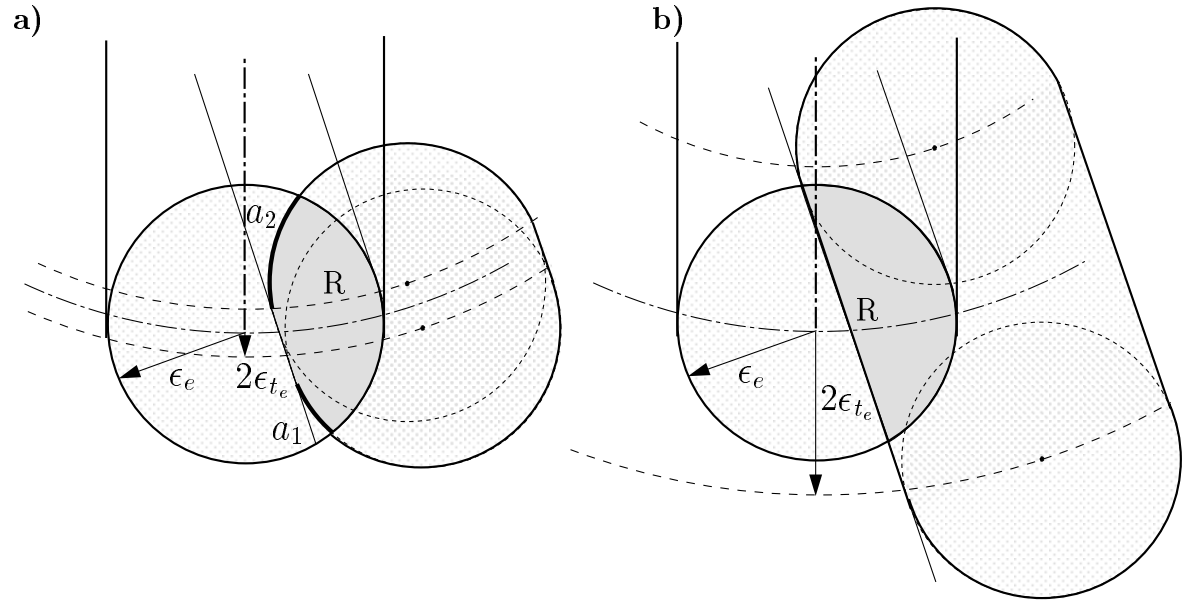

Figure 3.6: *Region* $\mathbf{R}(e, V_a, \beta)$ *for different values of* ϵ_{t_e}.

Proposition 3: *The region* $\mathbf{E}(\beta)$ *that contain all the possible realizations of* e *for a given deviation* β *in its orientation is the positive linear combination of the regions* $\mathbf{R}(e, V_a, \beta)$ *and* $\mathbf{R}(e, V_b, \beta)$.

Proof: The vertices V_a and V_b of any realization of e are inside the regions $\mathbf{R}(e, V_a, \beta)$ and $\mathbf{R}(e, V_b, \beta)$, respectively, and any point of e can be expressed as a positive linear combination of V_a and V_b. ◇

Figure 3.7 shows the region $\mathbf{E}(\beta)$ for two different deviations in the orientation of e for some given values of ϵ_e and ϵ_{t_e}.

$\mathbf{E}(\beta)$ can be partitioned into three disjoint figures $\mathbf{L}_r(\beta)$, $\mathbf{L}_{V_a}(\beta)$ and $\mathbf{L}_{V_b}(\beta)$, as shown in Figure 3.8a, being $\mathbf{L}_r(\beta)$ the rectangle of maximum area inscribed in $\mathbf{E}(\beta)$ with two of its sides over the parallel sides of the border of $\mathbf{E}(\beta)$. The width, $d(\beta)$, and length, $l(\beta)$, of the rectangle $\mathbf{L}_r(\beta)$ decrease with β in the following way:

$$d(\beta) = 2(\epsilon_e - \frac{l_0}{2}|\sin\beta|) \tag{3.21}$$

$$l(\beta) = l_0 \cos\beta \tag{3.22}$$

Let $\mathbf{L}(\beta)$ be the geometric figure obtained from $\mathbf{L}_{V_a}(\beta)$ and $\mathbf{L}_{V_b}(\beta)$ as shown in Figure 3.8b. $\mathbf{L}(\beta)$ will be used in Section 3.3.4 to compute the effect of uncertainty on the contact configurations. The center (c_x, c_y) of the maximum inscribed circle will be considered the center of $\mathbf{L}(\beta)$. If $\beta = 0$ region $\mathbf{L}(\beta)$ is a circle:

$$\mathbf{L}(0) = \mathbf{C}(c_x, c_y, \epsilon_e) \tag{3.23}$$

Corollary 3: The larger the deviation in the orientation the smaller $\mathbf{E}(\beta)$, since the area of $\mathbf{L}_r(\beta)$ decreases with β.

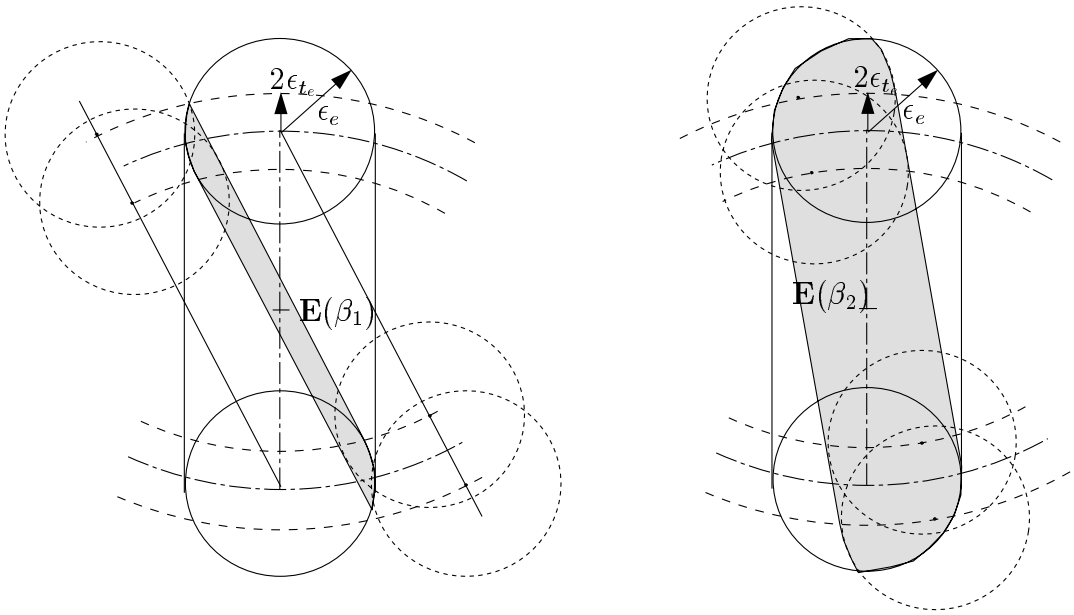

Figure 3.7: *Region* $\mathbf{E}(\beta)$ *of possible positions of the contact edge for two deviations in its orientation.*

3.2.2 Modelling uncertainty on the contact vertex

The vertices of the manipulated object lie inside uncertainty circles of radius ϵ_v centered on their nominal positions. Nevertheless, the position of the vertices depend on the deviation in the orientation of the adjacent edges. Let $V = (v_x, v_y)$ be the contact vertex and e_m and e_M be its adjacent edges, such that e_m is first encountered when the border of the object is followed clockwise. Let also α_m and α_M be the deviations in the orientations of e_m and e_M, respectively.

Proposition 4: *The region* $\mathbf{V}(\alpha_m, \alpha_M)$ *where the contact vertex lies is:*

$$\mathbf{V}(\alpha_m, \alpha_M) = \mathbf{R}(e_m, V, \alpha_m) \cap \mathbf{R}(e_M, V, \alpha_M) \tag{3.24}$$

Proof: From corollary 2.1 the region where V lies for any α_m and α_M is expressed by equation (3.24), since:

- $\mathbf{R}(e_m, V, \alpha_m)$ is the region where V lies for a given deviation α_m when $\alpha_M = 0$, and
- $\mathbf{R}(e_M, V, \alpha_M)$ is the region where V lies for a given deviation α_M when $\alpha_m = 0$.

$\diamond$

Corollary 4.1: If $\alpha_m = 0$ and $\alpha_M = 0$, then:

$$\mathbf{V}(0, 0) = \mathbf{C}(v_x, v_y, \epsilon_v) \tag{3.25}$$

since

$$\begin{aligned} \mathbf{R}(e_m, V, 0) &= \mathbf{C}(v_x, v_y, \epsilon_v) \\ \mathbf{R}(e_M, V, 0) &= \mathbf{C}(v_x, v_y, \epsilon_v) \end{aligned} \tag{3.26}$$

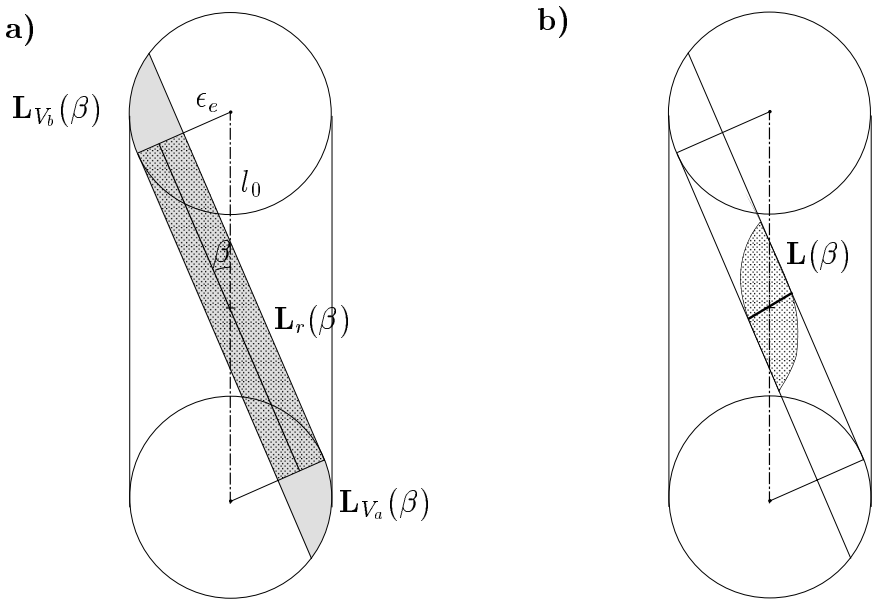

Figure 3.8: *a) Partition of* $\mathbf{E}(\beta)$ *into three disjoint regions* $\mathbf{L}_r(\beta)$, $\mathbf{L}_{V_a}(\beta)$ *and* $\mathbf{L}_{V_b}(\beta)$ *b) Geometric figure* $\mathbf{L}(\beta)$.

Corollary 4.2: For a given pair of deviations α_m, α_M, the range of orientations of the manipulated object that may produce contact is $[\phi_m - \alpha_m, \phi_M - \alpha_M]$, being $[\phi_m, \phi_M]$ the nominal range of contact orientations.

Corollary 4.3: The maximum values $\alpha_{m_{max}}$ and $\alpha_{M_{max}}$ of $|\alpha_m|$ and $|\alpha_M|$, respectively, have an expression analogous to that of the maximum value β_{max} of $|\beta|$ computed in proposition 1.

Figures 3.9a and 3.9b show the regions $\mathbf{R}(e_m, V, \alpha_m)$ and $\mathbf{R}(e_M, V, \alpha_M)$, respectively.

3.2.3 Sensing uncertainty

The sensing uncertainty in the robot position is expressed in equation (3.4). Its effect on the position of the topological element of the contact corresponding to the manipulated object is the following:

- *type-A*: The region where the contact edge lies is $\mathbf{E}(\beta)$ convolved with a circle of radius ϵ_{p_r}.
- *type-B*: The region where the contact vertex lies is $\mathbf{V}(\alpha_m, \alpha_M)$ convolved with a circle of radius ϵ_{p_r}.

These regions will be approximated by $\mathbf{E}(\beta)$ and $\mathbf{V}(\alpha_m, \alpha_M)$, respectively, computed with a larger uncertainty radius:

- *type-A*: $\epsilon_e = \epsilon_m + \epsilon_{p_r}$
- *type-B*: $\epsilon_v = \epsilon_m + \epsilon_{p_r}$

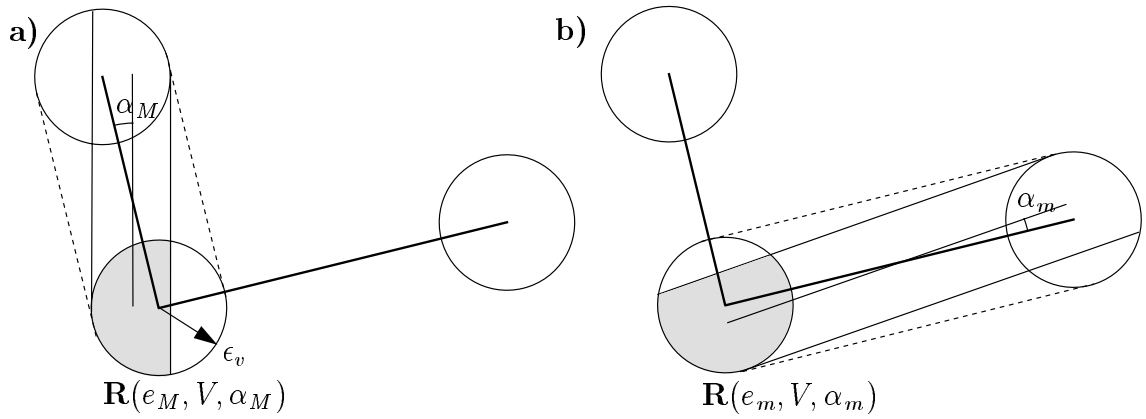

Figure 3.9: *a) Region* $\mathbf{R}(e_m, V, \alpha_M)$ *b) Region* $\mathbf{R}(e_M, V, \alpha_m)$.

Figure 3.10 shows the additional region introduced by this approximation.

The sensing uncertainty in the robot orientation is expressed in equation (3.8). Its effect is not directly considered in the position and orientation of the topological elements of the contact, but by explicitly considering the range where the actual orientation lies, as expressed in the following definition.

Definition: The observed configuration c_o is *compatible* with the occurrence of contact i iff this can take place at one or more orientations of the range $[\phi_{o_m}, \phi_{o_M}]$.

3.3 One basic contact situations

3.3.1 Nominal contact condition

Let $\mathcal{F}_i$ be the $\mathcal{C}$-face representing the nominal contact configurations for a given basic contact i between a vertex V_i and an edge e_i, and let $c_o = (x_o, y_o, \phi_o)$ be the observed configuration.

The nominal contact condition for contact i can be expressed in physical space, in $\mathcal{C}$-space and in $\mathcal{C}'$-space in the following way, respectively:

$$V_i \cap e_i \neq \emptyset \tag{3.27}$$

$$c_o \cap \mathcal{F}_i \neq \emptyset \tag{3.28}$$

$$(x_o, y_o) \cap f_i'(\phi_o) \neq \emptyset \tag{3.29}$$

The contact condition is satisfied if $\phi_o \in R^i_\phi$, i.e. $\phi_o \in R^i_\phi$ is a necessary condition for contact i to take place.

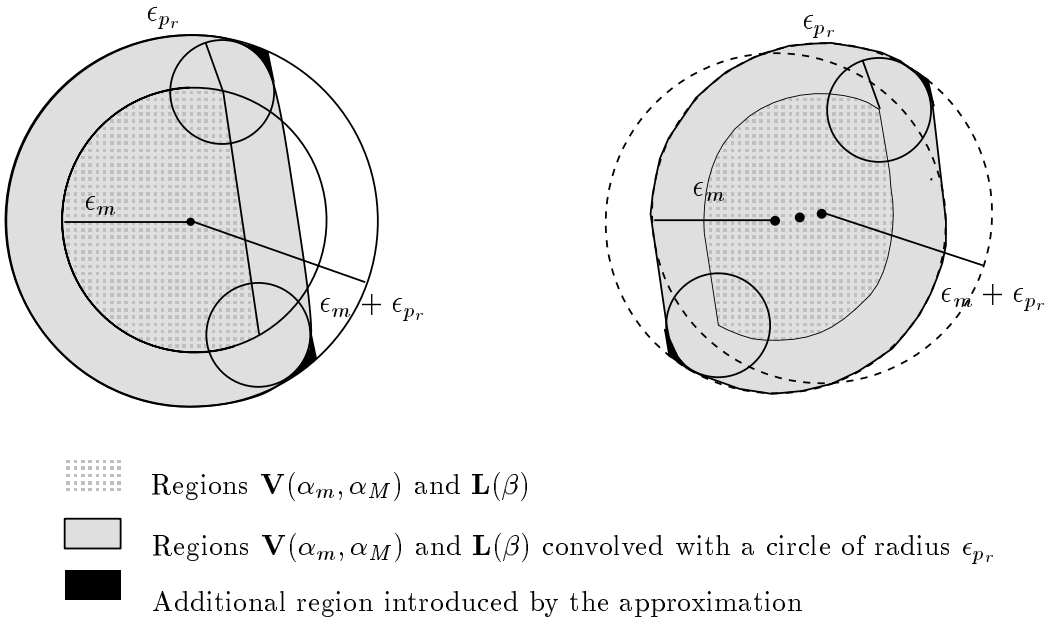

Figure 3.10: *Additional region introduced by approximating the convolution region by the uncertainty regions computed with radius $\epsilon_m + \epsilon_{p_r}$.*

3.3.2 Contact condition in the presence of uncertainty

The effect of the uncertainty in the contact configurations is tackled as follows:

- The nominal $\mathcal{C}$-space is used to determine if a observed configuration is a contact configuration.
- A set of configurations is associated to c_o and to each basic contact i such that contact i can take place iff this set intersects $\mathcal{F}_i$.

Proposition 5: *There exists an orientation $\phi_o^i \in [\phi_{o_m}, \phi_{o_M}]$ such that c_o is compatible with the occurrence of contact i iff this can take place at ϕ_o^i.*

The proof is found in Section 3.3.3.

The contact condition in the presence of uncertainty is expressed in physical space by the following proposition.

Proposition 6: *A basic contact can take place iff for orientation ϕ_o^i:*

$$\mathbf{V}(\alpha_m, \alpha_M) \cap \mathbf{E}(\beta) \neq \emptyset \tag{3.30}$$

for some values of the deviations α_m, α_M and β.

Proof: A point p_i satisfying $p_i \in [\mathbf{V}(\alpha_m, \alpha_M) \cap \mathbf{E}(\beta)]$ simultaneously satisfies $p_i \in \mathbf{V}(\alpha_m, \alpha_M)$ and $p_i \in \mathbf{E}(\beta)$. Therefore, it can simultaneously be a position where the contact vertex can lie and a position where a point of the contact edge can lie, i.e. a position where equation (3.27) is satisfied, and hence a position where the basic contact can take place. ◇

Proposition 7: *The condition*

$$\phi_o^i \in [\phi_m^i - \alpha_m + \beta,\ \phi_M^i - \alpha_M + \beta] \tag{3.31}$$

is a necessary condition for contact i to take place.

Proof: A contact is possible if the actual orientation of the robot lies inside the corresponding range of contact orientations. From corollaries 1 and 4.2, the range of nominal contact orientations is shifted by the deviations β, α_m and α_M. Considering all of them gives rise to expression (3.31). ◇

Corollary 7.1: From corollary 2.1 it follows that:

$$\begin{array}{lcll} \mathbf{L}(\beta_1) & \subset & \mathbf{L}(\beta_2) & \text{if } |\beta_1| > |\beta_2| \\ \mathbf{V}(\alpha_{m1}, \alpha_M) & \subset & \mathbf{V}(\alpha_{m2}, \alpha_M) & \text{if } |\alpha_{m1}| > |\alpha_{m2}| \\ \mathbf{V}(\alpha_m, \alpha_{M1}) & \subset & \mathbf{V}(\alpha_m, \alpha_{M2}) & \text{if } |\alpha_{M1}| > |\alpha_{M2}| \end{array} \tag{3.32}$$

Therefore, the uncertainty in the position of the topological elements of the contact for all the possible values of the deviations can be taken into account by only considering the uncertainty region defined by the deviations with minimum absolute value.

Corollary 7.2: If Δ_ϕ^i is defined as:

$$\Delta_\phi^i = \begin{cases} 0 & \text{if } \phi_o^i \in [\phi_m^i, \phi_M^i] \\ \phi_o^i - \phi_m^i & \text{if } \phi_o^i < \phi_m^i \\ \phi_o^i - \phi_M^i & \text{if } \phi_o^i > \phi_M^i \end{cases} \tag{3.33}$$

then, proposition 7 can be rewritten as:

$$\begin{array}{ll} \beta - \alpha_M \geq \Delta_\phi^i & \text{if } \phi_o^i > \phi_M^i \\ \beta - \alpha_m \leq \Delta_\phi^i & \text{if } \phi_o^i < \phi_m^i \end{array} \tag{3.34}$$

i.e. a contact can take place if the deviations in the orientations of the edges is enough to cover the orientation gap Δ_ϕ^i.

From corollaries 7.1 and 7.2, the following values of the deviations will be considered for the analysis of the contact configurations:

a) $\phi_o^i > \phi_M^i$:

$$\begin{aligned} \alpha_m &= 0 \\ \beta - \alpha_M &= \Delta_\phi^i \end{aligned} \tag{3.35}$$

The contact is possible for some given pairs (β, α_M) and for any value of α_m (Figure 3.11a). Therefore, $\mathbf{V}(\alpha_m, \alpha_M) = \mathbf{V}(0, \alpha_M) = \mathbf{R}(e_M, V, \alpha_M)$.

b) $\phi_o^i < \phi_m^i$:

$$\begin{aligned} \alpha_M &= 0 \\ \beta - \alpha_m &= \Delta_\phi^i \end{aligned} \tag{3.36}$$

The contact is possible for some given pairs (β, α_m), and for any value of α_M (Figure 3.11b). Therefore, $\mathbf{V}(\alpha_m, \alpha_M) = \mathbf{V}(\alpha_m, 0) = \mathbf{R}(e_m, V, \alpha_m)$.

c) $\phi_o^i \in R_\phi^i$:

$$\begin{aligned} \alpha_m &= 0 \\ \alpha_M &= 0 \\ \beta &= 0 \end{aligned} \tag{3.37}$$

The contact is possible for any value of the deviations. Therefore, the contact vertex and the vertices of the contact edge can lie anywhere within their uncertainty circles as expressed in equations (3.23) and (3.25).

Let α be defined as:

$$\alpha = \begin{cases} \alpha_m & \text{if } \phi_o^i < \phi_m \\ \alpha_M & \text{if } \phi_o^i > \phi_M \end{cases} \tag{3.38}$$

For a given basic contact i, the contact condition of equation (3.30) will be tested using the nominal $\mathcal{C}$-space by associating to c_o a set of configurations $\mathbf{U}^i(\alpha, \beta)$ such that contact i can take place iff $\mathbf{U}^i(\alpha, \beta)$ interects $\mathcal{F}_i$. $\mathbf{U}^i(\alpha, \beta)$ will be called Contact Position Region. Therefore, proposition 8 follows.

Proposition 8: *When equation* (3.30) *is satisfied, the Contact Position Region* $\mathbf{U}^i(\alpha, \beta)$ *satisfies:*

$$\mathbf{U}^i(\alpha, \beta) \cap f_i'(\phi_t^i) \neq \emptyset \tag{3.39}$$

where ϕ_t^i *is defined as:*

$$\phi_t^i = \phi_o^i + \Delta_\phi^i \tag{3.40}$$

Corollary 8.1: Proposition 8 can be rewritten as:

$$\begin{array}{lll} \mathbf{U}^i(0,0) \cap f_i'(\phi_o^i) \neq \emptyset & \text{if} & \phi_o^i \in [\phi_m^i, \phi_M^i] \\ \mathbf{U}^i(\alpha_M, \beta) \cap f_i'(\phi_M^i) \neq \emptyset & \text{if} & \phi_o^i > \phi_M^i \quad \text{with } \beta - \alpha_M = \Delta_\phi^i \\ \mathbf{U}^i(\alpha_m, \beta) \cap f_i'(\phi_m^i) \neq \emptyset & \text{if} & \phi_o^i < \phi_m^i \quad \text{with } \beta - \alpha_m = \Delta_\phi^i \end{array} \tag{3.41}$$

Corollary 8.2: Contact i can take place for an observed configuration c_o iff equation (3.39) is satisfied for a given set of values α and β.

Definition: The *Contact Position Domain* $\mathbf{U}^i(\Delta_\phi^i)$ is the union of the Contact Position Regions $\mathbf{U}^i(\alpha, \beta)$ for all the pairs of deviations α and β satisfying $\beta - \alpha = \Delta_\phi^i$:

$$\mathbf{U}^i(\Delta_\phi^i) = \bigcup_{\forall \alpha, \beta | \beta - \alpha = \Delta_\phi^i} \mathbf{U}^i(\alpha, \beta) \tag{3.42}$$

Proposition 9: *If equation* (3.30) *is satisfied for some given values* α *and* β*, the Contact Position Domain satisfies*:

$$\mathbf{U}^i(\Delta_\phi^i) \cap f_i'(\phi_t^i) \neq \emptyset \tag{3.43}$$

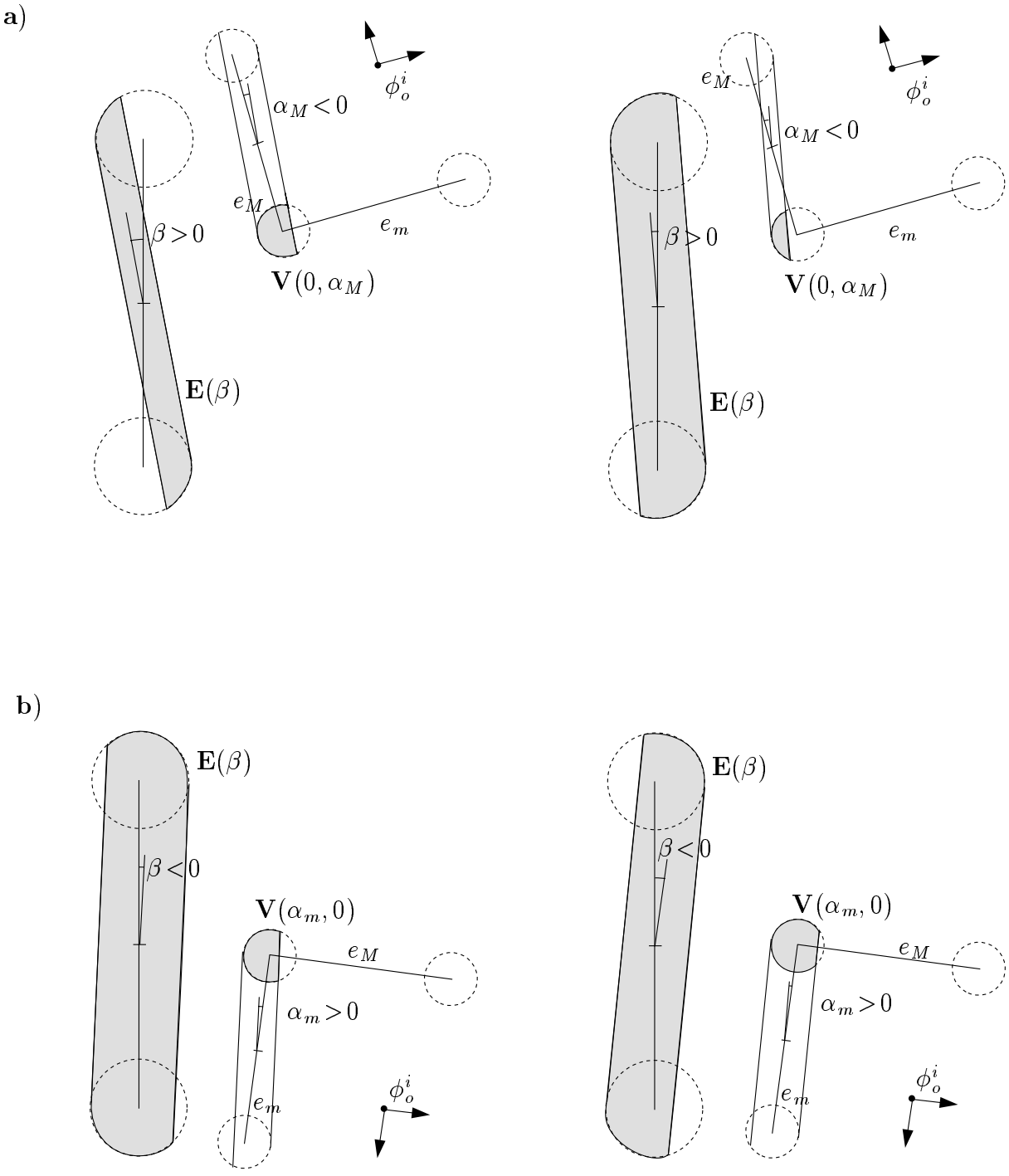

Figure 3.11: *Different values of* α_m, α_M *and* β *that satisfy equation* (3.31) *for orientations (a)* $\phi_o^i > \phi_M$ *and (b)* $\phi_o^i < \phi_m$.

Corollary 9: Contact i can take place for a observed configuration c_o iff equation (3.43) is satisfied.

3.3.3 The orientation ϕ_o^i

By proposition 5, the test to verify if c_o is compatible with the occurrence of contact i is performed at only one orientation. This Section gives the proof of this proposition and the procedure to compute this orientation.

Proposition 5: *There exists an orientation $\phi_o^i \in [\phi_{o_m}, \phi_{o_M}]$ such that c_o is compatible with the occurrence of contact i iff this can take place at ϕ_o^i.*

Proof: Let $d_p(\phi)$ be the distance from the observed position (x_o, y_o) to the line containing $f'(\phi)$, with $\phi \in R_\phi^i$:

$$d_p(\phi) = |D_p(\phi) - D_f(\phi)| \tag{3.44}$$

where (Figure 3.12a):

- $D_p(\phi)$ is the distance from the origin of $\{W\}$ to the observed position (x_o, y_o) in the direction ψ_W (for type-A basic contacts $\psi_W = \psi_T + \phi + \pi$ and for type-B basic contacts ψ_W is independent of ϕ):

$$D_p(\phi) = x_o \cos\psi_W + y_o \sin\psi_W \tag{3.45}$$

- $D_f(\phi)$ is the distance from the origin of $\{W\}$ to the line containing $f'(\phi)$, as defined in equations (2.4) and (2.5) for type A and type B basic contacts, respectively.

The distance d_p is minimum at one or two orientations of the range $[\phi_{o_m}, \phi_{o_M}]$. Let ϕ_o^i be one of these orientations. Then:

- If the contact can take place at orientation ϕ_o^i then c_o is compatible with the occurrence of contact i, since $\phi_o^i \in [\phi_{o_m}, \phi_{o_M}]$.
- If c_o is compatible with the occurrence of contact i, i.e. (3.43) is satisfied for an orientation $\phi \in [\phi_{o_m}, \phi_{o_M}]$, then (3.43) is also satisfied for orientation ϕ_o^i, since for this orientation the observed position is closest to the nominal contact positions. $\diamond$

Computing ϕ_o^i

Let introduce:

ϕ_l : orientation such that $d_p(\phi_l) = 0$.

$\frac{\partial d_p}{\partial \phi}$: the derivate of d_p with respect to ϕ.

ϕ_h : orientation such that $\left.\frac{\partial d_p}{\partial \phi}\right|_{\phi_h} = 0$.

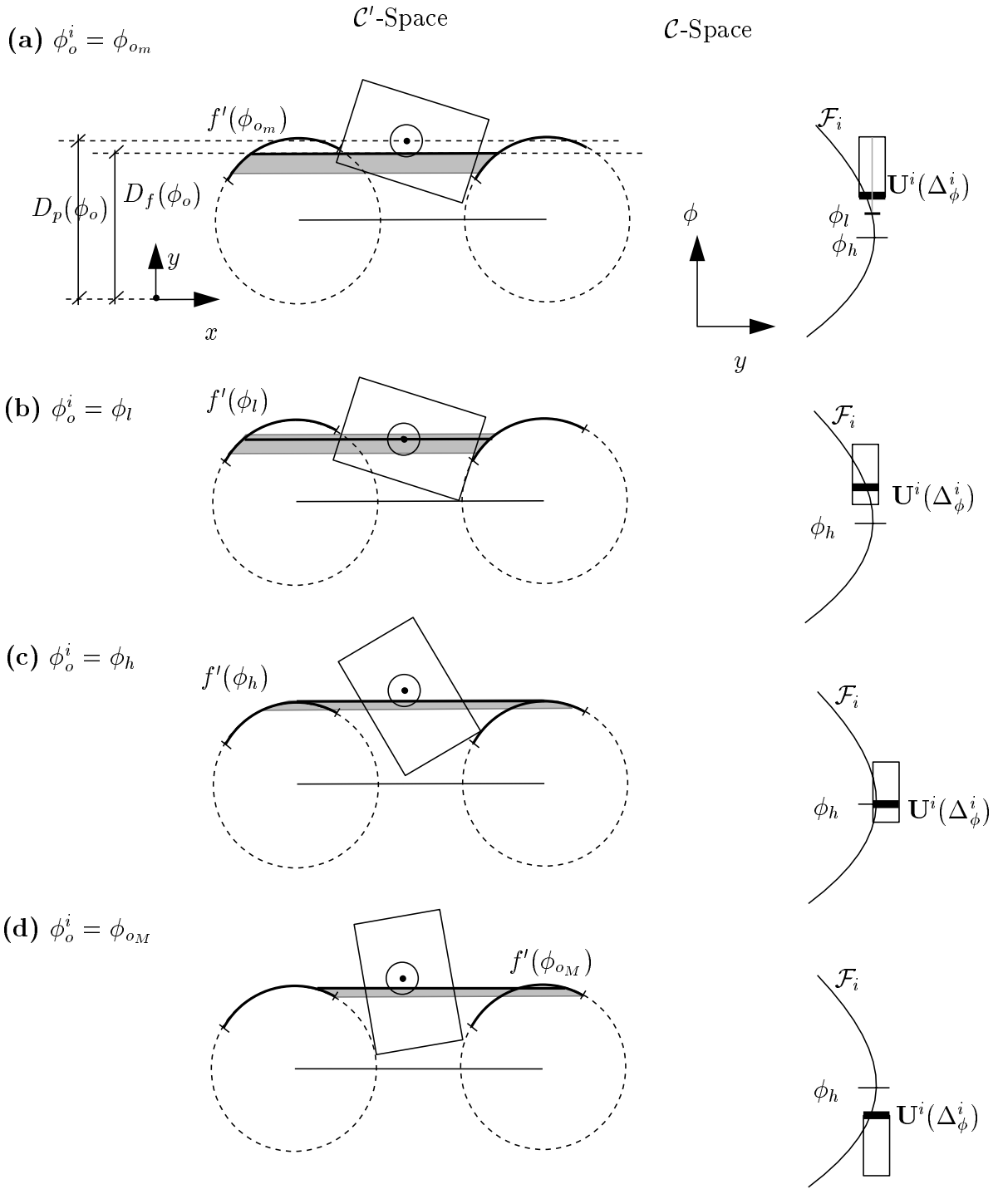

Figure 3.12: *Orientation ϕ_o^i for a type-B basic contact: (a) $\phi_o^i = \phi_{o_m}$ (b) $\phi_o^i = \phi_l$ (c) $\phi_o^i = \phi_h$ (d) $\phi_o^i = \phi_{o_M}$.*

For type-A basic contacts:

$$\phi_l = -\psi_T - \pi + 2\arctan\left(\frac{(x_i - x_o) \pm \sqrt{(x_i - x_o)^2 + (y_i - y_o)^2 - d_T^2}}{-(y_i - y_o) + d_T}\right) \tag{3.46}$$

$$\frac{\partial d_p}{\partial \phi} = \begin{cases} (x_i - x_o)\sin(\psi_T + \phi + \pi) - (y_i - y_o)\cos(\psi_T + \phi + \pi) & \text{if } D_p(\phi) \geq D_f(\phi) \\ -(x_i - x_o)\sin(\psi_T + \phi + \pi) + (y_i - y_o)\cos(\psi_T + \phi + \pi) & \text{if } D_p(\phi) < D_f(\phi) \end{cases} \tag{3.47}$$

$$\phi_h = \arctan\left(\frac{y_i - y_o}{x_i - x_o}\right) - k\pi - \psi_T \quad \text{with } k = \{0, 1\} \tag{3.48}$$

For type-B basic contacts:

$$\phi_l = \psi_W + \pi - \gamma_i - \arccos\left(\frac{x_o \cos\psi_w + y_o \sin\psi_W}{h_i}\right) \tag{3.49}$$

$$\frac{\partial d_p}{\partial \phi} = \begin{cases} -h\sin(\psi_W + \pi - \gamma_i - \phi) & \text{if } D_p(\phi) \geq D_f(\phi) \\ h\sin(\psi_W + \pi - \gamma_i - \phi) & \text{if } D_p(\phi) < D_f(\phi) \end{cases} \tag{3.50}$$

$$\phi_h = \psi_W + k\pi - \gamma_i \quad \text{with } k = \{0, 1\} \tag{3.51}$$

If $\left|\frac{x_o \cos\psi_w + y_o \sin\psi_W}{h_i}\right| > 1$ then ϕ_l does not exist, otherwise there are two possible values. If both of them satisfy $\phi_l \in [\phi_{o_m}, \phi_{o_M}]$ then one of them is arbitrarily chosen.

The algorithm to compute ϕ_o^i is as follows (Figure 3.12):

Find-orientation(c_o, i)

IF $[\phi_{om}, \phi_{oM}] \cap R_\phi^i = \emptyset$ RETURN the extreme of $[\phi_{om}, \phi_{oM}]$ closest to R_ϕ^i

ELSE

Compute ϕ_l

IF $\phi_l \in [\phi_{o_m}, \phi_{o_M}]$ RETURN ϕ_l

ELSE:

Compute $s_m = \left.\frac{\partial d_p}{\partial \phi}\right|_{\phi_{o_m}}$ and $s_M = \left.\frac{\partial d_p}{\partial \phi}\right|_{\phi_{o_M}}$

IF $s_m > 0$ and $s_M > 0$ RETURN ϕ_{o_m}

IF $s_m < 0$ and $s_M < 0$ RETURN ϕ_{o_M}

IF $s_m < 0$ and $s_M > 0$ THEN

Compute ϕ_h

RETURN ϕ_h

IF $s_m > 0$ and $s_M < 0$

Compute ϕ_h

IF $\phi_o > \phi_h$ RETURN ϕ_{o_M}

ELSE RETURN ϕ_{o_m}

END

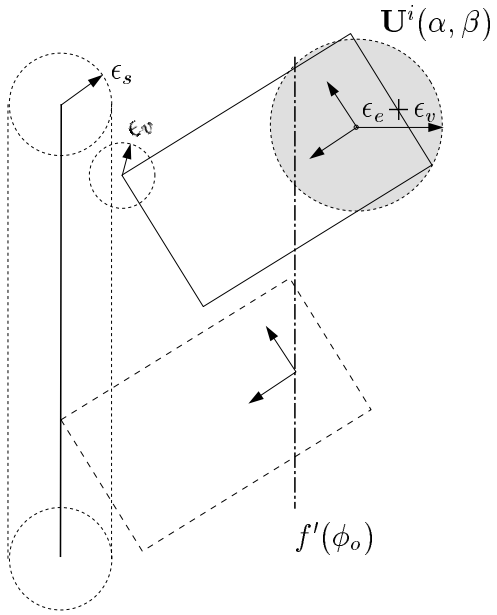

Figure 3.13: *Contact Position Region* $\mathbf{U}^i(\alpha,\beta)$ *when* $\phi_o^i \in R_\phi^i$.

3.3.4 Construction of the Contact Position Region

The Contact Position Region:

a) Is a circle of radius $(\epsilon_e + \epsilon_v + \epsilon_{pr})$ centered at the observed position (Figure 3.13) when $\phi_o^i \in R_\phi^i$, since $\alpha = \beta = 0$ and the contact vertex and the vertices of the contact edge can lie anywhere within their uncertainty circles.

b) Is a region that intersects $f'(\phi_m)$ or $f'(\phi_M)$ when the contact can take place at an orientation $\phi_o^i \notin R_\phi^i$ (equation (3.41)).

Let $\mathbf{V}(\alpha)$ be defined as follows:

$$\mathbf{V}(\alpha) = \begin{cases} \mathbf{V}(\alpha,0) & \text{if} \quad \phi_o^i < \phi_m^i \\ \mathbf{V}(0,\alpha) & \text{if} \quad \phi_o^i > \phi_M^i \end{cases} \tag{3.52}$$

Let $P_o = (P_{ox}, P_{oy})$ be the center of $\mathbf{U}^i(\alpha,\beta)$ which is obtained from (x_o, y_o) by:

(a) Rotating an angle α around the center (x_v, y_v) of the edge adjacent to the contact vertex:

$$\begin{aligned} x'_o &= x_v + (x_o - x_v)\cos\alpha - (y_o - y_v)\sin\alpha \\ y'_o &= y_v + (x_o - x_v)\sin\alpha + (y_o - y_v)\cos\alpha \end{aligned} \tag{3.53}$$

(b) Rotating an angle $-\beta$ around the center (x_e, y_e) of the contact edge:

$$\begin{aligned} x''_o &= x_e + (x'_o - x_e)\cos(-\beta) - (y'_o - y_e)\sin(-\beta) \\ y''_o &= y_e + (x'_o - x_e)\sin(-\beta) + (y'_o - y_e)\cos(-\beta) \end{aligned} \tag{3.54}$$

(c) Translating, in the direction of the nominal contact edge, a distance t:

$$t = \begin{cases} l_o(1-\cos\beta) & \text{if} \quad (\cos\psi, \sin\psi)(x_o - x_e, y_o - y_e) > 0 \\ -l_o(1-\cos\beta) & \text{otherwise} \end{cases} \tag{3.55}$$

ψ being the orientation normal to the nominal contact edge:

$$\begin{aligned} P_{ox} &= x_o'' + d\cos(\psi + \pi/2) \\ P_{ox} &= y_o'' + d\sin(\psi + \pi/2) \end{aligned} \tag{3.56}$$

Then, the algorithm to compute the Contact Position Region is the following:

$\mathbf{U}^i(\alpha,\beta)$-construction($c_o$)

IF $\phi_o^i \in R_\phi^i$ THEN $\mathbf{U}^i(\alpha,\beta) = \mathbf{C}(x_o, y_o, \epsilon_e + \epsilon_v)$.

ELSE

(1) Rotate $\mathbf{L}(\beta)$ and $\mathbf{V}(\alpha)$ an angle $-\beta$ around their respective centers.

(2) Find the convolution region of the regions obtained in the previous step.

(3) Center the obtained region at P_o.

END

The border of the convolution region of step (2) is obtained when the center of one figure traverse the border of the other. This border can be described by up to five arcs of circumferences and two straight segments, as detailed below, if the following approximations are done:

- $\mathbf{R}(e, V, \beta)$ is computed considering that the condition of corollary 2.2 is not satisfied, and therefore the border of $\mathbf{R}(e, V, \beta)$ does not have the arcs a_1 and a_2. As a consequence, the shape of $\mathbf{L}(\beta)$ is always that of Figure 3.14a.
- The region where the topological element of the contact corresponding to the manipulated object lies is approximated by (Section 3.2.3):

  type-A : Region $\mathbf{L}(\beta)$ computed with $\epsilon_e = \epsilon_m + \epsilon_{p_r}$

  type-B : Region $\mathbf{V}(\alpha)$ computed with $\epsilon_v = \epsilon_m + \epsilon_{p_r}$

The following nomenclature is used (Figure 3.14):

- The border of region $\mathbf{L}(\beta)$ is composed of two arcs and two straight segments, as in Figure 3.14a, which are described by the following variables:

  l_e: length of the contact edge

  ψ: orientation of the normal to the contact edge

  $r_e = \epsilon_e - (l_e/2)|\sin\beta|$, radius of the maximum inscribed circumference

  $\gamma_e = \arccos((2r_e - \epsilon_e)/\epsilon_e)$

  and the following points of $\mathbf{L}(\beta)$ described with respect to its center, P_β, once $\mathbf{L}(\beta)$ has been rotated an angle $-\beta$ around it:

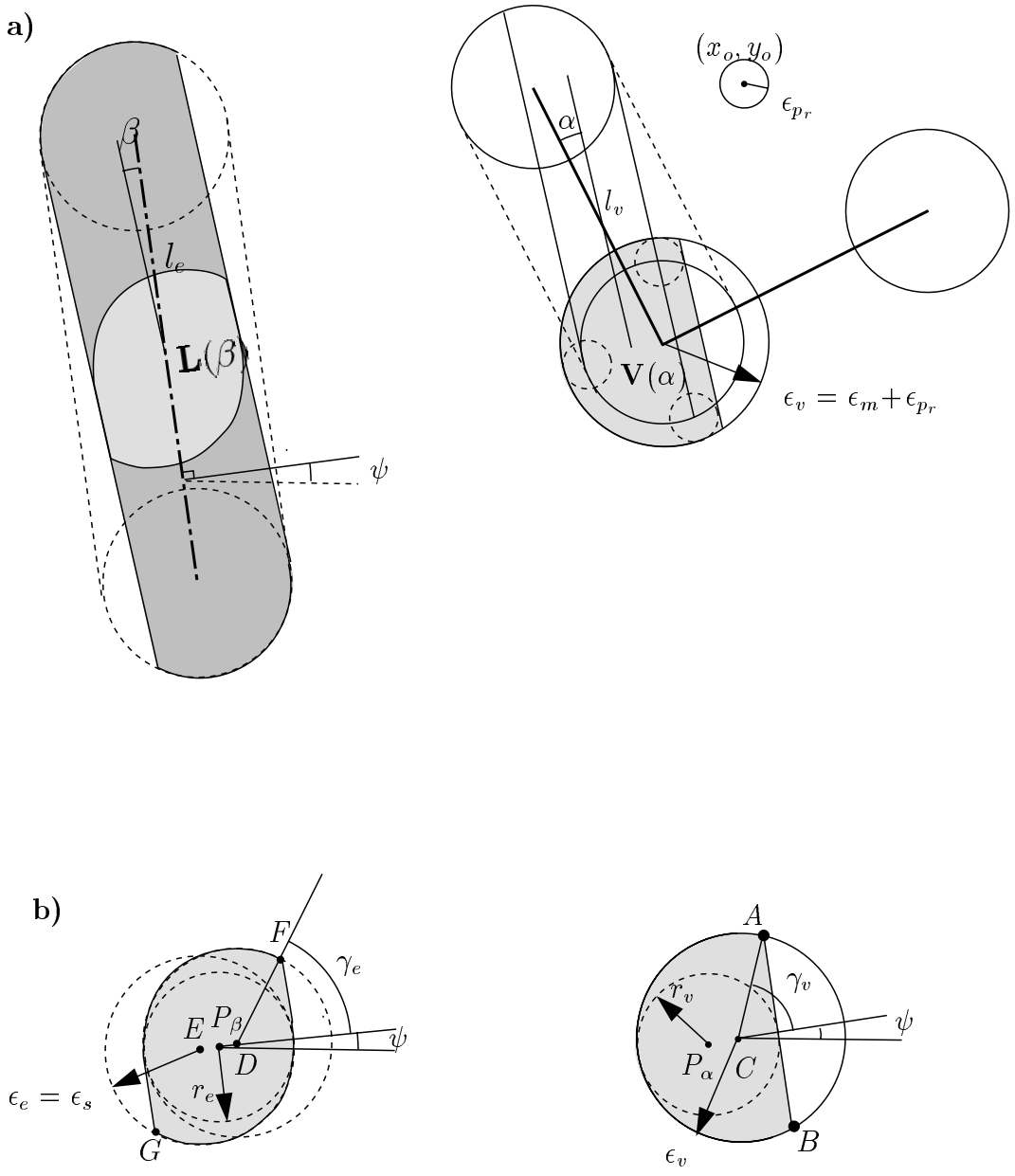

Figure 3.14: *a) Region* $\mathbf{L}(\beta)$ *and* $\mathbf{V}(\alpha)$*, where the uncertainty* ϵ_{p_r} *in the position of the robot is taken into account in* ϵ_v*, since it is a type-B basic contact b) Regions* $\mathbf{L}(\beta)$ *and* $\mathbf{V}(\alpha)$ *rotated* $-\beta$ *around the respective centers.*

$$D = ((\epsilon_e - r_e)\cos\psi, (\epsilon_e - r_e)\sin\psi)$$
$$E = (-(\epsilon_e - r_e)\cos\psi, -(\epsilon_e - r_e)\sin\psi)$$
$$F = (D_x + \epsilon_e\cos(\gamma_e + \psi), D_y + \epsilon_e\sin(\gamma_e + \psi))$$
$$G = (E_x + \epsilon_e\cos(\pi + \gamma_e + \psi), E_y + \epsilon_e\sin(\pi + \gamma_e + \psi))$$

- Region $\mathbf{V}(\alpha)$ is described by the following variables:

  l_v: length of the edge adjacent to the contact vertex

  $r_v = \epsilon_v - (l_v/2)|\sin(-\alpha)|$, radius of the maximum inscribed circumference.

  $\gamma_v = \arccos((2r_v - \epsilon_v)/\epsilon_v)$

  and the following points with respect of the center, P_α, once $\mathbf{L}(\beta)$ has been rotated an angle $-\beta$ around it:

  $$C = ((\epsilon_v - r_v)\cos\psi, (\epsilon_v - r_v)\sin\psi)$$
  $$A = (C_x + \epsilon_v\cos(\gamma_v + \psi), C_y + \epsilon_v\sin(\gamma_v + \psi))$$
  $$B = (C_x + \epsilon_v\cos(-\gamma_v + \psi), C_y + \epsilon_v\sin(-\gamma_v + \psi))$$

Then, the border of $\mathbf{U}^i(\alpha, \beta)$ is composed of the following arcs (Figure 3.15a), described with respect to its center P_o:

arc *a*: center: $C'_a = A + D$
$C''_a = F + C$
if $\overrightarrow{C_bC'_a} \times \overrightarrow{C_bC''_a} < 0$ then $C_a = C'_a$ else $C_a = C''_a$
radius: $R_a = \epsilon_e$ if $C_a = C'_a$ else $R_a = \epsilon_v$
limits: $[\gamma_e + \psi, \quad \arctan(C_b - C_a) + \psi]$

arc *b*: center: $C_b = E + C$
radius: $R_b = \epsilon_e + \epsilon_v$
limits: $[\arctan(C_b - C_a) + \psi, \quad \pi + \psi]$

arc *c*: center: $C_c = G + C$
radius: $R_c = \epsilon_v$
limits: $[\pi + \psi, \quad \arctan(C_d - C_c) + \psi]$

arc *d*: center: $C_d = E + C$
radius: $R_d = \epsilon_e + \epsilon_v$
limits: $[\arctan(C_d - C_c) + \psi, \quad \arctan(C_d - C_e) + \psi]$
The arc does not exist if $\overrightarrow{C_dC_c} \times \overrightarrow{C_dC_e} < 0$

arc *e*: center: $C_e = B + E$
radius: $R_e = \epsilon_e$
limits: $[\arctan(C_d - C_e) + \psi, \quad 2\pi + \psi]$

Figure 3.16 shows the obtained region $\mathbf{U}^i(\alpha, \beta)$ for two different pairs of values of α and β.

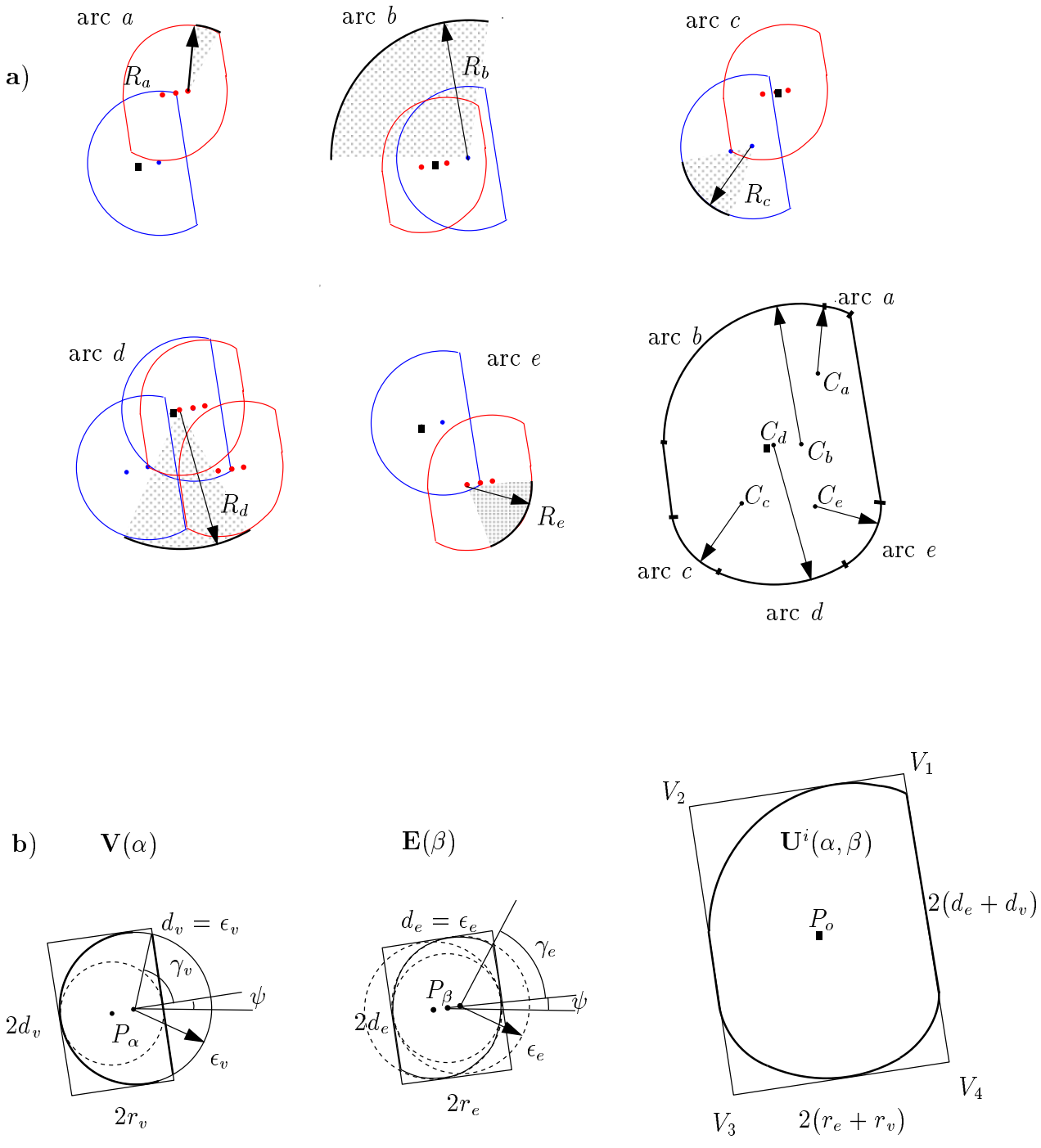

Figure 3.15: *a) Arcs that compose the border of* $\mathbf{U}^i(\alpha,\beta)$ *b) Bounding box* $Box(\mathbf{U}^i(\alpha,\beta))$ *that approximates* $\mathbf{U}^i(\alpha,\beta)$.

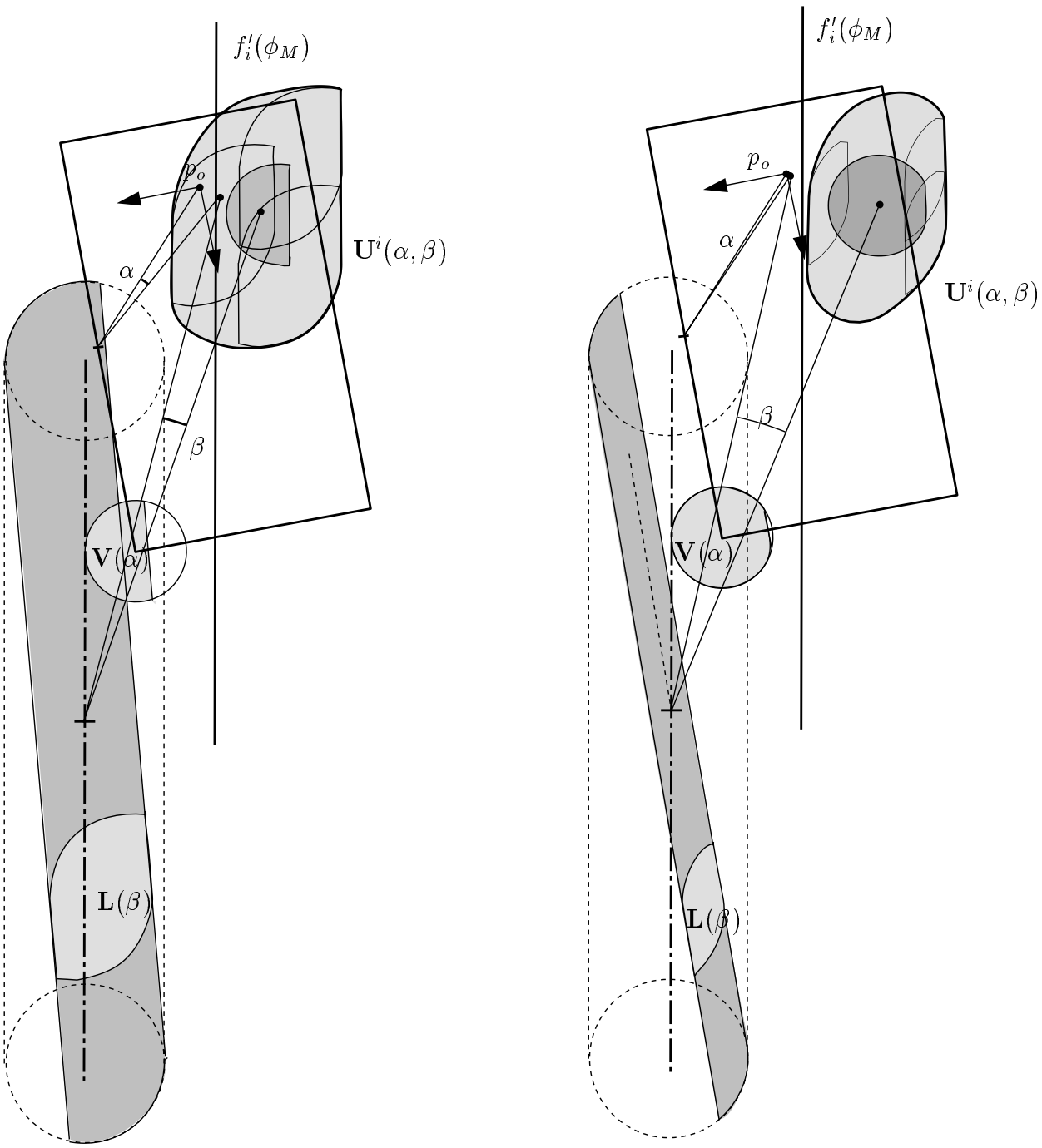

Figure 3.16: *Contact Position Region* $\mathbf{U}^i(\alpha,\beta)$ *when* $\phi_o^i > \phi_M$, *for two different pair of values* (α,β).

Bounding box

In order to simplify the contact identification algorithm (Section 3.3.6), an oriented bounding box $Box(\mathbf{U}^i(\alpha,\beta))$ is computed. The sides of the oriented bounding box are:

$$r = 2(r_e + r_v) = \epsilon_e - (l_e/2)|\sin\beta| \; + \; \epsilon_v - (l_v/2)|\sin(-\alpha)| \tag{3.57}$$

and

$$d = 2(d_e + d_v) \tag{3.58}$$

where d_e and d_v are defined as follows:

$$d_e = \begin{cases} \epsilon_e \sin\gamma_e & \text{if} \quad r_e < \epsilon_e/2 \\ \epsilon_e & \text{otherwise} \end{cases} \tag{3.59}$$

$$d_v = \begin{cases} \epsilon_v \sin\gamma_v & \text{if} \quad r_v < \epsilon_v/2 \\ \epsilon_v & \text{otherwise} \end{cases} \tag{3.60}$$

The vertices of $Box(\mathbf{U}^i(\alpha,\beta))$ with respect to P_o are (Figure 3.15b):

$$\begin{aligned} V_1 &= (-d\sin\psi + r\cos\psi, d\cos\psi + r\sin\psi) \\ V_2 &= (-d\sin\psi - r\cos\psi, d\cos\psi - r\sin\psi) \\ V_3 &= (d\sin\psi - r\cos\psi, -d\cos\psi - r\sin\psi) \\ V_4 &= (d\sin\psi + r\cos\psi, -d\cos\psi + r\sin\psi) \end{aligned} \tag{3.61}$$

In the worst case the area of $Box(\mathbf{U}^i(\alpha,\beta))$ is a 27% bigger than the area of $\mathbf{U}^i(\alpha,\beta)$. This can be shown by computing the areas when $\alpha = \beta = 0$, since for these values the difference is maximum. $\mathbf{U}^i(0,0)$ is a circle of radius $(\epsilon_v + \epsilon_e)$ and the corresponding bounding box is a square of sides $2(\epsilon_v + \epsilon_e)$. Let A_U and A_B be the areas of $\mathbf{U}^i(\alpha,\beta)$ and of $Box(\mathbf{U}^i(\alpha,\beta))$, respectively:

$$\begin{aligned} A_U &= \pi(\epsilon_v + \epsilon_e)^2 \\ A_B &= 4(\epsilon_v + \epsilon_e)^2 \end{aligned} \tag{3.62}$$

Then:

$$\frac{A_B - A_U}{A_U} = 27\% \tag{3.63}$$

Let D_{rm} and D_{rM} be the distances from the origin of $\{W\}$ to the sides of $Box(\mathbf{U}^i(\alpha,\beta))$ that are parallel to the contact edge, and D_{dm} and D_{dM} be the distances from the origin of $\{W\}$ to the sides of $Box(\mathbf{U}^i(\alpha,\beta))$ that are perpendicular to the contact edge:

$$\begin{aligned} D_{rm} &= P_{ox}\cos(\psi) + P_{oy}\sin(\psi) - r \\ D_{rM} &= P_{ox}\cos(\psi) + P_{oy}\sin(\psi) + r \\ D_{dm} &= P_{ox}\cos(\psi + \pi/2) + P_{oy}\sin(\psi + \pi/2) - d \\ D_{dM} &= P_{ox}\cos(\psi + \pi/2) + P_{oy}\sin(\psi + \pi/2) + d \end{aligned} \tag{3.64}$$

where (P_{ox}, P_{oy}) is the center of $\mathbf{U}^i(\alpha,\beta)$ defined in (3.56). These distances will be used to compute the bounding box of the Contact Position Domain.

3.3.5 Construction of the Contact Position Domain

The Contact Position Domain:

a) Is a circle of radius $(\epsilon_e + \epsilon_v + \epsilon_{p_r})$ centered at the observed position (Figure 3.13) when $\phi_o^i \in R_\phi^i$, since $\Delta_\phi^i = 0$.

b) Can be represented, when $\phi_o^i \notin R_\phi^i$, as the union of only a finite set of Contact Position Regions, in order to avoid the complexity of finding the border of the union of all the Contact Position Regions satisfying $\beta - \alpha = \Delta_\phi^i$ (equation (3.42)). The number of Contact Position Regions considered is such that the deviation in orientation between them is an order of magnitude less than the error in the orientation of the robot, i.e. $|\beta_i - \beta_{i+1}| < \epsilon_{\phi_r}/10$.

The algorithm to compute the Contact Position Domain is the following:

$\mathbf{U}^i(\Delta_\phi^i)$-construction($c_o$)

IF $\phi_o^i \in R_\phi^i$ THEN $\mathbf{U}^i(\alpha, \beta) = \mathbf{C}(x_o, y_o, \epsilon_e + \epsilon_v)$.

ELSE

Compute α_{max} and β_{max}, the maximum possible values of α and β from (3.14)

$\alpha_{min} = |\Delta_\phi^i| - \beta_{max}$

$\beta_{min} = |\Delta_\phi^i| - \alpha_{max}$

$\Delta_\alpha = \alpha_{max} - \alpha_{min}$

$\Delta_\beta = \beta_{max} - \beta_{min}$

$\delta = \epsilon_{\phi_r}/10$

$n = \mathrm{TRUNC}(\frac{\min(|\Delta_\phi^i|, \Delta_\alpha, \Delta_\beta)}{\delta} + 1)$

$\mathbf{U}^i(\Delta_\phi^i) = \emptyset$

FOR k=1 TO n

$\alpha_k = \alpha_{min} + k\Delta_\alpha/(n-1)$

$\beta_k = \Delta_\phi^i + \alpha$

$\mathbf{U}^i(\Delta_\phi^i) = \mathbf{U}^i(\Delta_\phi^i) \cup \mathbf{U}^i(\alpha_k, \beta_k)$

END

Figure 3.17 shows the approximation of $\mathbf{U}^i(\Delta_\phi^i)$ for three different orientations satisfying $\phi_o^i < \phi_m^i$.

Bounding box

An oriented bounding box, $Box(\mathbf{U}^i(\Delta_\phi^i))$, can also be computed for $\mathbf{U}^i(\Delta_\phi^i)$ in order to simplify the contact identification algorithm. The sides of $Box(\mathbf{U}^i(\Delta_\phi^i))$ are computed by finding the boxes $Box(\mathbf{U}^i(\alpha, \beta))$ whose sides are at a maximum or minimum distance

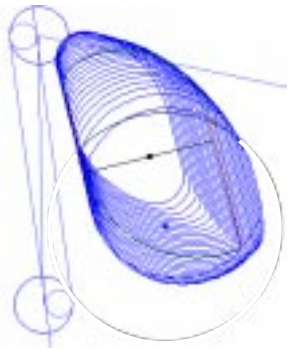

$n = 25$
$\Delta_\phi = 0.2269$
$\Delta_\alpha = 0.2139$
$\Delta_\beta = 0.2819$

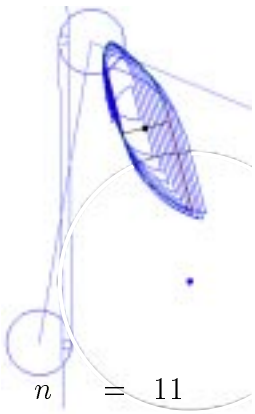

$n = 11$
$\Delta_\phi = 0.4161$
$\Delta_\alpha = 0.0927$
$\Delta_\beta = 0.0927$

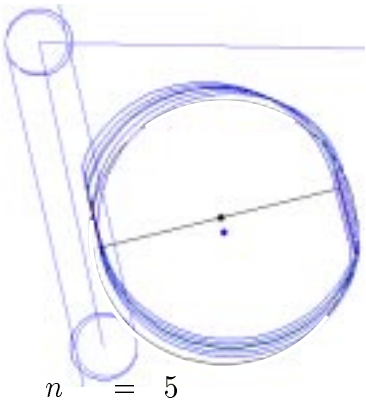

$n = 5$
$\Delta_\phi = 0.0377$
$\Delta_\alpha = 0.2136$
$\Delta_\beta = 0.2953$

Figure 3.17: *Approximation of* $\mathbf{U}^i(\Delta^i_\phi)$ *by the reunion of* $\mathbf{U}^i(\alpha,\beta)$ *for a finite set of pairs* (α,β)*, for three different orientations satisfying* $\phi^i_o < \phi^i_m$.

from the origin of $\{W\}$. Let:

- β_{rm} be the value of β such that D_{rm} is minimum
- β_{rM} be the value of β such that D_{rM} is maximum
- β_{dm} be the value of β such that D_{dm} is minimum
- β_{dM} be the value of β such that D_{dM} is maximum

where D_{rm}, D_{rM}, D_{dm} and D_{dM} where defined in (3.64). To compute these values of β, the derivates with respect to β of the distances expressed in (3.64) must be computed. Taking into account that:

- (x_e, y_e) is the center of the contact edge
- (x_v, y_v) is the center of the adjacent edge of the contact vertex used to compute the center P_o of $\mathbf{U}^i(\Delta^i_\phi)$
- P_o is expressed in equation (3.56)
- r is expressed in equation (3.57)
- $\text{sign}(\beta) = \frac{|\beta|}{\beta}$ if $\beta \neq 0$ and $\text{sign}(\beta) = 1$ otherwise
- α can be expressed as $\alpha = \beta - \Delta^i_\phi$
- the value of d expressed in (3.58) is approximated by $d = \epsilon_e + \epsilon_v$

then, the expressions of the derivates are the following:

$$\frac{\partial D_{rm}}{\partial \beta} = (y_v - y_e)\cos(\psi+\beta) - (x_v - x_e)\sin(\psi+\beta) + \text{sign}(\beta)(\frac{l_e}{2}\cos(\beta) - \frac{l_e}{2}\sin(\beta - \Delta^i_\phi)) \quad (3.65)$$

$$\frac{\partial D_{rM}}{\partial \beta} = (y_v - y_e)\cos(\psi+\beta) - (x_v - x_e)\sin(\psi+\beta) - \text{sign}(\beta)(\frac{l_e}{2}\cos(\beta) + \frac{l_e}{2}\sin(\beta - \Delta^i_\phi)) \quad (3.66)$$

$$\frac{\partial D_{dm}}{\partial \beta} = -(y_v - y_e)\sin(\psi+\beta) - (x_v - x_e)\cos(\psi+\beta) \quad (3.67)$$

$$\frac{\partial D_{dM}}{\partial \beta} = \frac{\partial D_{dm}}{\partial \beta} \quad (3.68)$$

Let D' be $\frac{\partial D}{\partial \beta}$, and let β_m and β_M be the minimum and maximum possible values of β for a given Δ^i_ϕ:

$$\text{if } \Delta^i_\phi \geq 0 \quad \begin{cases} \beta_M = \begin{cases} \Delta^i_\phi & \text{if } \beta_{max} > \Delta^i_\phi \\ \beta_{max} & \text{otherwise} \end{cases} \\ \beta_m = \begin{cases} 0 & \text{if } \alpha_{max} > \Delta^i_\phi \\ \Delta^i_\phi - \alpha_{max} & \text{otherwise} \end{cases} \end{cases}$$

$$\text{if } \Delta^i_\phi < 0 \quad \begin{cases} \beta_M = \begin{cases} 0 & \text{if } \alpha_{max} > -\Delta^i_\phi \\ \Delta^i_\phi + \alpha_{max} & \text{otherwise} \end{cases} \\ \beta_m = \begin{cases} \Delta^i_\phi & \text{if } \beta_{max} > -\Delta^i_\phi \\ -\beta_{max} & \text{otherwise} \end{cases} \end{cases}$$

where β_{max} and α_{max} are the maximum values of $|\beta|$ and $|\alpha|$, respectively, as computed in proposition 1 and corollary 4.3.

Then, the expressions of β_{rm}, β_{rM}, β_{dm} and β_{dM} are equal to:

- β_m or β_M when the derivates of the distances evaluated at these extreme values have the same sign,
- the value that satisfies $D' = 0$, otherwise.

$$\beta_{rm} = \begin{cases} \beta_m \text{ if } D'_{rm}(\beta_m) > 0 \text{ and } D'_{rm}(\beta_M) > 0 \\ \beta_M \text{ if } D'_{rm}(\beta_m) < 0 \text{ and } D'_{rm}(\beta_M) < 0 \\ \arctan(\frac{2(y_v-y_e)\cos(\psi) - 2(x_v-x_e)\sin(\psi) + \text{sign}(\beta)(l_e - l_v\sin(\Delta^i_\phi))}{2(y_v-y_e)\sin(\psi) + 2(x_v-x_e)\cos(\psi) + \text{sign}(\beta) l_v \sin(\Delta^i_\phi)}) \text{ , otherwise} \end{cases} \quad (3.69)$$

$$\beta_{rM} = \begin{cases} \beta_M \text{ if } D'_{rM}(\beta_m) > 0 \text{ and } D'_{rM}(\beta_M) > 0 \\ \beta_m \text{ if } D'_{rM}(\beta_m) < 0 \text{ and } D'_{rM}(\beta_M) < 0 \\ \arctan(\frac{2(y_v-y_e)\cos(\psi) - 2(x_v-x_e)\sin(\psi) - \text{sign}(\beta)(l_e - l_v\sin(\Delta^i_\phi))}{2(y_v-y_e)\sin(\psi) + 2(x_v-x_e)\cos(\psi) - \text{sign}(\beta) l_v \sin(\Delta^i_\phi)}) \text{ , otherwise} \end{cases} \quad (3.70)$$

$$\beta_{dm} = \begin{cases} \beta_M \text{ if } D'_{dm}(\beta_m) > 0 \text{ and } D'_{dm}(\beta_M) > 0 \\ \beta_m \text{ if } D'_{dm}(\beta_m) < 0 \text{ and } D'_{dm}(\beta_M) < 0 \\ -\psi - \arctan(\frac{x_v - x_e}{y_v - y_e}) \text{ , otherwise} \end{cases} \quad (3.71)$$

$$\beta_{dM} = \begin{cases} \beta_m \text{ if } D'_{dM}(\beta_m) > 0 \text{ and } D'_{dM}(\beta_M) > 0 \\ \beta_M \text{ if } D'_{dM}(\beta_m) < 0 \text{ and } D'_{dM}(\beta_M) < 0 \\ -\psi - \arctan(\frac{x_v - x_e}{y_v - y_e}) \text{ , otherwise} \end{cases} \quad (3.72)$$

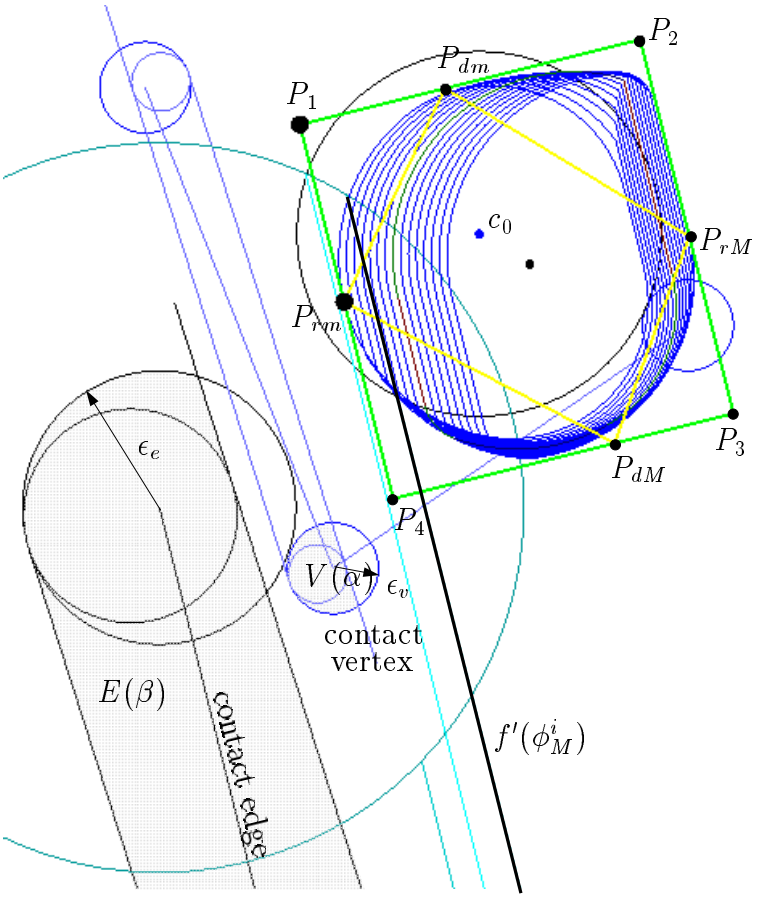

Figure 3.18: $Box(\mathbf{U}^i(\Delta_\phi^i))$.

Once these values of β have been obtained, the lines that contain the sides of $Box(\mathbf{U}^i(\Delta_\phi^i))$ can be expressed as:

$$x\cos(\psi) + y\sin\psi = x_{rm}\cos\psi + y_{rm}\sin\psi \quad (3.73)$$

$$x\cos(\psi) + y\sin\psi = x_{rM}\cos\psi + y_{rM}\sin\psi \quad (3.74)$$

$$x\cos(\psi+\pi/2) + y\sin(\psi+\pi/2) = x_{dm}\cos(\psi+\pi/2) + y_{dm}\sin(\psi+\pi/2) \quad (3.75)$$

$$x\cos(\psi+\pi/2) + y\sin(\psi+\pi/2) = x_{dM}\cos(\psi+\pi/2) + y_{dM}\sin(\psi+\pi/2) \quad (3.76)$$

where (Figure 3.18):

$$P_{rm} = (x_{rm}, y_{rm}) \begin{cases} x_{rm} = P_{ox}(\beta_{rm}) - r(\beta_{rm})\cos\psi \\ y_{rm} = P_{oy}(\beta_{rm}) - r(\beta_{rm})\sin\psi \end{cases} \quad (3.77)$$

$$P_{rM} = (x_{rM}, y_{rM}) \begin{cases} x_{rM} = P_{ox}(\beta_{rM}) + r(\beta_{rM})\cos\psi \\ y_{rM} = P_{oy}(\beta_{rM}) + r(\beta_{rM})\sin\psi \end{cases} \quad (3.78)$$

$$P_{dm} = (x_{dm}, y_{dm}) \begin{cases} x_{dm} = P_{ox}(\beta_{rm}) - d\cos(\psi+\pi/2) \\ y_{dm} = P_{oy}(\beta_{rm}) - d\sin(\psi+\pi/2) \end{cases} \quad (3.79)$$

$$P_{dM} = (x_{dM}, y_{dM}) \begin{cases} x_{dM} = P_{ox}(\beta_{rM}) + d\cos(\psi+\pi/2) \\ y_{dM} = P_{oy}(\beta_{rM}) + d\sin(\psi+\pi/2) \end{cases} \quad (3.80)$$

Finally, the vertices of $Box(\mathbf{U}^i(\Delta^i_\phi))$ can be obtained by projecting in the direction of ψ the points P_{dm} and P_{dM} into the lines that contain P_{rm} and P_{rM}. Let define:

$$d_1 = (x_{dm} - x_{rm}, y_{dm} - y_{rm}) \cdot (\cos(\psi + \pi/2), \sin(\psi + \pi/2)) \quad (3.81)$$
$$d_2 = (x_{dm} - x_{rM}, y_{dm} - y_{rM}) \cdot (\cos(\psi + \pi/2), \sin(\psi + \pi/2)) \quad (3.82)$$
$$d_3 = (x_{dM} - x_{rM}, y_{dM} - y_{rM}) \cdot (\cos(\psi + \pi/2), \sin(\psi + \pi/2)) \quad (3.83)$$
$$d_4 = (x_{dM} - x_{rm}, y_{dM} - y_{rm}) \cdot (\cos(\psi + \pi/2), \sin(\psi + \pi/2)) \quad (3.84)$$

Then, the vertices of $Box(\mathbf{U}^i(\Delta^i_\phi))$ are (Figure 3.18):

$$P_1 = (x_1, y_1) \begin{cases} x_1 = x_{rm} + d_1 \cos(\psi + \pi/2) \\ y_1 = y_{rm} + d_1 \sin(\psi + \pi/2) \end{cases} \quad (3.85)$$
$$P_2 = (x_2, y_2) \begin{cases} x_2 = x_{rM} + d_2 \cos(\psi + \pi/2) \\ y_2 = y_{rM} + d_2 \sin(\psi + \pi/2) \end{cases} \quad (3.86)$$
$$P_3 = (x_3, y_3) \begin{cases} x_3 = x_{rM} + d_3 \cos(\psi + \pi/2) \\ y_3 = y_{rM} + d_3 \sin(\psi + \pi/2) \end{cases} \quad (3.87)$$
$$P_4 = (x_4, y_4) \begin{cases} x_4 = x_{rm} + d_4 \cos(\psi + \pi/2) \\ y_4 = y_{rm} + d_4 \sin(\psi + \pi/2) \end{cases} \quad (3.88)$$

3.3.6 Contact identification

In the presence of uncertainty, a given observed configuration $c_o = (x_o, y_o, \phi_o)$ is a contact configuration of a basic contact i if equation (3.43) is satisfied:

$$\mathbf{U}^i(\Delta^i_\phi) \cap f'_i(\phi^i_t) \neq \emptyset$$

The algorithm Contact-Identification(c_o, $\mathbf{U}^i(\Delta^i_\phi)$) to test equation (3.43) uses the algorithm Contact-Identification(c_o, $\mathbf{U}^i(\alpha, \beta)$) that tests if equation (3.39) is satisfied for any given possible pair of values α and β:

$$\mathbf{U}^i(\alpha, \beta) \cap f'_i(\phi^i_t) \neq \emptyset$$

The algorithms are the following:

Contact-Identification(c_o, $\mathbf{U}^i(\Delta^i_\phi)$)

(1) IF $\phi^i_o \in R^i_\phi$ THEN

(1.1) IF $\mathbf{C}(x_o, y_o, \epsilon_e + \epsilon_v) \cap f'(\phi^i_o) \neq \emptyset$ RETURN TRUE

(1.2) ELSE RETURN FALSE

(2) ELSE

(2.1) IF $Box(\mathbf{U}^i(\Delta^i_\phi)) \cap f'(\phi^i_t) = \emptyset$ RETURN FALSE

(2.2) FOR k=1 TO n

r = Contact-Identification(c_o, $\mathbf{U}^i(\alpha_k, \beta_k)$)

IF r = TRUE THEN RETURN TRUE

(2.3) RETURN FALSE

END

Contact-Identification(c_o, $\mathbf{U}^i(\alpha, \beta)$)

(1) IF $Box(\mathbf{U}^i(\alpha, \beta)) \cap f'(\phi^i_t) = \emptyset$ RETURN FALSE

(2) IF the perpendicular projection of the center of $\mathbf{U}^i(\alpha, \beta)$ into the line containing $f'(\phi^i_t)$ belongs to $f'(\phi^i_t)$ THEN RETURN TRUE

(3) ELSE

(3.1) IF $f'(\phi^i_t)$ intersects any of the arcs of $\mathbf{U}^i(\alpha, \beta)$ RETURN TRUE

(3.2) ELSE RETURN FALSE

END

As an example Figure 3.19 shows:

a) An edge of an static object and a vertex of a manipulated object (with its adjacent edges) which can produce a type-B basic contact.

b) A situation where the observed configuration may correspond to a contact configuration, since $\mathbf{U}^i(\Delta^i_\phi) \cap f'_i(\phi^i_t) \neq \emptyset$ and hence $\mathbf{E}(\beta) \cap \mathbf{V}(\alpha) \neq \emptyset$, (where $\beta = \alpha = 0$ since $\phi^i_o \in R^i_\phi$).

c) A situation where the observed configuration may not correspond to a contact configuration, since $\mathbf{U}^i(\alpha_1, \beta_1) \cap f'_i(\phi^i_t) = \emptyset$ and hence $\mathbf{E}(\beta_1) \cap \mathbf{V}(\alpha_1) = \emptyset$ (where $\beta_1 - \alpha_1 = \phi^i_o - \phi_M$, since $\phi^i_o \notin R^i_\phi$).

d) The previous situation for different values of the deviations. Since $\mathbf{U}^i(\alpha_2, \beta_2) \cap f'_i(\phi^i_t) \neq \emptyset$ and hence $\mathbf{E}(\beta_2) \cap \mathbf{V}(\alpha_2) \neq \emptyset$, for these deviations the contact is possible. Therefore the observed configuration is considered a possible contact configuration.

The same is illustrated in Figure 3.20 for a type-A basic contact.

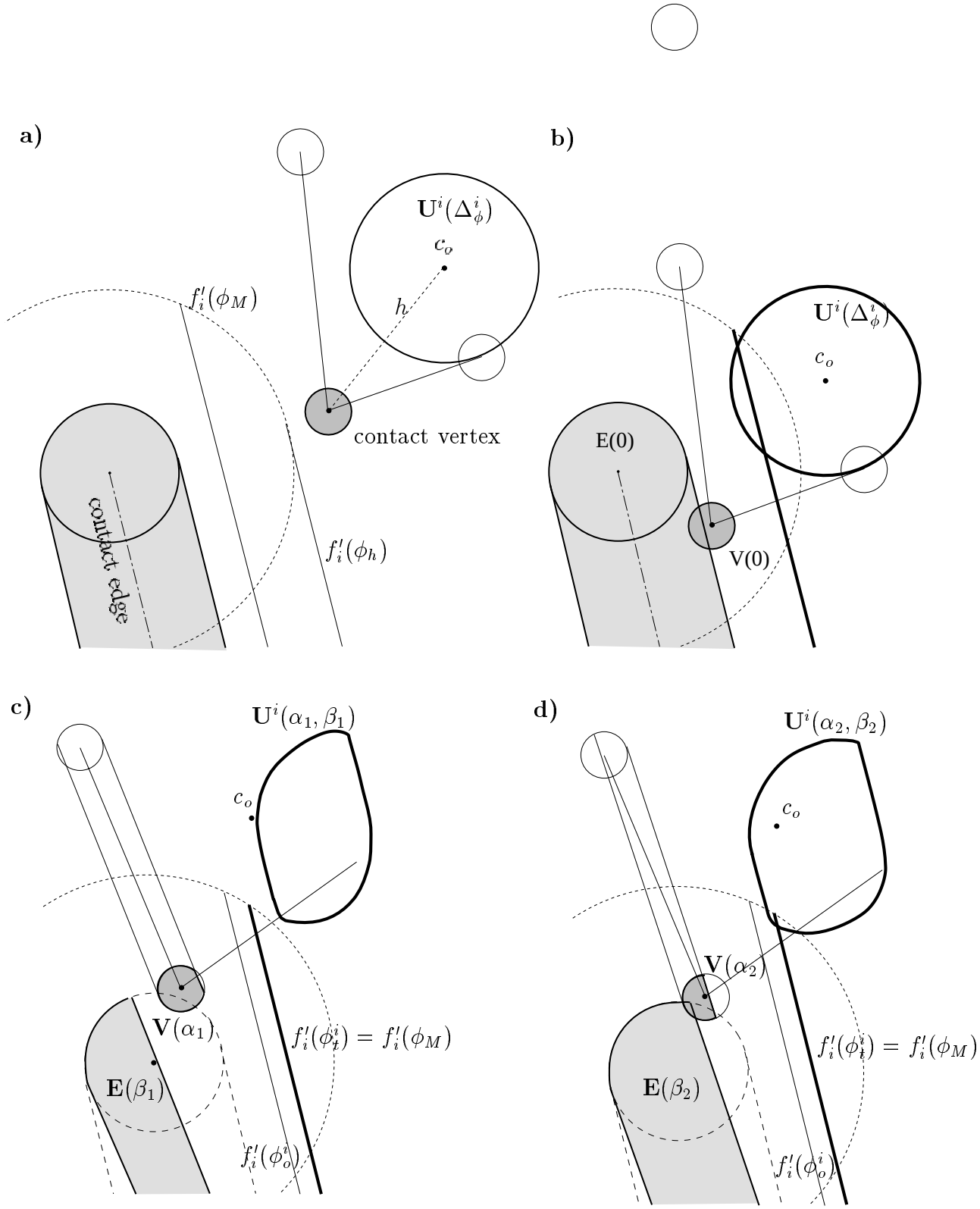

Figure 3.19: *Contact identification of a type-B basic contact.*

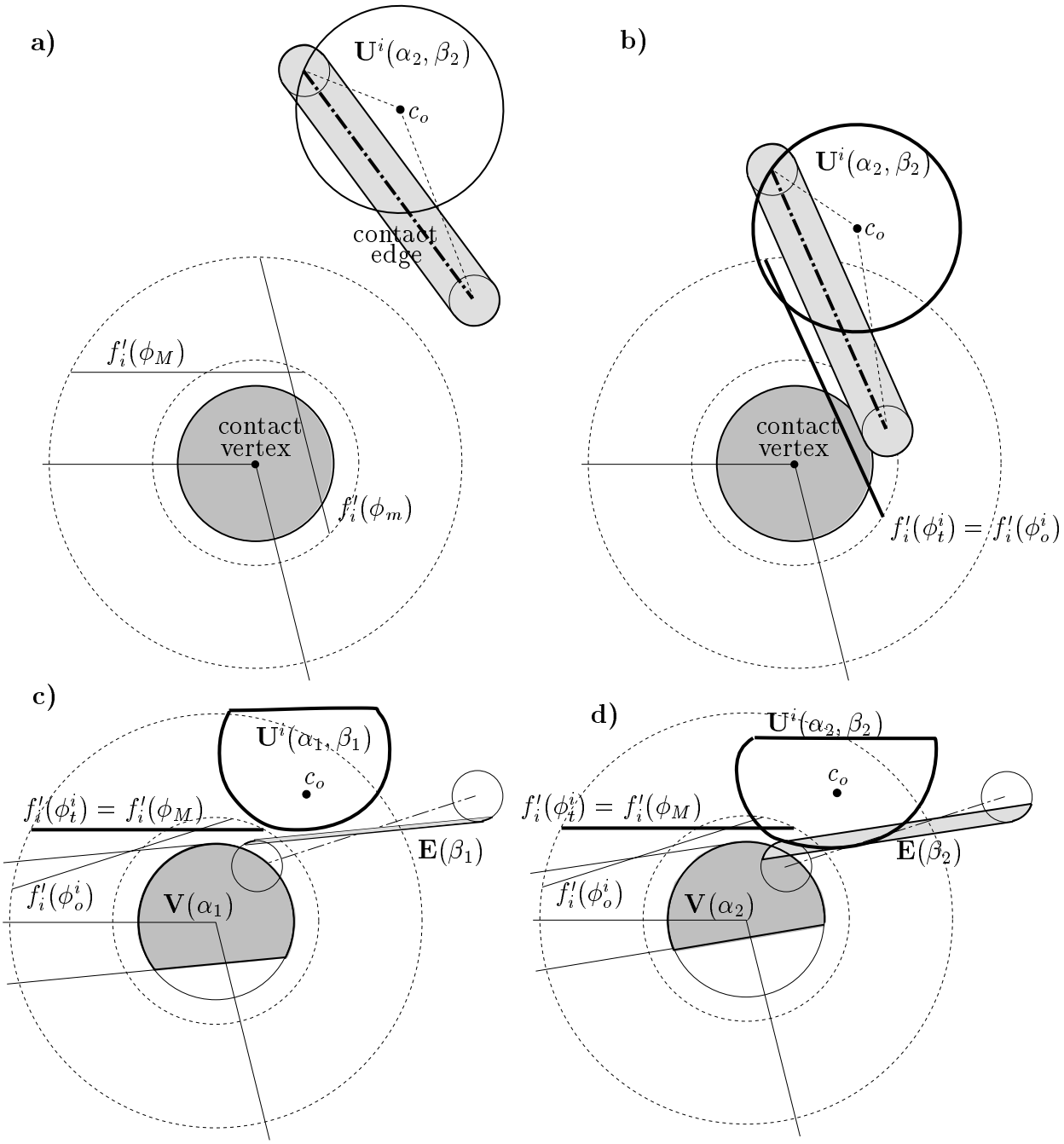

Figure 3.20: *Contact identification of a type-A basic contact.*

Simplified contact identification algorithm

A simplified contact identification procedure can be used, which only takes into account the bounding boxes. This results in:

- A faster test (since the test with the arcs of circumferences is avoided).
- The possible occurrence of false positives (i.e. the identification of a contact for a configuration where the contact is not possible).

The algorithm is as follows:

Simplified-Contact-Identification(c_o, $\mathbf{U}^i(\Delta^i_\phi)$)
(1) IF $\phi^i_o \in R^i_\phi$ THEN
  (1.1) IF $\mathbf{C}(x_o, y_o, \epsilon_e + \epsilon_v) \cap f'(\phi^i_o) \neq \emptyset$ RETURN TRUE
  (1.2) ELSE RETURN FALSE
(2) ELSE
  (2.1) IF $Box(\mathbf{U}^i(\Delta^i_\phi)) \cap f'(\phi^i_t) = \emptyset$ RETURN FALSE
  (2.2) FOR k=1 TO n
    IF $Box(\mathbf{U}^i(\alpha_k, \beta_k)) \cap f'(\phi^i_t) \neq \emptyset$ RETURN TRUE
  (2.3) RETURN FALSE
END

3.4 More than one basic contact situations

Let:

$c_o = (x_o, y_o, \phi_o)$: be the observed configuration.

S: be a set of basic contacts.

C_S: be the nominal contact situation involving the basic contacts of S.

Proposition 10: *There exists an orientation $\phi^S_o \in [\phi_{o_m}, \phi_{o_M}]$ such that c_o is compatible with the occurrence of contact situation C_S iff C_S can take place at ϕ^S_o.*

Proof: Let $d_e(\phi)$ be the distance from the observed position (x_o, y_o) to the closest nominal contact position of C_S corresponding to orientation ϕ. Let ϕ^S_o be an orientation of the range $[\phi_{om}, \phi_{oM}]$ such that d_e is minimum. Then:

- If the contact can take place at orientation ϕ^S_o then c_o is compatible with the occurrence of contact situation C_S, since $\phi^S_o \in [\phi_{o_m}, \phi_{o_M}]$.
- If c_o is compatible with the occurrence of contact situation C_S, then the contact can take place at orientation ϕ^S_o, since for this orientation takes place the minimum possible distance between the observed position and a nominal contact position. $\diamond$

The orientation ϕ_o^S is computed as follows:

- If C_S only involves one basic contact i then $\phi_o^S = \phi_o^i$, where ϕ_o^i is obtained by using the algorithm Find-orientation(c_o, i) of Section 3.3.3.
- Otherwise, if $[\phi_{om}, \phi_{oM}] \cap R_\phi^S = \emptyset$, then ϕ_o^S is the extreme of $[\phi_{om}, \phi_{oM}]$ closest to R_ϕ^S.
- Otherwise, if C_S involves two basic contacts and R_ϕ^{ij} is a unique orientation $\phi_e \in [\phi_{om}, \phi_{oM}]$, then $\phi_o^S = \phi_e$.
- Otherwise, if C_S involves more than two basic contacts and $\phi_v \in [\phi_{om}, \phi_{oM}]$ is the orientation of the nominal $\mathcal{C}$-vertex, then $\phi_o^S = \phi_v$.
- Otherwise, ϕ_o^S is computed as follows. Let $(e_x(\phi), e_y(\phi))$ be the position of the $\mathcal{C}'$-edge for a given orientation ϕ, $(e'_x(\phi), e'_y(\phi))$ its derivate, and $(t_x(\phi), t_y(\phi))$ be the unitary vector in the direction $(e'_x(\phi), e'_y(\phi))$, i.e. in the direction of the tangent to the $\mathcal{C}'$-edge at a given orientation ϕ. Let also define the following vectors (Figure 3.21):

$$\vec{v}_m = (e_x(\phi_{om}) - x_o, e_y(\phi_{om}) - y_o) \quad (3.89)$$
$$\vec{v}_M = (e_x(\phi_{oM}) - x_o, e_y(\phi_{oM}) - y_o) \quad (3.90)$$
$$\vec{w}_e = (e_x(\phi_{oM}) - e_x(\phi_{om}), e_y(\phi_{oM}) - e_y(\phi_{om})) \quad (3.91)$$
$$\vec{v}_e = \frac{\vec{w}_e}{|\vec{w}_e|} \quad (3.92)$$

The distance $d_e(\phi)$ is:

$$d_e(\phi) = \sqrt{(e_x(\phi) - x_o)^2 + (e_y(\phi) - y_o)^2} \quad (3.93)$$

And its derivate is:

$$d'_e(\phi) = \frac{(e_x(\phi) - x_o)e'_x(\phi) + (e_x(\phi) - x_o)e'_y(\phi)}{d_e(\phi)} \quad (3.94)$$

The minimum of d_e occurs:

- At one of the extremes of $[\phi_{om}, \phi_{oM}]$ if $d'_e(\phi_{om})$ and $d'_e(\phi_{oM})$ have the same sign. The sign of $d'_e(\phi)$ is the same as the sign of the following scalar product:

$$(e_x(\phi) - x_o, e_y(\phi) - y_o) \cdot (t_x(\phi), t_y(\phi)) \quad (3.95)$$

If the range $[\phi_{om}, \phi_{oM}]$ is small, then $(t_x(\phi_{om}), t_y(\phi_{om}))$ and $(t_x(\phi_{oM}), t_y(\phi_{oM}))$ can both be approximated by $\vec{v}_e$. Therefore, the sign of $d'_e(\phi_{om})$ and $d'_e(\phi_{oM})$ can be determined as the sign of $\vec{v}_m \cdot \vec{v}_e$ and $\vec{v}_M \cdot \vec{v}_e$, respectively. If both signs are negative it means that the minimum of d_e occurs for the maximum

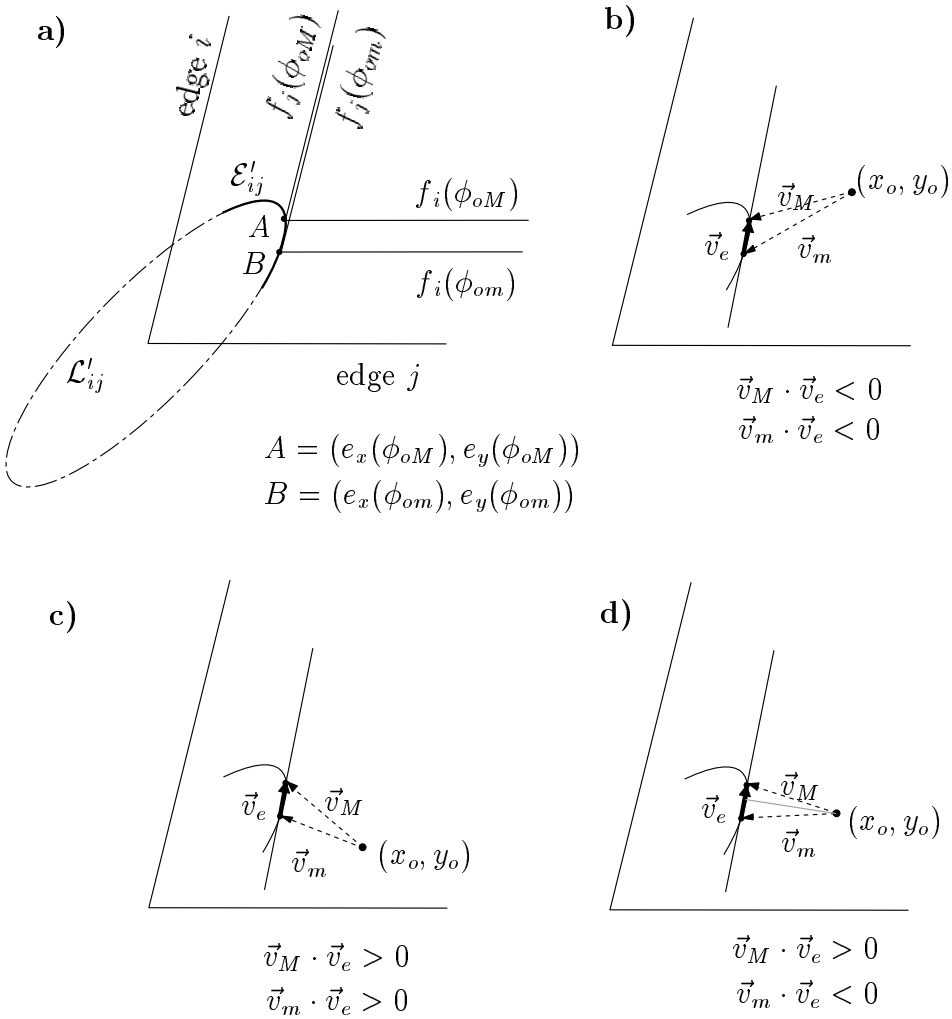

Figure 3.21: *a) $\mathcal{C}'$-edge of a contact situation involving two type-B basic contacts, b) An example where $\phi_o^S = \phi_{oM}$, since for the given observed position $\vec{v}_M \cdot \vec{v}_e < 0$ and $\vec{v}_m \cdot \vec{v}_e < 0$, c) An example where $\phi_o^S = \phi_{om}$, since $\vec{v}_M \cdot \vec{v}_e > 0$ and $\vec{v}_m \cdot \vec{v}_e > 0$, d) An example where $\phi_o^S \in [\phi_{om}, \phi_{oM}]$, since $\vec{v}_M \cdot \vec{v}_e > 0$ and $\vec{v}_m \cdot \vec{v}_e < 0$*

value of the range, i.e. $\phi_o^S = \phi_{oM}$ (Figure 3.21b). If both signs are positive it means that the minimum of d_e occurs for the minimum value of the range, i.e. $\phi_o^S = \phi_{om}$ (Figure 3.21c).

– At the orientation $\phi \in [\phi_{om}, \phi_{oM}]$ such that $d'_e(\phi) = 0$ if $d'_e(\phi_{om})$ and $d'_e(\phi_{oM})$ have different sign. Assuming that ϕ varies linearly along the line that connects $(e_x(\phi_{om}), e_y(\phi_{om}))$ and $(e_x(\phi_{oM}), e_y(\phi_{oM}))$, then the value ϕ_o^S that satisfies $d'_e(\phi_o^S) = 0$ is approximated by (Figure 3.21d):

$$\phi_o^S = \phi_{om} - \frac{\vec{v}_m \cdot \vec{v}_e}{|\vec{v}_m|}(\phi_{oM} - \phi_{om})$$

The algorithm to compute ϕ_o^S is as follows:

Find-orientation(c_o, C_S)

IF C_S only involves one basic contact i THEN RETURN Find-orientation(c_o, i)

ELSE IF $[\phi_{om}, \phi_{oM}] \cap R_\phi^S = \emptyset$ RETURN the extreme of $[\phi_{om}, \phi_{oM}]$ closest to R_ϕ^S

ELSE IF C_S involves more than two basic contacts THEN RETURN ϕ_v

ELSE IF C_S involves two basic contacts and
R_ϕ^{ij} is a unique orientation THEN RETURN ϕ_e

ELSE

IF $\vec{v}_m \cdot \vec{v}_e > 0$ and $\vec{v}_M \cdot \vec{v}_e > 0$ RETURN ϕ_{om}

ELSE IF $\vec{v}_m \cdot \vec{v}_e < 0$ and $\vec{v}_M \cdot \vec{v}_e < 0$ RETURN ϕ_{oM}

ELSE RETURN $\phi_{om} - \frac{\vec{v}_m \cdot \vec{v}_e}{|\vec{v}_m|}(\phi_{oM} - \phi_{om})$

END

3.4.1 Contact uncertainty dependence

Definition: Given a set S of basic contacts, a source of uncertainty is *independent* if it can give rise to complementary contact situations, and it is *dependent* otherwise.

- Given the deviation produced by a dependent source of uncertainty on a toplogical element of S, then the deviation produced by this source of uncertainty on all the other topological elements is determined. The following sources of uncertainty are dependent:
  a) The uncertainty in the position and orientation of the robot.
  b) The uncertainty in the positioning of the manipulated object in the robot gripper.
  c) The uncertainty in the positioning of an static object when all the contacts of S involve the same static object.
- Given the deviation produced by an independent source of uncertainty on a toplogical element of S, then the deviation produced by this source of uncertainty on all the other topological elements is not known, although it may be constrained to a subset of all the possible deviations (e.g. the manufacturing tolerances when the involved topological elements are contiguous[1]). The sources of uncertainty not considered in the previous item are independent.

Let:

D: be the set of dependent sources of uncertainty affecting the basic contacts of S.

I: be the set of independent sources of uncertainty affecting the basic contacts of S.

ϵ_D: be the sum of the maximum deviations in the contact position due to D.

ϵ_I: be the sum of the maximum deviations in the contact position due to I.

[1]Two edges are contiguous if both end at the same vertex, two vertices are contiguous if they are the endpoints of the same edge, and a vertex and an edge are contiguous if the edge ends at the vertex.

The values of ϵ_D and ϵ_I are the following:

a) If the contacts involve the same static object:

$$\epsilon_D = \epsilon_{p_r} + \epsilon_s - \epsilon_{t_s} + \epsilon_m - \epsilon_{t_m} \quad (3.96)$$

$$\epsilon_I = \epsilon_{t_m} + \epsilon_{t_s} \quad (3.97)$$

b) If the contacts involve different static objects:

$$\epsilon_D = \epsilon_{p_r} + \epsilon_m - \epsilon_{t_m} \quad (3.98)$$

$$\epsilon_I = \epsilon_{t_m} + \epsilon_s \quad (3.99)$$

Weighting the effect of dependent and independent sources of uncertainty

Let $\Delta_\phi^{S_i}$ be the deviation in orientation of contact $i \in S$:

$$\Delta_\phi^{S_i} = \begin{cases} 0 & \text{if } \phi_o^S \in R_\phi^i \\ \phi_o^S - \phi_m^i & \text{if } \phi_o^S < \phi_m^i \\ \phi_o^S - \phi_M^i & \text{if } \phi_o^S > \phi_M^i \end{cases} \quad (3.100)$$

$\Delta_\phi^{S_i}$ may be due to the dependent and the independent sources of uncertainty:

$$|\Delta_\phi^{S_i}| = |\Delta_{\phi_D}^S| + |\Delta_{\phi_I}^{S_i}| \quad (3.101)$$

where $\Delta_{\phi_I}^{S_i}$ is the deviation in orientation due to the independent sources of uncertainty that affect contact i, and $\Delta_{\phi_D}^S$ is the the deviation in orientation due to the dependent sources of uncertainty that affect all the contacts of S (Figure 3.22a).

The balance between dependent and independent sources of uncertainty that will be considered is such that the uncertainty in the contact position is maximum. The value of $\Delta_{\phi_D}^S$ is choosen such that for each contact $i \in S$, the sum of the areas of the associated Contact Position Domains due to the dependent and independent source of uncertainty is maximum.

$\Delta_{\phi_D}^S$ is computed as follows. Let approximate the area of a Contact Position Region by the area A of its bounding box:

$$A = r\ d \quad (3.102)$$

Where r and d are computed as follows:

- If the values of $|\Delta_\phi^{S_i}|$ are small enough to approximate $\sin|\Delta_\phi^{S_i}|$ by $|\Delta_\phi^{S_i}|$, and the values of $|\alpha|$ and $|\beta|$ are expressed as a function of $|\Delta_\phi^{S_i}|$:

$$|\beta| = q|\Delta_\phi^{S_i}| \quad (3.103)$$

$$|\alpha| = (1-q)|\Delta_\phi^{S_i}| \quad (3.104)$$

  where $q \in [0,1]$, then equation (3.57) becomes:

$$r = (\epsilon_e + \epsilon_v) - (\frac{l_e}{2}q + \frac{l_v}{2}(1-q))|\Delta_\phi^{S_i}| \quad (3.105)$$

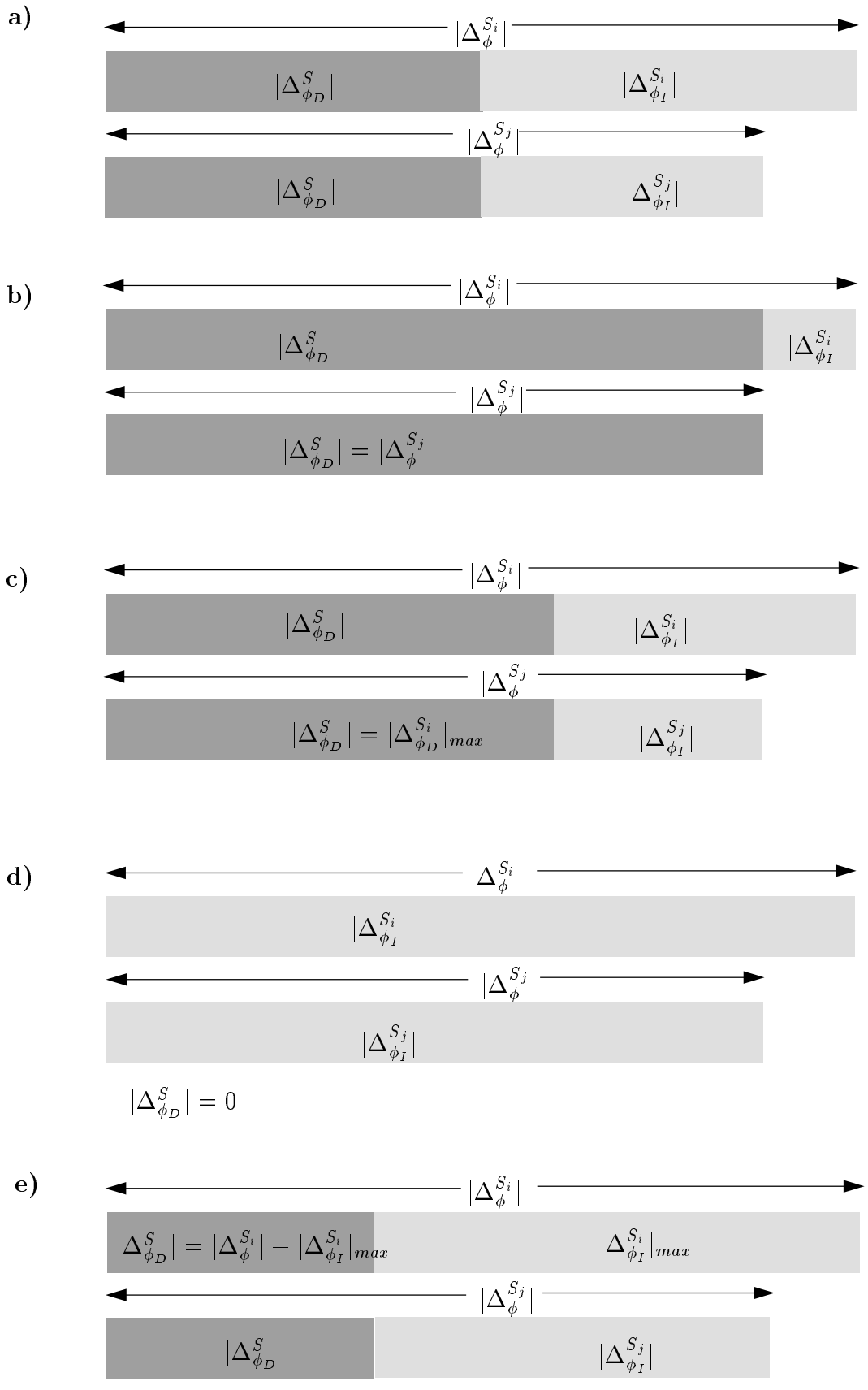

Figure 3.22: *Balance between dependent and independent sources of uncertainty.*

- d is approximated by:

$$d = \epsilon_e + \epsilon_v \tag{3.106}$$

Therefore, the area A is:

$$\begin{aligned} A &= r\, d \\ &= (\epsilon_e + \epsilon_v)^2 - (\epsilon_e + \epsilon_v)(\frac{l_e}{2}q + \frac{l_v}{2}(1-q))|\Delta_\phi^{S_i}| \\ &= A_{max} - k|\Delta_\phi^{S_i}| \end{aligned} \tag{3.107}$$

where:

$$A_{max} = (\epsilon_e + \epsilon_v)^2 \tag{3.108}$$

$$k = (\epsilon_e + \epsilon_v)(\frac{l_e}{2}q + \frac{l_v}{2}(1-q)) \tag{3.109}$$

Considering the Contact Position Regions due to the dependent and independent sources of uncertainty, equation (3.107) is particularized as:

$$A_D = A_{Dmax} - k_D|\Delta_{\phi_D}^S| \tag{3.110}$$

$$A_I = A_{Imax} - k_I|\Delta_{\phi_I}^{S_i}| \tag{3.111}$$

where:

$$A_{Dmax} = \epsilon_D^2 \tag{3.112}$$

$$A_{Imax} = \epsilon_I^2 \tag{3.113}$$

$$k_D = \epsilon_D(\frac{l_e}{2}q + \frac{l_v}{2}(1-q)) \tag{3.114}$$

$$k_I = \epsilon_I(\frac{l_e}{2}q + \frac{l_v}{2}(1-q)) \tag{3.115}$$

Then, the sum of A_D and A_I is:

$$\begin{aligned} A_T &= A_D + A_I \\ &= A_{Dmax} + A_{Imax} - k_I|\Delta_{\phi_I}^{S_i}| - k_D|\Delta_{\phi_D}^S| \end{aligned} \tag{3.116}$$

Taking into account (3.101), A_T can be expressed as:

$$A_T = A_{Dmax} + A_{Imax} - k_I|\Delta_\phi^{S_i}| + (k_I - k_D)|\Delta_{\phi_D}^S| \tag{3.117}$$

To determine the value of $|\Delta_{\phi_D}^S|$ that maximizes A_T, the following derivate is computed:

$$\frac{\partial A_T}{\partial|\Delta_{\phi_D}^S|} = (k_I - k_D) \tag{3.118}$$

Then, the maximum of A_T is found for the minimum or for the maximum value of $|\Delta_{\phi_D}^S|$:

- The choosen extreme depends on the values of ϵ_I and ϵ_D:

  If $\epsilon_I > \epsilon_D$, since $(\frac{l_e}{2}q + \frac{l_r}{2}(1-q))$ is always positive, then $(k_I - k_D) > 0$; therefore the maximum of A_T is found for the maximum value of $|\Delta^S_{\phi_D}|$.

  Otherwise, if $\epsilon_I < \epsilon_D$, the maximum of A_T is found for the minimum value of $|\Delta^S_{\phi_D}|$.

- The minimum and maximum values of $|\Delta^S_{\phi_D}|$ are computed as follows. Let $|\Delta^{S_i}_{\phi_D}|_{max}$ be the maximum absolute value of the deviation in orientation of contact $i \in S$ due to the dependent sources of uncertainty. Then, the range of possible contact orientations of contact i considering the dependent sources of uncertainty is:

$$[\phi^i_m - |\Delta^{S_i}_{\phi_D}|_{max},\ \phi^i_M + |\Delta^{S_i}_{\phi_D}|_{max}] \tag{3.119}$$

  Let $|\Delta^{S_i}_{\phi_I}|_{max}$ be defined in a similar way for the independent sources of uncertainty. The values of $|\Delta^{S_i}_{\phi_D}|_{max}$ and $|\Delta^{S_i}_{\phi_I}|_{max}$ are the sum of the corresponding maximum values of $|\alpha|$ and $|\beta|$. Therefore the extremes of $|\Delta^S_{\phi_D}|$ are:

  a) *Maximum of* $|\Delta^S_{\phi_D}|$: The maximum value of $|\Delta^S_{\phi_D}|$ is bounded either by $|\Delta^{S_i}_{\phi}|$ as in Figure 3.22b, or by $|\Delta^{S_i}_{\phi_D}|_{max}$ as in Figure 3.22c, for any contact $i \in S$:

$$\min_{\forall i \in S}(|\Delta^{S_i}_{\phi_D}|_{max}, |\Delta^{S_i}_{\phi}|) \tag{3.120}$$

  b) *Minimum of* $|\Delta^S_{\phi_D}|$: The minimum value of $|\Delta^S_{\phi_D}|$ depends on weather the orientation gap $|\Delta^{S_i}_{\phi}|$ for each contact $i \in S$ can be covered by the independent uncertainty sources (Figure 3.22d), or not (Figure 3.22e):

$$\max_{\forall i \in S}(|\Delta^{S_i}_{\phi}| - |\Delta^{S_i}_{\phi_I}|_{max}, 0) \tag{3.121}$$

The following algorithm computes the value of $|\Delta^S_{\phi_D}|$ and $|\Delta^{S_i}_{\phi_I}|\ \forall i \in S$, such that A_T is maximum for a given ϕ^S_o.

Uncertainty-balance(ϕ^S_o)

Compute $|\Delta^{S_i}_{\phi}|\ \ \forall i \in S$

IF $\epsilon_I > \epsilon_D$ THEN $|\Delta^S_{\phi_D}| = \min_{\forall i \in S}(|\Delta^{S_i}_{\phi_D}|_{max}, |\Delta^{S_i}_{\phi}|)$

ELSE $|\Delta^S_{\phi_D}| = \max_{\forall i \in S}(|\Delta^{S_i}_{\phi}| - |\Delta^{S_i}_{\phi_I}|_{max}, 0)$

Compute $|\Delta^{S_i}_{\phi_I}| = |\Delta^{S_i}_{\phi}| - |\Delta^S_{\phi_D}|\ \ \forall i \in S$

RETURN $|\Delta^S_{\phi_D}|$ and $|\Delta^{S_i}_{\phi_I}|\ \forall i \in S$

END

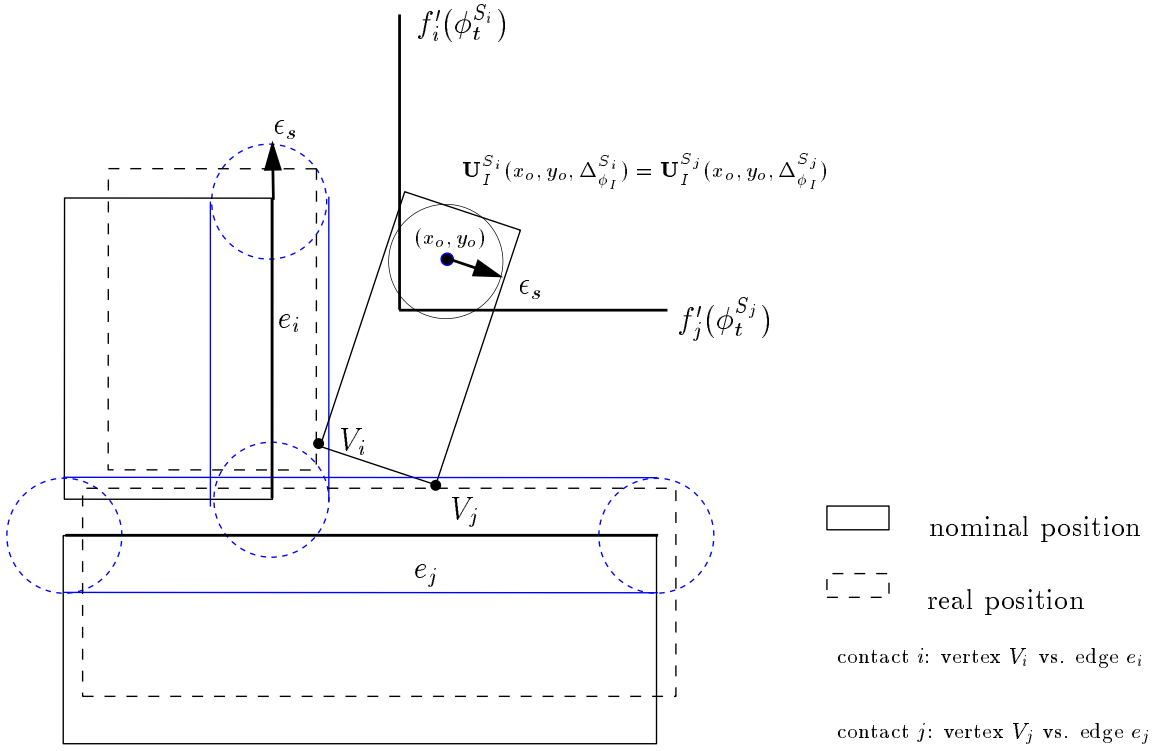

Figure 3.23: *Effect of independent sources of uncertainty: the current configuration of the manipulation object is at a possible contact configuration of a nominal two-basic contact situation, since* $\mathbf{U}_I^{S_i}(x_o, y_o, \Delta_{\phi_I}^{S_i}) \cap f_i'(\phi_t^{S_i}) \neq \emptyset$ *and* $\mathbf{U}_I^{S_j}(x_o, y_o, \Delta_{\phi_I}^{S_j}) \cap f_j'(\phi_t^{S_j}) \neq \emptyset$.

3.4.2 Independent sources of uncertainty

Let $\mathbf{U}_I^{S_i}(x, y, \Delta_{\phi_I}^{S_i})$ be the Contact Position Domain $\mathbf{U}^i(\Delta_{\phi_I}^{S_i})$ built considering $D = \emptyset$ and $I \neq \emptyset$, and located with respect to (x, y)[2]. $\mathbf{U}_I^{S_i}(x, y, \Delta_{\phi_I}^{S_i})$ is a circle of radius ϵ_I centered at (x, y) when $\phi_o^S \in R_\phi^i$, since in this case $\Delta_{\phi_I}^{S_i} = 0$.

Proposition 11: *Assuming* $D = \emptyset$, c_o *may be a contact configuration of* C_S *iff:*

$$\mathbf{U}_I^{S_i}(x_o, y_o, \Delta_{\phi_I}^{S_i}) \cap f_i'(\phi_t^{S_i}) \neq \emptyset \quad \forall i \in S \tag{3.122}$$

where $\phi_t^{S_i}$ *is defined as:*

$$\phi_t^{S_i} = \phi_o^S + \Delta_\phi^{S_i} \tag{3.123}$$

Proof: From corollary 9, the observed configuration is compatible with the occurrence of all the basic contacts of S, when equation (3.122) is satisfied. This occurrence can be simultaneous, since the uncertainties are independent. ◇

[2]The construction algorithm of Section 3.3.4 locates the Contact Position Domains with respect to the observed position (x_o, y_o).

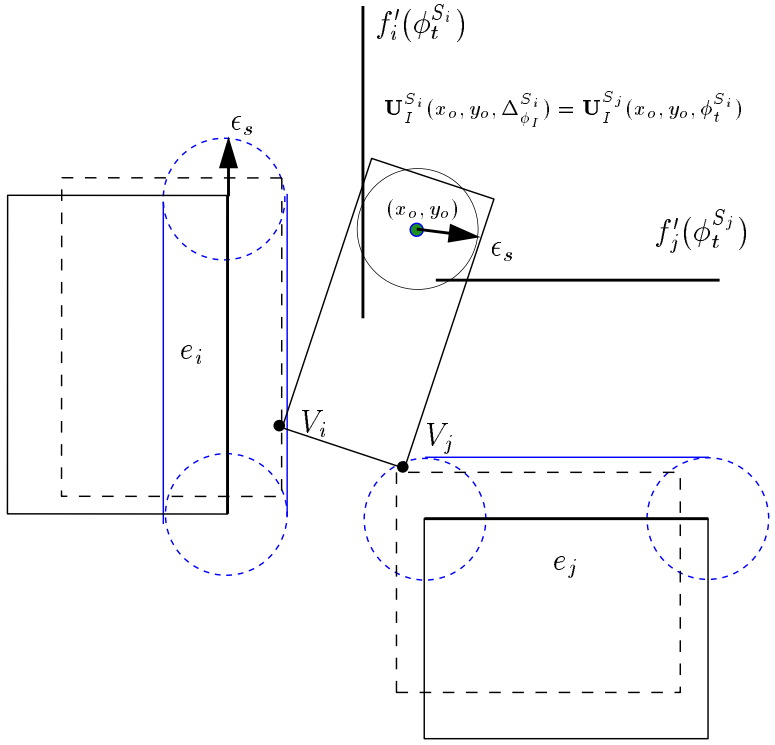

Figure 3.24: *Effect of independent sources of uncertainty: the current configuration of the manipulation object is at a possible contact configuration of a complementary two-basic contact situation, since* $\mathbf{U}_I^{S_i}(x_o, y_o, \Delta_{\phi_I}^{S_i}) \cap f_i'(\phi_t^{S_i}) \neq \emptyset$ *and* $\mathbf{U}_I^{S_j}(x_o, y_o, \Delta_{\phi_I}^{S_i}) \cap f_j'(\phi_t^{S_j}) \neq \emptyset$.

As an example Figure 3.23 shows a contact situation with two type-B basic contacts i and j involving different static objects. Only the sources of uncertainty affecting the static objects are considered, which in this case are independent sources of uncertainty (i.e. $\epsilon_I = \epsilon_s$). In this example, since $\phi_o^S \in R_\phi^i$ and $\phi_o^S \in R_\phi^j$:

$\Delta_{\phi_I}^{S_i} = \Delta_{\phi_I}^{S_j} = 0$

$\phi_t^{S_i} = \phi_t^{S_j} = \phi_o^S$

$\mathbf{U}_I^{S_i}(x_o, y_o, \Delta_{\phi_I}^{S_i})$ and $\mathbf{U}_I^{S_j}(x_o, y_o, \Delta_{\phi_I}^{S_j})$ are both equal to a circle of radius ϵ_s.

The current configuration of the manipulated object may correspond to a contact configuration, since equation (3.122) is satisfied, i.e. $\mathbf{U}_I^{S_i}(x_o, y_o, \Delta_{\phi_I}^{S_i}) \cap f_i'(\phi_t^{S_i}) \neq \emptyset$ and $\mathbf{U}_I^{S_j}(x_o, y_o, \Delta_{\phi_I}^{S_j}) \cap f_j'(\phi_t^{S_j}) \neq \emptyset$.

Complementary contact situations may arise due to independent sources of uncertainty, since equation (3.122) can be satisfied regardless of the existence of the nominal contact situation. Figure 3.24 shows a contact situation similar to Figure 3.23, where in this case the manipulated object is at a configuration that is compatible with the occurrence of a complementary two-contact situation.

3.4.3 Dependent sources of uncertainty

Let:

$P_S(\phi)$: be the nominal contact position of C_S for an orientation ϕ:

$$P_S(\phi) = \bigcap_{\forall i \in S} f_i'(\phi) \tag{3.124}$$

$\mathbf{U}_D^{S_i}(\Delta_{\phi_D}^S)$: be the Contact Position Domain $\mathbf{U}^i(\Delta_{\phi_D}^S)$ built considering $D \neq \emptyset$ and $I = \emptyset$. It is a circle of radius ϵ_D centered at (x_o, y_o) when $\phi_o^S \in R_\phi^i$, since in this case $\Delta_{\phi_D}^S = 0$.

Proposition 12: *Assuming $I = \emptyset$, c_o may be a contact configuration of C_S iff:*

$$P_S(\phi_t^S) \in \mathbf{U}_D^{S_i}(\Delta_{\phi_D}^S) \quad \forall i \in S \tag{3.125}$$

where ϕ_t^S is defined as:

$$\phi_t^S = \phi_o^S + \Delta_{\phi_D}^S \tag{3.126}$$

Proof: If equation (3.125) is satisfied then:

$$\mathbf{U}_D^{S_i}(\Delta_{\phi_D}^S) \cap f_i'(\phi_t^S) \neq \emptyset \quad \forall i \in S \tag{3.127}$$

is satisfied and therefore, from corollary 9, the observed configuration is compatible with the occurrence of all the basic contacts of S, and from equation (3.124) this occurrence is simultaneous. ◇

As an example Figure 3.25 shows a nominal contact situation with two type-B basic contacts i and j involving different static objects. The only uncertainty source considered is the uncertainty in the positioning of the robot, which is a dependent uncertainty source (i.e. $\epsilon_D = \epsilon_{p_r}$). In this example $\phi_o^S \in R_\phi^{ij}$, and therefore, $\mathbf{U}_D^S(\Delta_{\phi_D}^S)$ is a circle of radius ϵ_D, since $\Delta_{\phi_D}^S = 0$. The current configuration of the manipulated object may correspond to a contact configuration, since equation (3.125) is satisfied, i.e. $P_S(\phi_t^S) = [f_i'(\phi_t^S) \cap f_j'(\phi_t^S)]$ satisfies $P_S(\phi_t^S) \in \mathbf{U}_D^{S_i}(\Delta_{\phi_D}^S)$ and $P_S(\phi_t^S) \in \mathbf{U}_D^{S_j}(\Delta_{\phi_D}^S)$.

3.4.4 Dependent and independent sources of uncertainty

Let $\mathbf{U}_D^S(\Delta_{\phi_D}^S)$ be defined as:

$$\mathbf{U}_D^S(\Delta_{\phi_D}^S) = \bigcap_{\forall i \in S} \mathbf{U}_D^{S_i}(\Delta_{\phi_D}^S) \tag{3.128}$$

$\mathbf{U}_D^S(\Delta_{\phi_D}^S)$ is a circle of radius ϵ_D centered at (x_o, y_o) when $\phi_o^S \in R_\phi^S$, otherwise it will be approximated by the intersection of the corresponding bounding boxes.

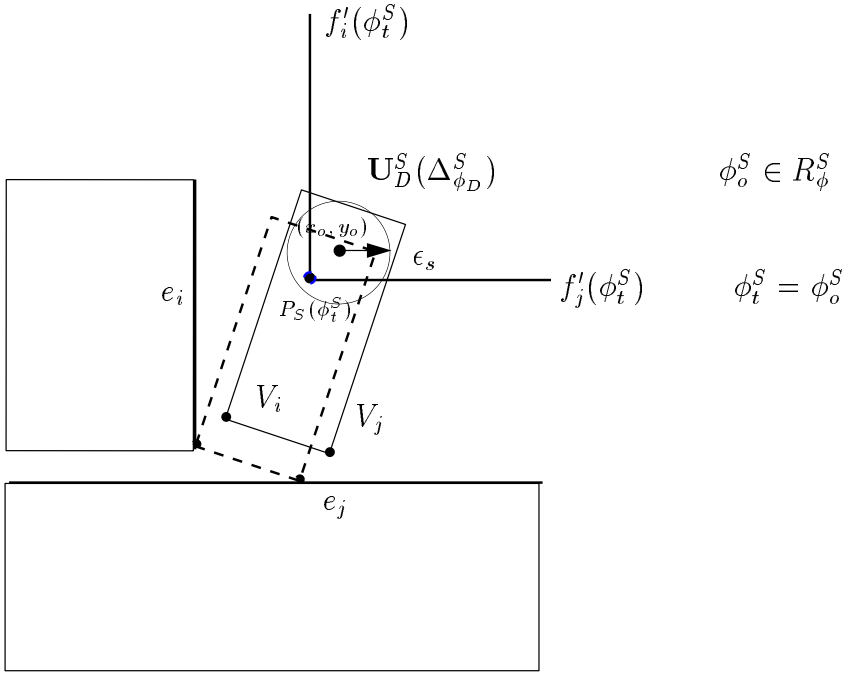

Figure 3.25: *Effect of dependent sources of uncertainty: the current configuration of the manipulation object is at a possible contact configuration of a nominal two-basic contact situation, since* $P_S(\phi_t^S) \in \mathbf{U}_D^S(\Delta_{\phi_D}^S)$.

Proposition 13: *The observed configuration* c_o *may be a contact configuration of* C_S *iff:*

$$\mathbf{U}_I^{S_i}(x_t, y_t, \Delta_{\phi_I}^{S_i}) \cap f_i'(\phi_t^{S_i}) \neq \emptyset \quad \forall i \in S \tag{3.129}$$

where (x_t, y_t) is the point of $\mathbf{U}_D^S(\Delta_{\phi_D}^S)$ such that $\mathbf{U}_I^{S_i}(x_t, y_t, \Delta_{\phi_I}^{S_i})$ is closest to $f_i'(\phi_t^{S_i})$ $\forall i \in S$.

Proof: If equation (3.129) is satisfied, from corollary 9, the observed configuration is compatible with the occurrence of all the basic contacts of S. This occurrence can be simultaneous, since the Contact Position Domains of (3.129) are built considering independent sources of uncertainty, and are all located with respect to (x_t, y_t), which is a position compatible with the observed position (x_o, y_o) considering the dependent sources of uncertainty. ◇

Determination of (x_t, y_t) **when** $\phi_o^S \in R_\phi^S$

Let first consider two basic contacts i and j, and let define the following nomenclature (Figure 3.26):

- l_i and l_j: lines that contain $f_i'(\phi_o^S)$ and $f_j'(\phi_o^S)$, respectively.
- D_{l_i} and D_{l_j}: distances from (x_t, y_t) to l_i and l_j, respectively.

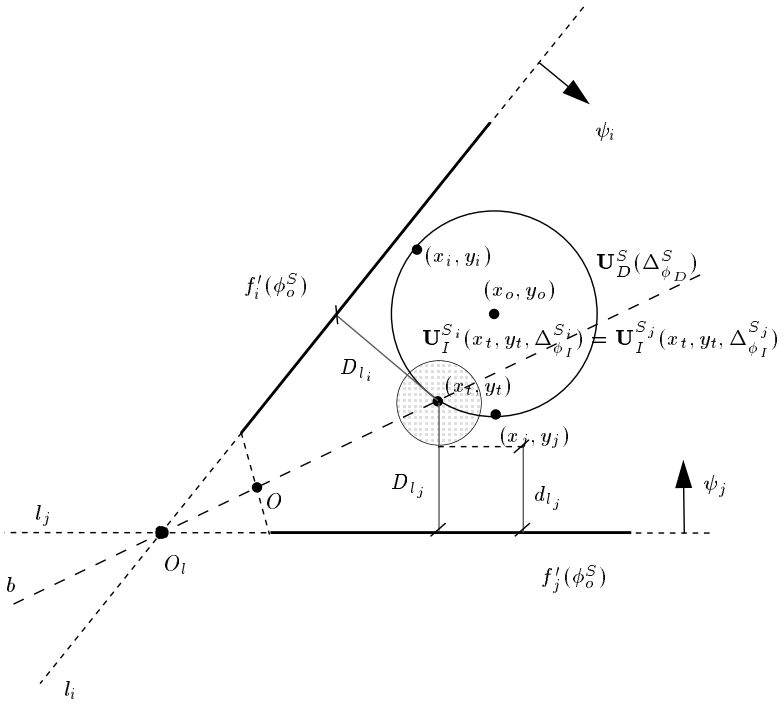

Figure 3.26: *Nomenclature.*

- d_{l_i} and d_{l_j}: distances from $\mathbf{U}_I^{S_i}(x_t, y_t, \Delta_{\phi_I}^{S_i})$ and $\mathbf{U}_I^{S_j}(x_t, y_t, \Delta_{\phi_I}^{S_j})$ to l_i and l_j, respectively.
- b: line such that $d_{l_i} = d_{l_j}$ is satisfied when $(x_t, y_t) \in b$.
- O_l: intersection of l_i and l_j.
- O: point that coincides with O_l if $f_i'(\phi_o^S)$ and $f_j'(\phi_o^S)$ intersect, or otherwise O is the point computed as follows:

  1- compute the intersections of b with the four segments formed with the extremes of $f_i'(\phi_o^S)$ and $f_j'(\phi_o^S)$.

  2- O is the intersection point which is closest to O_l.
- (x_i, y_i): point of $\mathbf{U}_D^S(\Delta_{\phi_D}^S)$ which is closest to l_i.
- (x_j, y_j): point of $\mathbf{U}_D^S(\Delta_{\phi_D}^S)$ which is closest to l_j.

When $\phi_o^S \in R_\phi^S$ then:

- $\Delta_{\phi_D}^S = 0$
- $\Delta_{\phi_I}^{S_i} = \Delta_{\phi_I}^{S_j} = 0$
- $\phi_t^{S_i} = \phi_t^{S_j} = \phi_o^S$
- $\mathbf{U}_D^S(\Delta_{\phi_D}^S)$ is a circle of radius ϵ_D centered at (x_o, y_o):

$$\mathbf{U}_D^S(\Delta_{\phi_D}^S) = \mathbf{C}(x_o, y_o, \epsilon_D) \tag{3.130}$$

- $\mathbf{U}_I^{S_i}(x_t, y_t, \Delta_{\phi_I}^{S_i})$ and $\mathbf{U}_I^{S_j}(x_t, y_t, \Delta_{\phi_I}^{S_j})$ coincide and are equal to a circle of radius ϵ_I centered at (x_t, y_t):

$$\mathbf{U}_I^{S_i}(x_t, y_t, \Delta_{\phi_I}^{S_i}) = \mathbf{U}_I^{S_j}(x_t, y_t, \Delta_{\phi_I}^{S_j}) = \mathbf{C}(x_t, y_t, \epsilon_I) \tag{3.131}$$

Then, since equation (3.131) holds:

$d_{l_i} = D_{l_i} - \epsilon_I$.

$d_{l_j} = D_{l_j} - \epsilon_I$.

b is the bisecting line of l_i and l_j.

$(x_i, y_i) = (x_o, y_o) - \epsilon_D(\cos\psi_i, \sin\psi_i)$

$(x_j, y_j) = (x_o, y_o) - \epsilon_D(\cos\psi_j, \sin\psi_j)$

Therefore, (x_t, y_t) is computed by the following algorithm, which is illustrated in Figure 3.27:

Determine-position$(c_o, \Delta_{\phi_D}^S, \Delta_{\phi_I}^{S_i})$

IF $O \in \mathbf{U}_D^S(\Delta_{\phi_D}^S)$ RETURN O

ELSE

Intersect b with $\mathbf{U}_D^S(\Delta_{\phi_D}^S)$

IF the intersection exists RETURN the intersection point closest to O

ELSE

IF $\mathbf{U}_D^S(\Delta_{\phi_D}^S)$ belongs to the angular sector defined by b and l_i RETURN (x_j, y_j)

ELSE RETURN (x_i, y_i)

END

For more than two basic contacts, the position (x_t, y_t) is computed as the mid-point of the positions obtained for each pair of basic contacts.

Determination of (x_t, y_t) when $\phi_o^S \notin R_\phi^S$

When $\phi_o^S \notin R_\phi^S$ the algorithm to determine (x_t, y_t) is the same as the one detailed in the previous Section, but some of the variables used vary in order to consider the following items:

(1) The center of $\mathbf{U}_I^{S_i}(x_t, y_t, \Delta_{\phi_I}^{S_i})$ is determined from (x_t, y_t) by the two rotations described in the algorithm $\mathbf{U}^i(\alpha, \beta)$-construction of Section 3.3.4

(2) The shape of $\mathbf{U}_I^{S_i}(x_t, y_t, \Delta_{\phi_I}^{S_i})$ and $\mathbf{U}_D^S(\Delta_{\phi_D}^S)$ depend on the values of $\Delta_{\phi_I}^{S_i}$ and $\Delta_{\phi_D}^S$. The corresponding bounding boxes will be considered to simplify the computations.

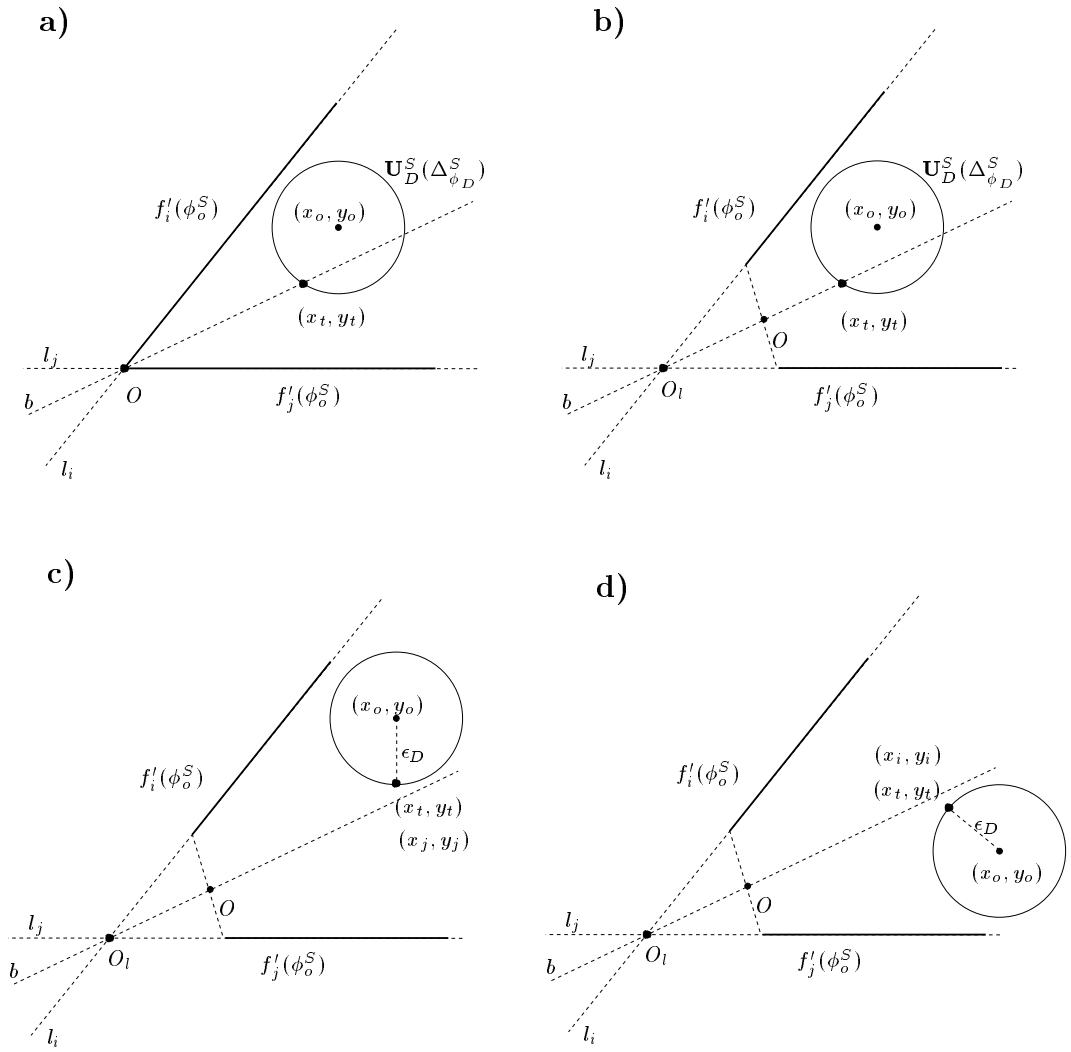

Figure 3.27: *Determination of* (x_t, y_t).

The changes are the following:

a) *Lines* l_i *and* l_j:

Taking (1) into account, the minimum distance from the center of $\mathbf{U}_I^{S_i}(x_t, y_t, \Delta_{\phi_I}^S)$ to $f_i'(\phi_t^{S_i})$ can be computed as the distance from (x_t, y_t) to a line l_i obtained from the line that contains $f_i'(\phi_t^{S_i})$ by:

- Rotating an angle β_{rm_i} around the center of the corresponding contact edge, where β_{rm_i} is the deviation for which $\mathbf{U}_I^{S_i}(x_t, y_t, \Delta_{\phi_I}^S)$ is closest to $f_i'(\phi_t^{S_i})$ (Section 3.3.5).
- Translating in its perpendicular direction a distance:

$$d_{\alpha i} = (x_o - x_o')\cos(\psi_i + \beta_{rm_i}) + (y_o - y_o')\sin(\psi_i + \beta_{rm_i}) \tag{3.132}$$

where (x_o', y_o') is defined in equation (3.53).

The line l_j is computed in a similar way.

b) *Distances* d_{l_i} *and* d_{l_j}:

Taking (2) into account, if $r_{Ii}(\beta_{rm_i})$ and $r_{Ij}(\beta_{rm_j})$ are the widths r of $Box(\mathbf{U}_I^{S_i})$ and $Box(\mathbf{U}_I^{S_j})$ computed for the deviations β_{rm_i} and β_{rm_j}, respectively, then:

$$d_{l_i} = D_{l_i} - r_{Ii}(\beta_{rm_i}) \quad (3.133)$$
$$d_{l_j} = D_{l_j} - r_{Ij}(\beta_{rm_j}) \quad (3.134)$$

c) *Line b*:

Is the line defined by the point O_l and the vector:

$$\vec{v} = (d_{l_i}\cos\psi_i + d_{l_j}\cos\psi_j, d_{l_i}\sin\psi_i + d_{l_j}\sin\psi_j) \quad (3.135)$$

d) *Points* (x_j, y_j) *and* (x_i, y_i):

Taking (2) into account, if $r_{Di}(\beta_{rm_i})$ and $r_{Dj}(\beta_{rm_j})$ are the widths r of $Box(\mathbf{U}_D^S)$ and $Box(\mathbf{U}_D^S)$ computed for the deviations β_{rm_i} and β_{rm_j}, respectively, then:

$$(x_i, y_i) = (x_o, y_o) - r_{Di}(\beta_{rm_i})(\cos\psi_i, \sin\psi_i) \quad (3.136)$$
$$(x_j, y_j) = (x_o, y_o) - r_{Dj}(\beta_{rm_j})(\cos\psi_j, \sin\psi_j) \quad (3.137)$$

Examples

As an example, Figure 3.28 shows a contact situation with two type-B basic contacts i and j involving different static objects. Since $\phi_o^S \in R_\phi^{ij}$ then:

$\Delta_{\phi_I}^{S_i} = \Delta_{\phi_I}^{S_i} = \Delta_{\phi_D}^S = 0$

$\phi_t^{S_i} = \phi_t^{S_j} = \phi_o^S$

$\mathbf{U}_D^S(\Delta_{\phi_D}^S)$ is a circle of radius ϵ_D centered at the observed position (x_o, y_o).

$\mathbf{U}_I^{S_i}(x_t, y_t, \Delta_{\phi_I}^{S_i})$ and $\mathbf{U}_I^{S_j}(x_t, y_t, \Delta_{\phi_I}^{S_j})$ are circles of radius ϵ_I centered at (x_t, y_t).

In this example, the current configuration of the manipulated object may correspond to a contact configuration, since equation (3.129) is satisfied, i.e. $\mathbf{U}_I^{S_i}(x_t, y_t, \Delta_{\phi_I}^{S_i}) \cap f_i'(\phi_t^{S_i}) \neq \emptyset$ and $\mathbf{U}_I^{S_j}(x_t, y_t, \Delta_{\phi_I}^{S_j}) \cap f_j'(\phi_t^{S_j}) \neq \emptyset$.

Figure 3.29 shows a similar example to that of Figure 3.28 but in this case $\phi_o^S \in R_\phi^i$ and $\phi_o^S \notin R_\phi^j$. In this example:

$\Delta_{\phi_D}^S = 0$

$\Delta_{\phi_I}^{S_i} = 0$

$\Delta_{\phi_I}^{S_j} = \phi_o^S - \phi_M^j$

$\phi_t^{S_i} = \phi_o^S$ and $\phi_t^{S_j} = \phi_M^j$

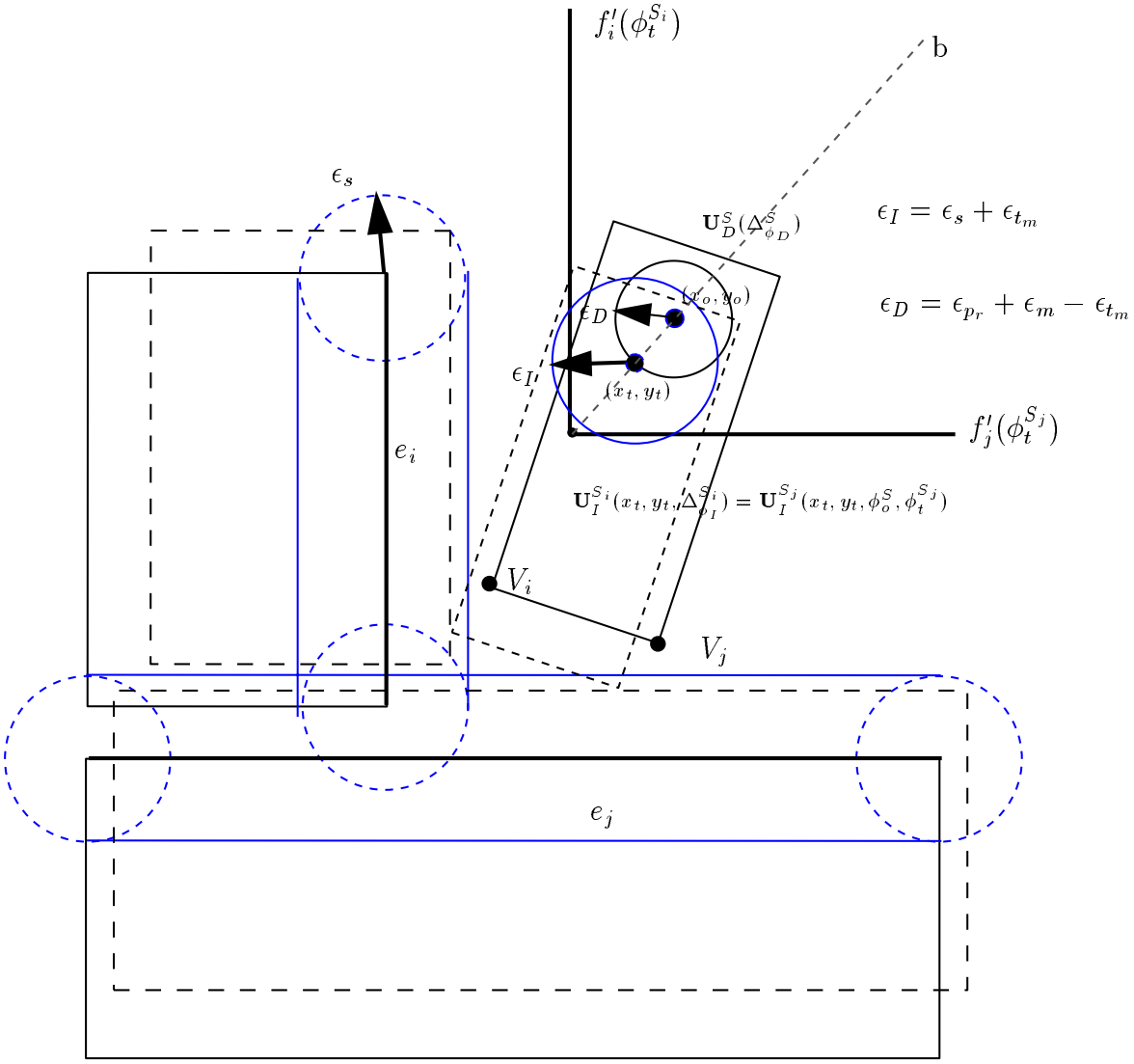

Figure 3.28: *Effect of dependent and independent sources of uncertainty: The current configuration of the manipulation object is at a possible contact configuration of a nominal two-basic contact situation, since* $\mathbf{U}_I^{S_i}(x_t, y_t, \Delta_{\phi_I}^{S_i}) \cap f_i'(\phi_t^{S_i}) \neq \emptyset$ *and* $\mathbf{U}_I^{S_j}(x_t, y_t, \Delta_{\phi_I}^{S_i}) \cap f_j'(\phi_t^{S_j}) \neq \emptyset$. *In this example* $\phi_t^{S_i} = \phi_t^{S_j} = \phi_o^S$.

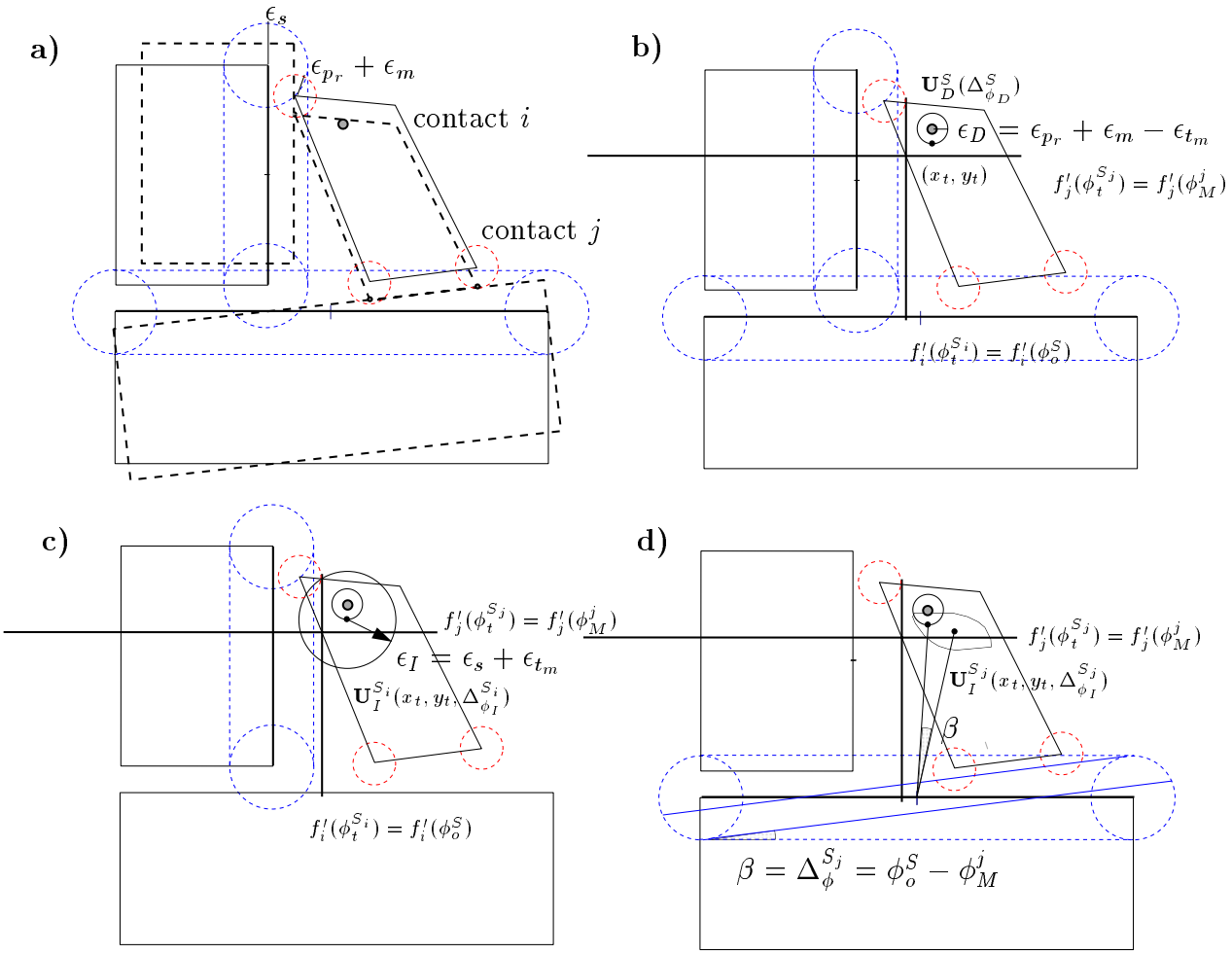

Figure 3.29: *Two-basic contact situation where ϕ_o^S satisfies $\phi_o^S \in R_\phi^i$, $\phi_o^S \notin R_\phi^j$. In this example the deviations in the orientation of the topological elements of the contact are considered to be produced only by the independent uncertainty sources.*

$\mathbf{U}_D^S(\Delta_{\phi_D}^S)$ is the circle of radius ϵ_D, shown in Figure 3.29b together with a point $(x_t, y_t) \in \mathbf{U}_D^S(\Delta_{\phi_D}^S)$

$\mathbf{U}_I^{S_i}(x_t, y_t, \Delta_{\phi_I}^{S_i})$ is the circle of radius ϵ_I centered at (x_t, y_t) shown in Figure 3.29c

$\mathbf{U}_I^{S_j}(x_t, y_t, \Delta_{\phi_I}^{S_j})$ is the Contact Position Domain $\mathbf{U}^j(\Delta_{\phi_I}^{S_j})$ located with respect to (x_t, y_t), shown in Figure 3.29d

Since $\mathbf{U}_I^{S_i}(x_t, y_t, \Delta_{\phi_I}^{S_i}) \cap f_i'(\phi_t^{S_i}) \neq \emptyset$ and $\mathbf{U}_I^{S_j}(x_t, y_t, \Delta_{\phi_I}^{S_j}) \cap f_j'(\phi_t^{S_j}) \neq \emptyset$, the configuration of the manipulated object can be a contact configuration of the two-contact situation.

3.4.5 Contact identification

The contact identification procedure for contact situations involving more than one basic contact must consider the dependencies between the sources of uncertainty. Given an observed configuration $c_o = (x_o, y_o, \phi_o)$ and contact situation C_S involving a set S of basic contacts then, for proposition 13, the contact identification procedure must verify $\mathbf{U}_I^{S_i}(x_t, y_t, \Delta_{\phi_I}^{S_i}) \cap f_i'(\phi_t^{S_i}) \neq \emptyset$ for all the contacts of S.

Given the position (x_t, y_t) and the deviation in orientation due to dependent sources of uncertainty $\Delta_{\phi_D}^S$, this is done by using the contact identification algorithms for one basic contact detailed in Section 3.3.6.

The contact identification algorithm is the following:

Contact-Identification(c_o, C_S)

IF C_S only involves one basic contact i THEN
  r = Contact-Identification(c_o, $\mathbf{U}^i(\Delta_\phi^i)$)
  RETURN r
ELSE
  ϕ_o^S = Find-orientation(c_o, C_S)
  $\{|\Delta_{\phi_D}^S|, \Delta_{\phi_I}^{S_i}\}$ = Uncertainty-balance(ϕ_o^S)
  (x_t, y_t) = Determine-position($c_o, \Delta_{\phi_D}^S, \Delta_{\phi_I}^{S_i}$)
  FOR $i = 1$ TO S
    r = Contact-Identification(c_o, $\mathbf{U}_I^{S_i}(x_t, y_t, \Delta_{\phi_I}^{S_i})$)
    IF r = FALSE THEN RETURN FALSE
  RETURN TRUE
END

3.5 Uncertainty reduction

The sensory information of configuration and force may be used during the execution of the assembly task to:

- Estimate the position and orientation of the topological elements involved in the contacts.
- Reduce the uncertainty.

Therefore, it is possible to make the task execution more reliable as it evolves towards its goal, since:

- The commands to be executed may be modified with the estimated values and hence the motion may become more accurate.
- The estimation of the current contact situation may become more exact.

Given a basic contact i compatible with a observed configuration, the following items are tackled in this section:

- Estimation of the orientation of the contact edge (Section 3.5.1)
- Estimation of the position of the contact vertex (Section 3.5.2)
- Estimation of the position of the contact edge (Section 3.5.3)
- Use of the previous estimations to modify the $\mathcal{C}$-arcs where the contact i is involved (Section 3.5.4)

3.5.1 Estimation of the orientation of the contact edge

Let R_β be the range of possible values of the deviation β in the orientation of the contact edge. From the geometry of the contact, $R_\beta = [-\beta_{max}, \beta_{max}]$, where the value of β_{max} was determined in proposition 1. Figure 3.30a shows the topological elements of a type-B basic contact and Figure 3.30d shows the minimum and the maximum deviations in the orientation of the contact edge.

Proposition 14: *If contact i takes place at a given observed orientation c_o, then $R_\beta \subseteq [-\beta_{max}, \beta_{max}]$.*

Proof: Let define (Figure 3.30b):

ψ: orientation of the normal to the contact edge.

V_a and V_b: vertices of de contact edge such that V_a is first encountered when the border of the object is followed clockwise.

A and B: extremes of $f_i'(\phi_o)$ corresponding to V_a and V_b.

$\vec{\omega}_A = c_o - A$

$\vec{v} = B - A$

$\delta_A = \arcsin(\frac{\vec{v}\times\vec{\omega}_A}{|\vec{v}||\vec{\omega}_A|})$

$\xi_A = \arcsin(\frac{\epsilon_e+\epsilon_v}{|\vec{\omega}_A|})$

S_A: boundle of lines crossing the circumference where the contact vertex lies and the circumference where V_a lies.

S_A can be computed in $\mathcal{C}'$-space as the boundle of lines crossing A and the circumference of radius $\epsilon_e + \epsilon_v$ centered at c_o. The orientations of the lines of S_A belong to the range $[\psi + \pi/2 + \beta^A_{min}, \psi + \pi/2 + \beta^A_{max}]$, where:

$$\begin{aligned} \beta^A_{min} &= \delta_A - \xi_A \\ \beta^A_{max} &= \delta_A + \xi_A \end{aligned} \tag{3.138}$$

Let $\vec{\omega}_B$, δ_B, ξ_B, S_B, β^B_{min} and β^B_{max} be defined in a similar way (Figure 3.30c).

Provided that contact i is taking place at the current observed configuration, the supporting line l of the contact edge satisfies:

$$l \in S_A \text{ AND } l \in S_B \tag{3.139}$$

Therefore, the range R_β is (Figure 3.30e):

$$R_\beta = [-\beta_m, \beta_M] \tag{3.140}$$

$$\beta_m = \max(-\beta_{max}, \beta^A_{min}, \beta^B_{min}) \tag{3.141}$$

$$\beta_M = \min(\beta_{max}, \beta^A_{max}, \beta^B_{max}) \tag{3.142}$$

$\diamond$

For each new observed contact configuration, R_β is updated:

$$\begin{aligned} \beta_m &= \max(\beta_m, \beta^A_{min}, \beta^B_{min}) \\ \beta_M &= \min(\beta_M, \beta^A_{max}, \beta^B_{max}) \end{aligned} \tag{3.143}$$

The contact identification becomes more precise if this reduction in the uncertainty of the orientation of the contact edge is taken into account to built the Contact Position Domain. On the other hand, once R_β has been determined, an estimated value of the deviation, β_e, is used to modify the robot commands by changing the orientation ψ of the contact edge by $(\psi + \beta_e)$ (Section 3.5.4). From corollary 2.1, the estimated value is the deviation with smallest absolute value:

$$\beta_e \in R_\beta \quad \text{such that} \quad |\beta_e| < |\beta_i| \;\; \forall \beta_i \in R_\beta \tag{3.144}$$

The initial estimated value is $\beta_e = 0$, since initially $R_\beta = [-\beta_{max}, \beta_{max}]$.

3.5.2 Estimation of the position of the contact vertex

The position of the contact vertex corresponding to a basic contact i is estimated as follows, when contact i occurs at the current observed configuration $c_o = (x_o, y_o, \phi_o)$.

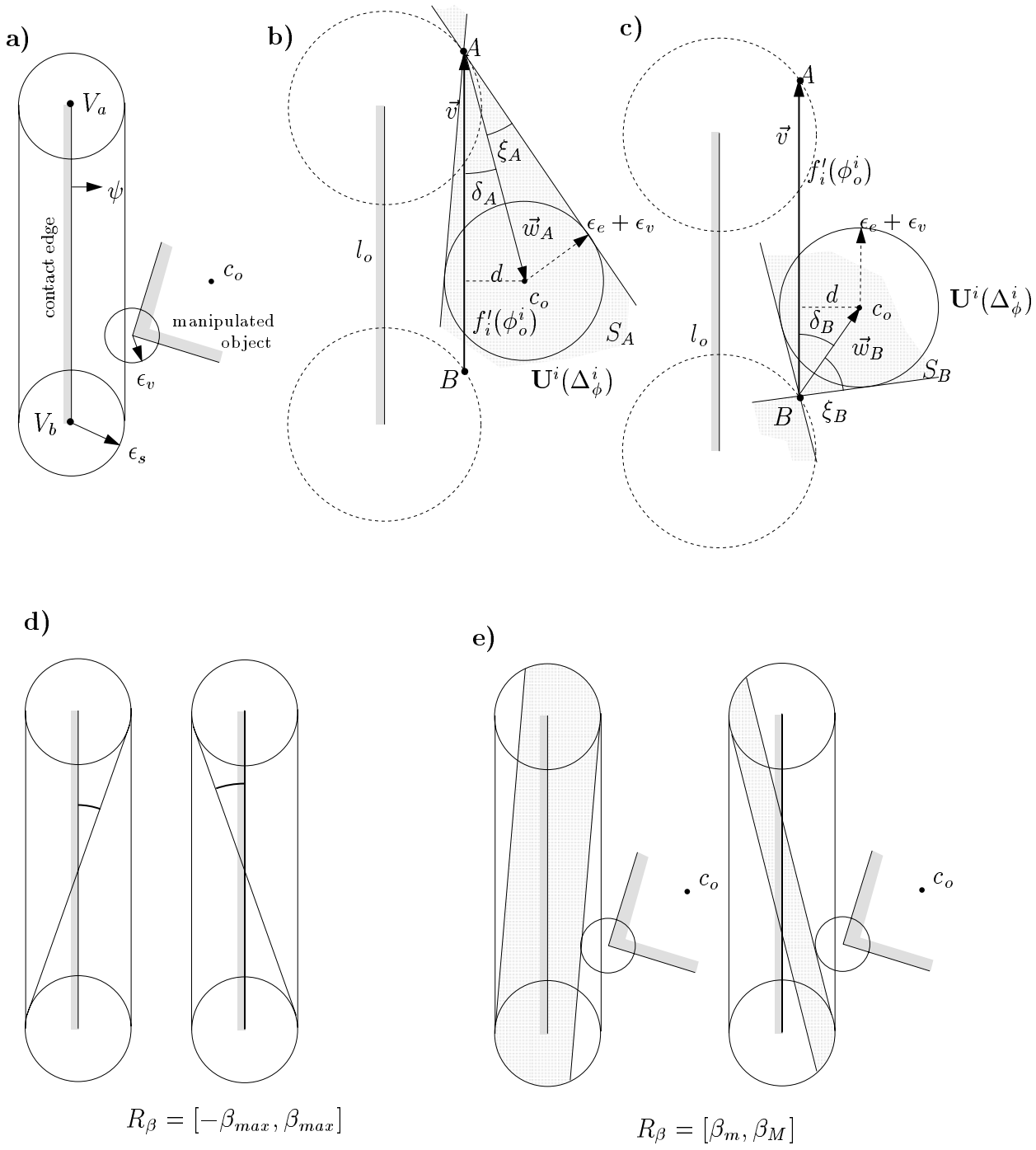

Figure 3.30: *a) Topological elements involved in a type-B basic contact, b) c) boundle of lines, S_A and S_B, crossing the circumference where the contact vertex lies and the circumferences where V_a and V_b lie, respectively, computed in $\mathcal{C}'$-space, d) minimum and maximum deviation of the orientation of the contact edge due to uncertainty, e) minimum and maximum deviation of the orientation of the contact edge due to uncertainty, for a given observed contact configuration c_o.*

Let define (Figures 3.31 and 3.32):

$$d_1 = D_p(\phi_o) - D_f(\phi_o) \quad (3.145)$$

$$d_2 = \epsilon_e + \epsilon_v - |d_1| \quad (3.146)$$

$$d_3 = [\epsilon_v - \frac{d_2}{2}]\text{sign}(d_1) \quad (3.147)$$

where $\text{sign}(d_1) = \frac{|d_1|}{d_1}$ if $d_1 \neq 0$ and $\text{sign}(d_1) = 1$ otherwise, and $D_p(\phi_o)$ and $D_f(\phi_o)$ were defined in Section 3.3.3 as:

- $D_p(\phi_o) = x_o \cos\psi_W + y_o \sin\psi_W$: the component of the vector from the origin of $\{W\}$ to the observed position (x_o, y_o) in the direction ψ_W (for type-A basic contacts $\psi_W = \psi_T + \phi_o + \pi$ and for type-B basic contacts ψ_W is independent of ϕ).
- $D_f(\phi_o)$: the distance from the origin of $\{W\}$ to the line containing $f'(\phi_o)$ as defined in equations (2.4) and (2.5) for type A and type B basic contacts, respectively.

The region where the actual contact vertex lies when contact i occurs at the current observed configuration $c_o = (x_o, y_o, \phi_o)$ is:

(1) $\mathbf{V}(\alpha)$ if $\phi_o \notin R^i_\phi$

(2) $\mathbf{V}(0,0)$ if $\phi_o \in R^i_\phi$ and $\mathbf{V}(0,0) \subset \mathbf{E}(0)$.

(3) $\mathbf{V}(0,0) \cap \mathbf{E}(0)$, otherwise (the shaded region of Figure 3.31a).

Then, the vertex with nominal position (v_x, v_y) is estimated as:

(1) the center of $\mathbf{V}(\alpha)$ if $\phi_o \notin R^i_\phi$

(2) the nominal vertex if $\phi_o \in R^i_\phi$ and $\mathbf{V}(0,0) \subset \mathbf{E}(0)$.

(3) otherwise as:

$$V_e = (v_{x_e}, v_{y_e}) = (v_x + d_3 \cos\psi, v_y + d_3 \sin\psi) \quad (3.148)$$

For type-B basic contacts the estimated vertex will be expressed as:

$$h_e = \sqrt{v_{x_e}^2 + v_{y_e}^2}$$
$$\gamma_e = \arctan(v_{y_e}/v_{x_e}) \quad (3.149)$$

For the analysis of the reaction forces (Section 3.6.1), the region where the actual vertex lies may be approximated by a segment, l_v, which has the following extremes (Figure 3.32):

$$M_x = v_{x_e} + d_v \cos(\psi + \pi/2)$$
$$M_y = v_{y_e} + d_v \sin(\psi + \pi/2)$$
$$N_x = v_{x_e} + d_v \cos(\psi - \pi/2)$$
$$N_y = v_{y_e} + d_v \sin(\psi - \pi/2) \quad (3.150)$$

where, respectively:

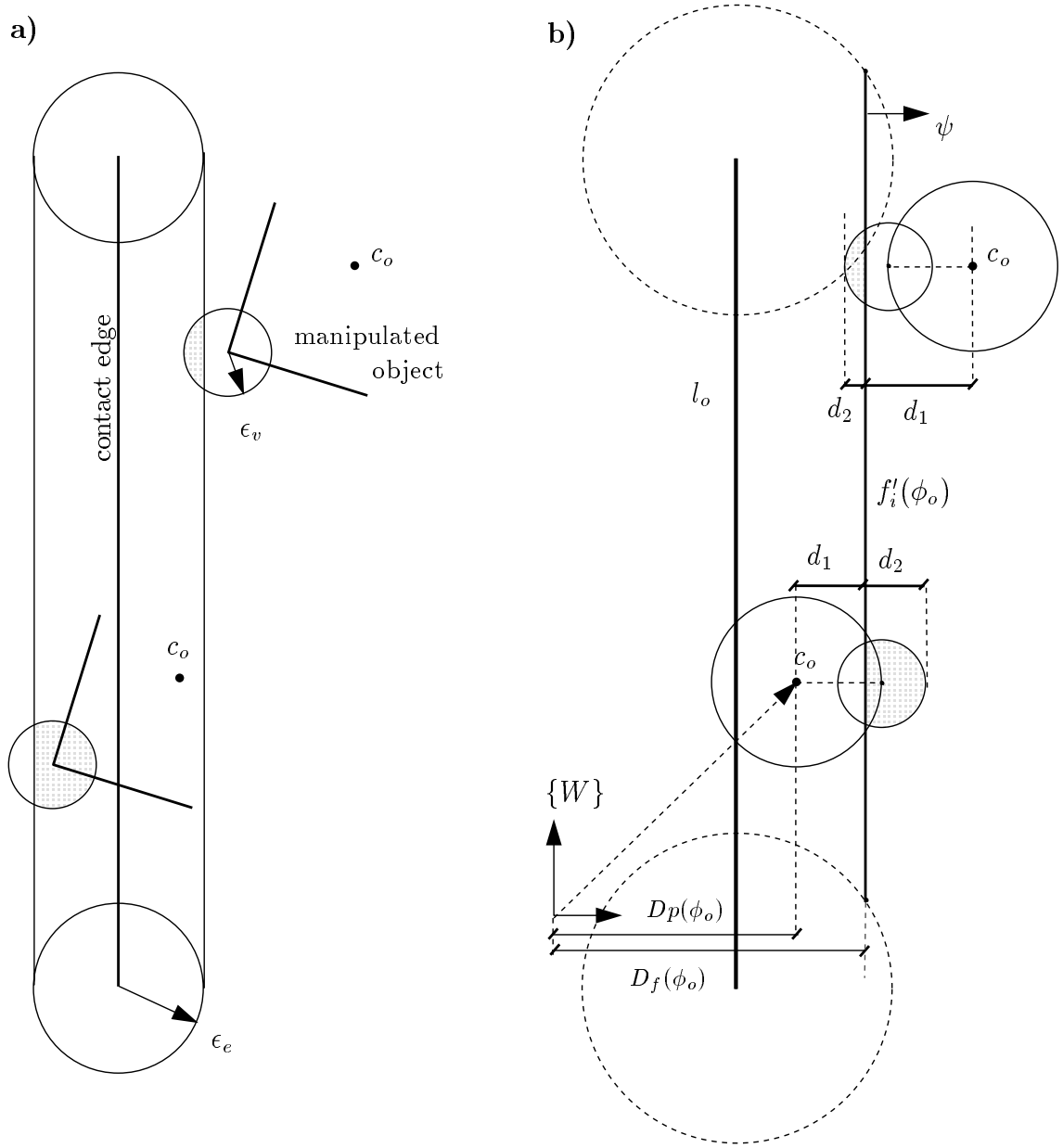

Figure 3.31: *a) Topological elements involved in a type-B basic contact at two configurations of the manipulated object, b) Distances d_1 and d_2.*

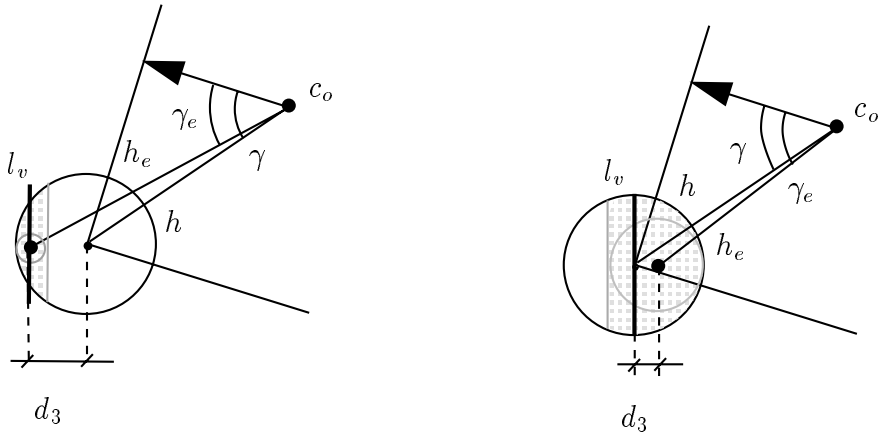

Figure 3.32: *Estimation of the position of the contact edge (h_e and γ_e).*

(1) d_v is expressed by (3.60)

(2) $d_v = \epsilon_v$

(3) d_v is expressed as:

$$d_v = \begin{cases} \epsilon_v \sin[\arccos(\frac{d_2 - \epsilon_v}{\epsilon_v})] & \text{if } d_2 < \epsilon_v \\ \epsilon_v & \text{otherwise} \end{cases} \tag{3.151}$$

3.5.3 Estimation of the position of the contact edge

Given a basic contact i which can occur at a given observed configuration $c_o = (x_o, y_o, \phi_o)$, and the following estimated values:

- β_e, v_{x_e} and v_{y_e} for a type-A basic contact
- β_e, h_e and γ_e for a type-B basic contact

then, the distances d_T and d_W, which determine the position of the contact edge, are estimated as:

$$d_{Te} = D(\phi_o) - v_{x_e}\cos(\psi_T + \phi_o + \pi) - v_{y_e}\sin(\psi_T + \phi_o + \pi) \tag{3.152}$$

$$d_{We} = D(\phi_o) - h_e\cos(\psi_W + \beta_e + \pi - \gamma_e - \phi_o) \tag{3.153}$$

where $D(\phi_o) = x_o\cos(\psi_W + \beta_e) + y_o\sin(\psi_W + \beta_e)$

3.5.4 Modification of the $\mathcal{C}$-arcs

The $\mathcal{C}$-arcs (both $\mathcal{C}_c$-arcs and $\mathcal{C}_f$-arcs) were determined in Chapter 2, being any configuration of the $\mathcal{C}$-arcs expressed as a function of the $\mathcal{C}$-edges of the $\mathcal{C}$-item or $\mathcal{C}$-prism where the $\mathcal{C}$-arc is defined.

The expression of the $\mathcal{C}$-edges were described in equation (2.11) as:

$$\begin{aligned} x &= \frac{D_i \sin(\psi_{Wj}) - D_j \sin(\psi_{Wi})}{\sin(\psi_{Wj} - \psi_{Wi})} \\ y &= -\frac{D_i \cos(\psi_{Wj}) - D_j \cos(\psi_{Wi})}{\sin(\psi_{Wj} - \psi_{Wi})} \\ q &= \rho\phi \end{aligned}$$

where D_k with $k = \{i, j\}$ was described in equations (2.5) and (2.4), depending on the type of basic contact:

$$\begin{aligned} D_k &= x_k \cos\psi_W + y_k \sin\psi_W + d_T \quad \text{for type-A basic contacts} \\ D_k &= h_k \cos(\psi_W + \pi - \gamma_k - \phi) + d_W \quad \text{for type-B basic contacts} \end{aligned} \tag{3.154}$$

Therefore, the $\mathcal{C}$-arcs, which were off-line determined from the nominal geometry, can be on-line modified by changing the nominal values describing the position of the contact vertex and the position and orientation of the contact edge by the corresponding estimated values computed in the previous Sections.

3.6 Force analysis

Let assume that the force sensor has its reference frame coincident with $\{T\}$, the reference frame of the manipulated object.

Definition: The Generalized Force Domain $\mathbf{G}_S$, associated to a observed configuration c_o compatible with a contact situation C_S involving a set S of basic contacts, is the set of the generalized reaction forces that may arise when C_S takes place at configuration c_o.

Let $\mathbf{G}'_S$ be the dual representation of $\mathbf{G}_S$.

3.6.1 One basic contact situations

The Generalized Force Domain $\mathbf{G}_i$ of a contact situation with only one basic contact i is composed of the forces satisfying the following two conditions:

- *Contact-point condition:* the line of the reaction force must intersect the region where the contact vertex may lie for the current observed contact configuration c_o.
- *Direction condition:* The direction of the reaction force must be in the range $[\psi - \epsilon_\psi, \psi + \epsilon_\psi]$ where ψ is the normal to the contact edge and ϵ_ψ is the deviation that takes into account the effect of friction and of the uncertainties affecting the direction of the reaction force.

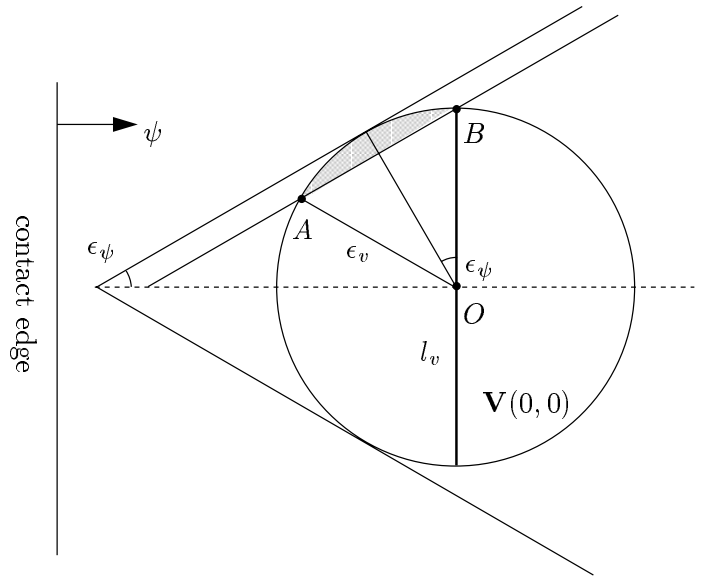

Figure 3.33: *Approximation of region* $\mathbf{V}(0,0)$ *by the segment* l_v.

Contact-point condition

The region where the contact vertex may lie for the observed contact configuration c_o has been determined in Section 3.5.2. The maximum area of this region is obtained for the deviation α with minimum absolute value, and for the orientation ϕ_o^i. In order to compute $\mathbf{G}_i$, this region is approximated by the segment l_v, since nearly all the lines of forces intersecting this region will intersect l_v. The maximum error introduced by this approximation is produced when the region is the circle $\mathbf{V}(0,0)$. This maximum error is computed as follows (Figure 3.33). Let A_{sector} and $A_{triangle}$ be the areas of the sector and the triangle formed with the points A, B and the origin O. Then the area A of the shadded region represents the area not considered by the approximation:

$$A = A_{sector} - A_{triangle} = \epsilon_v^2(\epsilon_\psi - \sin\epsilon_\psi \cos\epsilon_\psi) \tag{3.155}$$

Then:

$$\text{error} = \frac{A}{A_{\mathbf{V}(0,0)}} = \frac{\epsilon_v^2(\epsilon_\psi - \sin\epsilon_\psi\cos\epsilon_\psi)}{\pi\epsilon_v^2} = \frac{\epsilon_\psi - \sin\epsilon_\psi\cos\epsilon_\psi}{\pi} \tag{3.156}$$

For example, if $\epsilon_\psi = \pi/6$ then the error is 12%.

Direction condition

The reaction force direction is determined by the direction ψ of the normal to the contact edge when no uncertainty and friction are considered. When these effects are taken into account, the reaction force direction belongs to the range:

$$[\psi + \beta^m - \arctan\mu - \frac{\Delta\phi_l}{2}, \psi + \beta^M + \arctan\mu + \frac{\Delta\phi_l}{2}] \tag{3.157}$$

where:

- $[-\arctan\mu, \arctan\mu]$ is the range of deviations due to the effect of friction, μ being the friction coefficient.
- $[\beta^m, \beta^M]$ is the range of deviations due to the uncertainty in the orientation of the contact edge (Section 3.5.1).
- $[-\frac{\Delta\phi_l}{2}, \frac{\Delta\phi_l}{2}]$ is the range of deviations due to the uncertainty in the orientation of the robot, taking into account the current observed configuration:

$$\Delta\phi_l \leq \phi_{o_M} - \phi_{o_m} \tag{3.158}$$

$\Delta\phi_l$ is computed as follows. Let define (Figure 3.34):

$(x_{o_m}, y_{o_m}) = (x_o - (\epsilon_e + \epsilon_v)\cos\psi, y_o - (\epsilon_e + \epsilon_v)\sin\psi)$

$(x_{o_M}, y_{o_M}) = (x_o + (\epsilon_e + \epsilon_v)\cos\psi, y_o + (\epsilon_e + \epsilon_v)\sin\psi)$

$D_{p_m}(\phi_o^i) = x_{o_m}\cos\psi_W + y_{o_m}\sin\psi_W$

$D_{p_M}(\phi_o^i) = x_{o_M}\cos\psi_W + y_{o_M}\sin\psi_W$

$d_{p_m}(\phi_o^i)$: distance from the line containing $f'(\phi_o^i)$ to the position (x_{o_m}, y_{o_m})

$$d_{p_m}(\phi_o^i) = |D_{p_m}(\phi_o^i) - D_f(\phi_o^i)| \tag{3.159}$$

$d_{p_M}(\phi_o^i)$: distance from the line containing $f'(\phi_o^i)$ to the position (x_{o_M}, y_{o_M})

$$d_{p_M}(\phi_o^i) = |D_{p_M}(\phi_o^i) - D_f(\phi_o^i)| \tag{3.160}$$

ϕ_{l_m}, ϕ_{l_M}: orientations that satisfy $d_{p_m}(\phi_{l_m}) = 0$ and $d_{p_M}(\phi_{l_M}) = 0$, respectively. They are obtained from equations (3.46) and (3.49) for type-A and type-B basic contacts, respectively:

If $\phi_{l_m} < \phi_{o_m}$ or if ϕ_{l_m} does not exist, then $\phi_{l_m} = \phi_{o_m}$

If $\phi_{l_M} > \phi_{o_M}$ or if ϕ_{l_M} does not exist, then $\phi_{l_M} = \phi_{o_M}$

Finally, $\Delta\phi_l = \phi_{l_M} - \phi_{l_m}$.

Estimation of the orientation of the contact edge

The observed generalized force can also be used to constrain R_β (as done in Section 3.5.1 from the configuration information), when the basic contact i is the only one compatible with the observed configuration and force. Let define (Figure 3.35):

$\vec{f}$: the observed force

Ψ: orientation of the observed force with respect to the world reference frame

δ: maximum deviation in the direction of the force due to the force sensor uncertainty

μ: friction coefficient

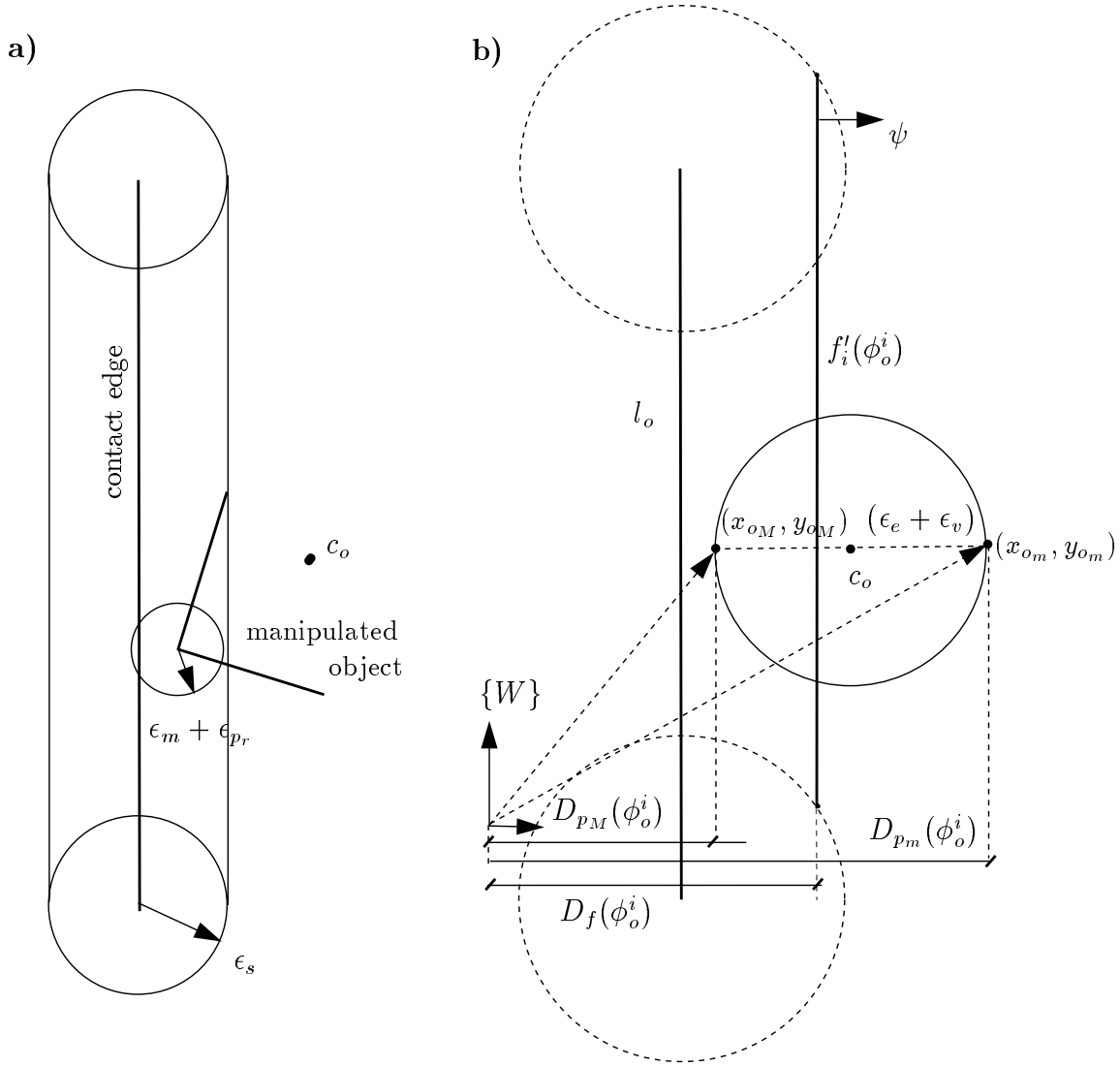

Figure 3.34: *a) Topological elements involved in a type-B basic contact b) Positions* (x_{o_m}, y_{o_m}) *and* (x_{o_M}, y_{o_M}) *involved in the computation of* $\Delta\phi_l$.

Then, the minimum and maximum values of β compatible with the observed force are:

$$\begin{aligned} \beta^f_{min} &= \Psi - \delta - \arctan\mu - \psi \\ \beta^f_{max} &= \Psi + \delta + \arctan\mu - \psi \end{aligned} \tag{3.161}$$

and then, the range R_β is updated as:

$$\begin{aligned} \beta_m &= \max(\beta_m, \beta^f_{min}) \\ \beta_M &= \min(\beta_M, \beta^f_{max}) \end{aligned} \tag{3.162}$$

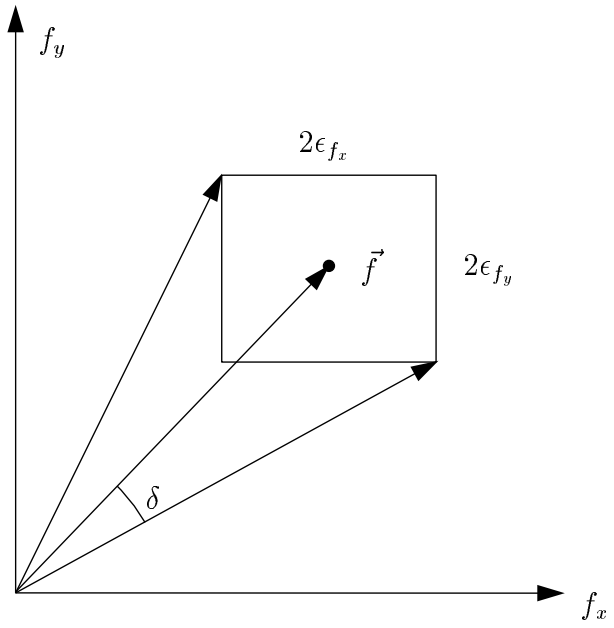

Figure 3.35: *Uncertainty in the direction of the reaction force.*

Dual representation of $\mathbf{G}_i$

The dual representation of the Force Generalized Domain $\mathbf{G}_i$ is computed as follows. Let define (Figure 3.36):

a, c : lines with orientation $\psi + \beta^m - \arctan\mu - \frac{\Delta\phi_l}{2}$ passing through the extremes of the segment l_v.

b, d : lines with orientation $\psi + \beta^M + \arctan\mu + \frac{\Delta\phi_l}{2}$ passing through the extremes of the segment l_v.

$\mathbf{W}$: region where the lines of forces of $\mathbf{G}_i$ lie; it is the union of cones $\widehat{ab}$ and $\widehat{cd}$.

$\mathbf{W}_0$: region $\mathbf{W}$ computed when $\mu = 0$.

The dual region representing the forces satisfying the contact-point condition is the cone $\widehat{m'n'}$, where m' and n' are the dual lines of the extremes M and N of the segment l_v, i.e. the cone $\widehat{m'n'}$ is the set of dual points of the lines of forces crossing l_v (property 5 in Appendix B).

The dual region representing the forces satisfying the direction condition is the cone $\widehat{a'b'}$, where a' and b' are lines perpendicular to a and b, respectively, passing through the origin, i.e. the cone $\widehat{a'b'}$ is the set of dual points of all the lines of forces with orientation within the range defined by the orientations of a and b, i.e. $[\psi + \beta^m - \arctan\mu - \frac{\Delta\phi_l}{2}, \psi + \beta^M + \arctan\mu + \frac{\Delta\phi_l}{2}]$ (property 3 in Appendix B).

Then, $\mathbf{G}'_i$ is:

$$\mathbf{G}'_i = \widehat{m'n'} \cap \widehat{a'b'} \tag{3.163}$$

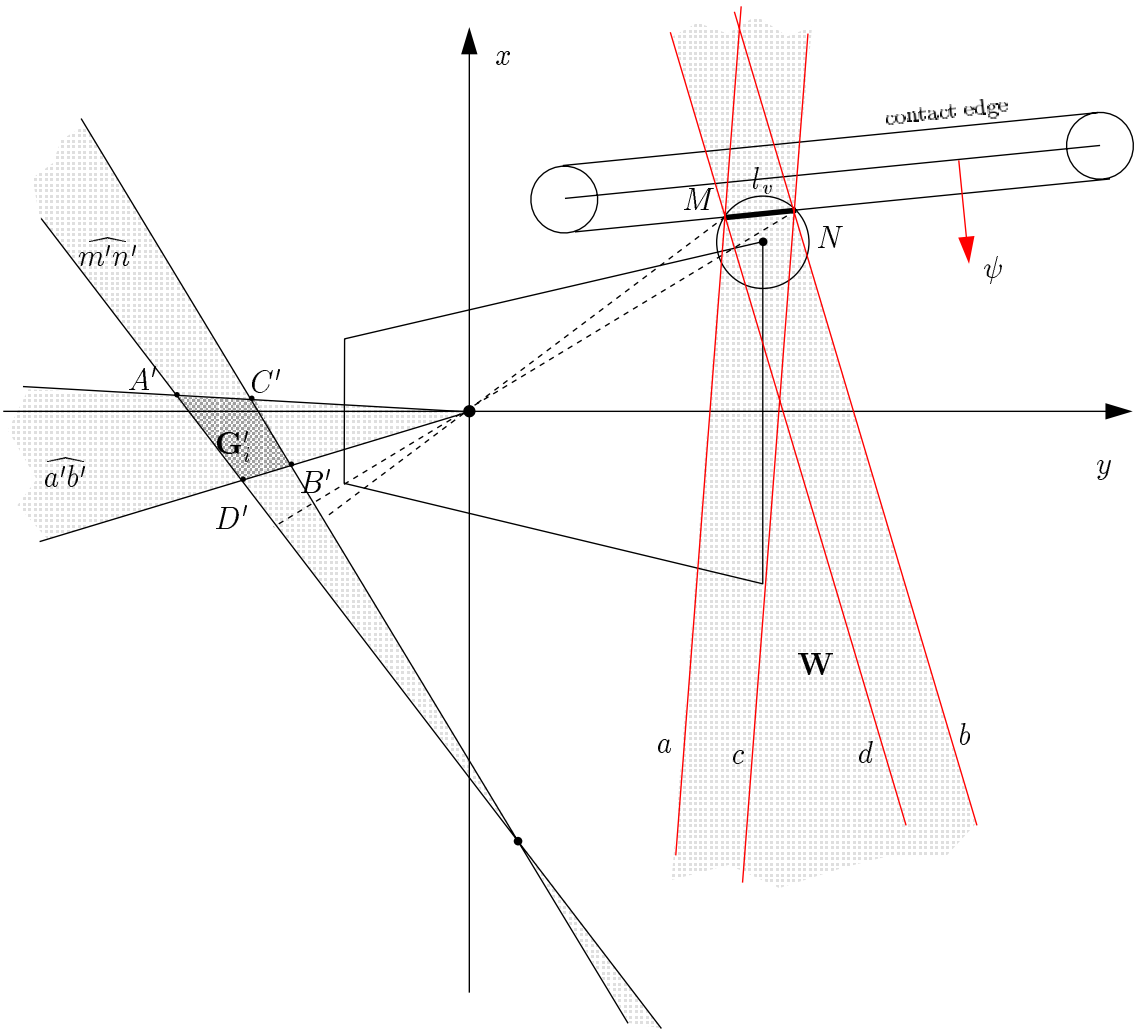

Figure 3.36: *Dual representation of* $\mathbf{G}_i$.

Let $\mathcal{H}(P_1, ..., P_n)$ be the convex hull defined by the points $P_1, ..., P_n$. The points of $\mathbf{G}'_i$ are the dual points of the lines of $\mathbf{W}$, and its vertices are the dual points A', B', C' and D' of the lines a, b, c and d, respectively. Then:

$$\mathbf{G'}_i = \mathcal{H}(A', B', C'D') \tag{3.164}$$

Partition of the dual plane

The dual plane has been partitioned in Section 2.8.3 into regions that bound the directions of applied forces that produce similar movements of the manipulated object (i.e. produce the same sense of sliding and rotation about the contact point, or produce sticking at it). The border of these regions is determined by the dual lines π'_t, π'_f and π'_r representing the planes defined by the *contact reference frame* (Π_t, Π_f and Π_r, respectively).

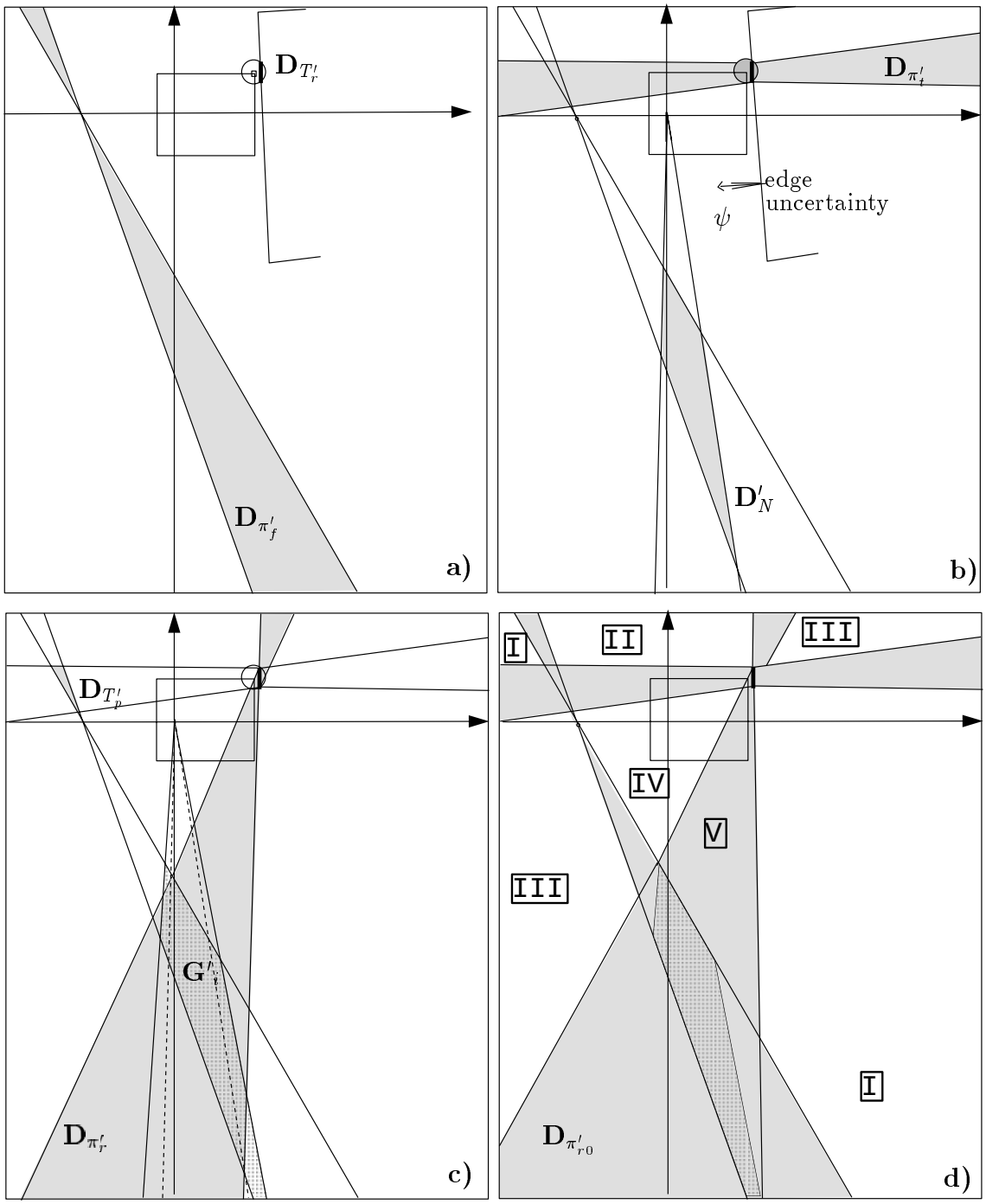

Figure 3.37: *a) Regions* $\mathbf{D}_{T'_r}$ *and* $\mathbf{D}_{\pi'_f}$ *b) Regions* $\mathbf{D}_{N'}$ *and* $\mathbf{D}_{\pi'_t}$ *c) Regions* $\mathbf{D}_{T'_p}$ *and* $\mathbf{D}_{\pi'_r}$ *d) Partition of the dual plane.*

Let $\mathbf{D}_{\pi'_t}$, $\mathbf{D}_{\pi'_f}$, $\mathbf{D}_{\pi'_r}$ $\mathbf{D}_{T'_r}$, $\mathbf{D}_{N'}$ and $\mathbf{D}_{T'_p}$ be the regions where the dual lines π'_t, π'_f and π'_r, and the dual points T'_r, N' and T_p may lie due to uncertainty (Figure 3.37). Then, the algorithm to partition the dual plane shown in Section 2.8.3 is modified as follows when uncertainty is considered.

Dual-plane-partition()

(1) Compute $\mathbf{D}_{T'_r}$ as the segment l_v

(2) Compute $\mathbf{D}_{\pi'_f}$ as the cone $\widehat{mn}$ (the dual region of l_v)

(3) Compute $\mathbf{D}_{\pi'_t}$ as the region $\mathbf{W}_0$

(4) Compute $\mathbf{D}_{N'}$ as the dual region of $\mathbf{D}_{\pi'_t}$

(5) Compute $\mathbf{G}'_i$ as the dual region of $\mathbf{W}$

(6) Compute $\mathbf{D}_{T'_p}$ as the resulting parallelogram of the intersection of $\mathbf{D}_{\pi'_f}$ and $\mathbf{D}_{\pi'_t}$.

(7) Compute $\mathbf{D}_{\pi'_r}$ as the dual region of $\mathbf{D}_{T'_p}$.

(8) Compute $\mathbf{D}_{\pi'_{r0}}$ as the dual region of $\mathbf{D}_{\pi'_f} \cap \mathbf{W}$

END

In step (4), the edges of $\mathbf{D}_{N'}$ can be obtained by computing the dual segments of the cones composed with the lines of the border of $\mathbf{D}_{\pi'_t}$. In step (7), the dual region of $\mathbf{D}_{T'_p}$ can be computed as the union of the dual cones of the edges of $\mathbf{D}_{T'_p}$.

The partition of the dual plane considering uncertainty is used in Chapter 4 to determine if an applied velocity command can produce an error-corrective compliant motion.

3.6.2 More than one basic contact situations

The Generalized Force Domain $\mathbf{G}_S$ of a contact situation involving a set S of basic contacts, which can simultaneously ocurr taking into account the uncertainties, is the set of the forces resulting from the composition of all possible compatible reaction forces, one at each basic contact. Therefore, the dual representation $\mathbf{G}'_S$ is the set of all non-negative linear combinations of possible compatible dual reaction forces, one at each basic contact.

Let s be any sub-set of S with $\inf(n-1, 3)$ basic contacts.

Proposition 14:

$$\mathbf{G}_S \supset \bigcup_{\forall s \subset S} \mathbf{G}_s \tag{3.165}$$

Proof: If a generalized reaction force $\vec{g}_o$ satisfies $\vec{g} \in \mathbf{G}_s$, then it is the resultant of one force at each of the basic contacts of s and zero force at the other(s). Therefore $\vec{g} \in \mathbf{G}_S$.

$\diamond$

From proposition 14, $\mathbf{G}'_S$ can be expressed as:

$$\mathbf{G}'_S = \left[\bigcup_{\forall s \subset S} \mathbf{G}'_s \right] \cup [\mathbf{H}'_S] \tag{3.166}$$

$\mathbf{H}'_S$ being a dual region associated to the basic contacts of S.

Proposition 15: For a contact situation with only one basic contact i, $\mathbf{H}'_i = \mathbf{G}'_i$.

Proof: For $n = 1$ the sets s are empty sets then $\bigcup_{\forall s \subset S} \mathbf{G}'_s = \emptyset$. ◇

Proposition 16: For a contact situation with two basic contacts i and j, $\mathbf{G}'_{ij} = \mathbf{G}'_i \cup \mathbf{G}'_j \cup \mathbf{H}'_{ij}$, with $\mathbf{H}'_{ij} = \mathcal{H}(A'_i, B'_i, A'_j, B'_j) \cup \mathcal{H}(A'_i, B'_i, C'_j, D'_j) \cup \mathcal{H}(C'_i, D'_i, A'_j, B'_j) \cup \mathcal{H}(C'_i, D'_i, C'_j, D'_j)$.

Figure 3.38 shows the four convex hulls that compose the region $\mathbf{H}'_{ij}$ and Figure 3.39 shows the domain $\mathbf{G}'_{ij} = \mathbf{G}'_i \cup \mathbf{G}'_j \cup \mathbf{H}'_{ij}$.

Proof:

Claim 1: Since $\mathbf{G}'_i$ is a trapezium, any point $F'_i \in \mathbf{G}'_i$ can be expressed as a linear combination of two points, F'_{1i} and F'_{2i}, belonging to the diagonals $\overline{A'B'}$ and $\overline{C'D'}$, respectively, (i.e. $F'_i \in \overline{F'_{1i}F'_{2i}}$) and satisfying $\overline{F'_{1i}F'_{2i}} \subset \mathbf{G}'_i$.

Claim 2: $\forall F'_{ij} \in \mathbf{G}'_{ij}$ there exists a trapezium $\mathbf{Q}'_F$ with border $\partial\mathbf{Q}'_F$ such that $F'_{ij} \in \mathbf{Q}'_F$ and $\partial\mathbf{Q}'_F \subset (\mathbf{G}'_i \cup \mathbf{G}'_j \cup \mathbf{H}'_{ij})$. Being $F'_{ij} \in \mathbf{G}'_{ij}$ a linear combination with positive coefficients of $F'_i \in \mathbf{G}'_i$ and $F'_j \in \mathbf{G}'_j$, then, from claim 1, $F'_{ij} \in \mathbf{Q}'_F$, with $\mathbf{Q}'_F = \mathcal{H}(F'_{1i}, F'_{2i}, F'_{1j}, F'_{2j})$. The edges of $\partial\mathbf{Q}'_F$ whose vertices are on the same domain belong to that domain (from claim 1). The edges of $\partial\mathbf{Q}'_F$ whose vertices are on different domains belong to $\mathbf{H}'_{ij}$ because the vertices are on the diagonals of the domains and these diagonals are the segments that define $\mathbf{H}'_{ij}$.

Claim 3: $\mathbf{G}'_i \cup \mathbf{G}'_j \cup \mathbf{H}'_{ij}$ has no holes. Each of the four trapeziums that define $\mathbf{H}'_{ij}$ can be decomposed into two trapeziums sharing the edge formed by the intersection points of the two diagonals of each domain. The union of trapeziums sharing an edge has no holes, then as $\mathbf{H}'_{ij}$ is the result of the union of eight trapeziums sharing an edge, it results that $\mathbf{H}'_{ij}$ has no holes. On the other side, as neither $\mathbf{G}'_i$ nor $\mathbf{G}'_j$ have holes and all the vertices of $\mathbf{H}'_{ij}$ belong to $\mathbf{G}'_i$ or $\mathbf{G}'_j$, the union of $\mathbf{G}'_i$, $\mathbf{G}'_j$ and $\mathbf{H}'_{ij}$ have no holes.

Claim 4: $\mathbf{G}'_{ij} \subset (\mathbf{G}'_i \cup \mathbf{G}'_j \cup \mathbf{H}'_{ij})$. From claim 2 and 3, $\forall F'_{ij} \in \mathbf{G}'_{ij}$ there exists a trapezium $\mathbf{Q}'_F$ that satisfies $F'_{ij} \in \mathbf{Q}'_F$ and $\mathbf{Q}'_F \subset (\mathbf{G}'_i \cup \mathbf{G}'_j \cup \mathbf{H}'_{ij})$.

Claim 5: $(\mathbf{G}'_i \cup \mathbf{G}'_j \cup \mathbf{H}'_{ij}) \subset \mathbf{G}'_{ij}$. $\mathbf{H}'_{ij} \subset \mathbf{G}'_{ij}$ because the trapeziums that determine $\mathbf{H}'_{ij}$ are build with the diagonals of $\mathbf{G}'_i$ and $\mathbf{G}'_j$. Also, by definition, $\mathbf{G}'_i \subset \mathbf{G}'_{ij}$ and $\mathbf{G}'_j \subset \mathbf{G}'_{ij}$.

From claims 4 and 5 $\mathbf{G}'_{ij} = \mathbf{G}'_i \cup \mathbf{G}'_j \cup \mathbf{H}'_{ij}$. ◇

Proposition 17: For a contact situation with three basic contacts i, j and k, $\mathbf{G}'_{ijk} = \mathbf{G}'_{ij} \cup \mathbf{G}'_{ik} \cup \mathbf{G}'_{jk} \cup \mathbf{H}'_{ijk}$, with $\mathbf{H}'_{ijk} = \mathcal{H}(F'_i, F'_j, F'_k)$, for any $F'_i \in \mathbf{G}'_i$, $F'_j \in \mathbf{G}'_j$ and $F'_k \in \mathbf{G}'_k$.

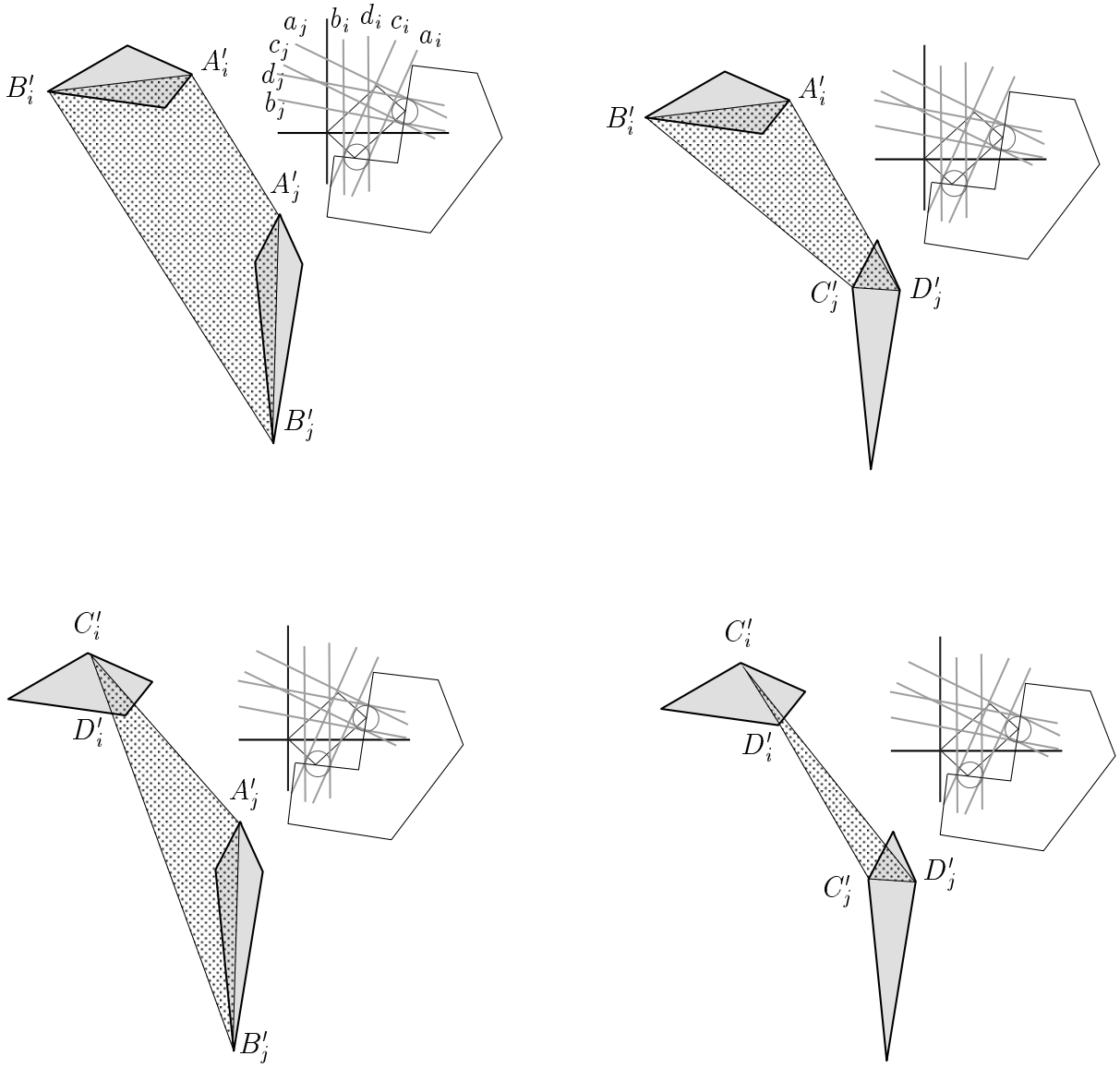

Figure 3.38: Regions $\mathcal{H}(A_i', B_i', A_j', B_j')$, $\mathcal{H}(A_i', B_i', C_j', D_j')$, $\mathcal{H}(C_i', D_i', A_j', B_j')$ and $\mathcal{H}(C_i', D_i', C_j', D_j')$.

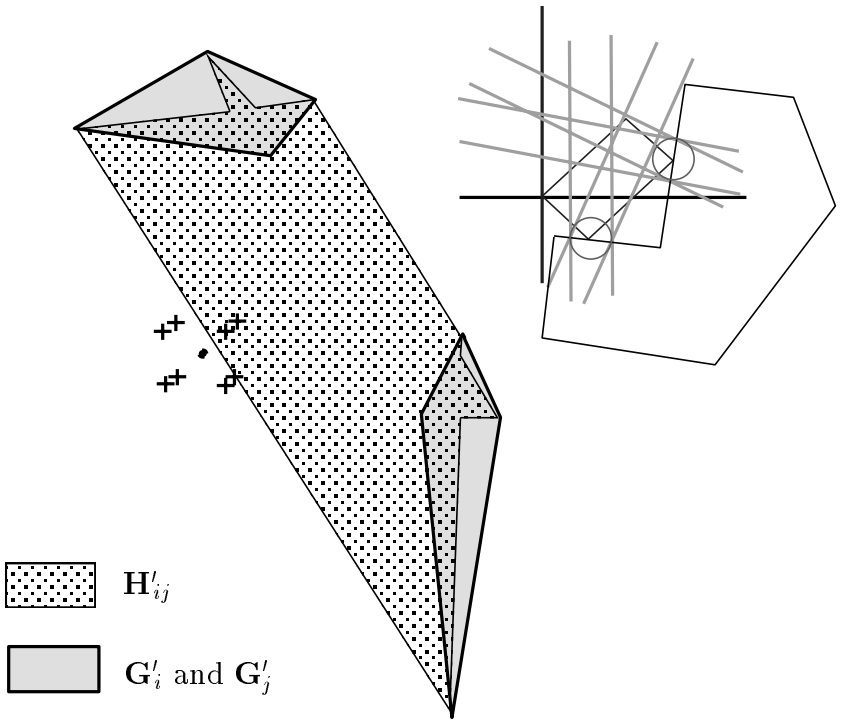

Figure 3.39: Generalized Force Domain $\mathbf{G}'_{ij} = \mathbf{G}'_i \cup \mathbf{G}'_j \cup \mathbf{H}'_{ij}$.

Proof: Let $F'_{ijk} \in \mathbf{G}'_{ijk}$ be a linear combination of any $N'_i \in \mathbf{G}'_i$, $N'_j \in \mathbf{G}'_j$ and $N'_k \in \mathbf{G}'_k$ and let define $\mathbf{N}' = \mathcal{H}(N'_i, N'_j, N'_k)$.

Claim 1: The border of $\mathbf{N}'$ *satisfies* $\partial\mathbf{N}' \subset (\mathbf{G}'_{ij} \cup \mathbf{G}'_{ik} \cup \mathbf{G}'_{jk} \cup \mathbf{H}'_{ijk})$. By construction, $\partial\mathbf{N}' = \overline{N'_iN'_j} \cup \overline{N'_iN'_k} \cup \overline{N'_jN'_k}$ and $\overline{N'_iN'_j} \subset \mathbf{G}'_{ij}$, $\overline{N'_iN'_k} \subset \mathbf{G}'_{ik}$ and $\overline{N'_jN'_k} \subset \mathbf{G}'_{jk}$.

Claim 2: $\mathbf{G}'_{rs} \cap \mathbf{G}'_{rt}$ *is a connected region* $\forall\ r, s, t \in \{i, j, k\}$. Since $\mathbf{G}'_r$ is a connected region that satisfies $\mathbf{G}'_r \subset (\mathbf{G}'_{rs} \cap \mathbf{G}'_{rt})$ then $\forall P' \in (\mathbf{G}'_{rs} \cap \mathbf{G}'_{rt})$ such that $P' \notin \mathbf{G}'_r$, there should exist a path p that connects P' with $\mathbf{G}'_r$ and that satisfies $p \subset (\mathbf{G}'_{rs} \cap \mathbf{G}'_{rt})$. Let $R'_s \in \partial\mathbf{G}'_r$, $R'_t \in \partial\mathbf{G}'_r$, $S' \in \mathbf{G}'_s$ and $T' \in \mathbf{G}'_t$ be points that satisfy $P' \in \overline{R'_sS'}$, $P' \in \overline{R'_tT'}$, $\overline{P'R'_t} \not\subset \mathbf{G}'_r$ and $\overline{P'R'_s} \not\subset \mathbf{G}'_r$ (Figure 3.40); then:

a) $\overline{P'R'_s} \subset \mathbf{G}'_{rs}$, since $\overline{P'R'_s} \subset \overline{R'_sS'}$ and $\overline{R'_sS'} \subset \mathbf{G}'_{rs}$.

b) $\overline{P'R'_s} \subset \mathbf{G}'_{rt}$ since as $\overline{R'_tT'} \subset \mathbf{G}'_{rt}$, $\overline{R'_sT'} \subset \mathbf{G}'_{rt}$ and $\partial\mathbf{G}'_r$ is a closed line, then $\forall Q' \in \overline{P'R'_s}$ there exists a segment $\overline{R'T'}$ with $R' \in \partial\mathbf{G}'_r$ such that $Q' \in \overline{R'T'}$ and therefore as $\overline{R'T'} \subset \mathbf{G}'_{rt}$ then $Q' \in \mathbf{G}'_{rt}$.

From a) and b) $\overline{P'R'_s}$ is the path p that connects P' with $\mathbf{G}'_r$ and that satisfies $p \subset (\mathbf{G}'_{rs} \cap \mathbf{G}'_{rt})$.

Claim 3: $(\mathbf{G}'_{ij} \cup \mathbf{G}'_{ik} \cup \mathbf{G}'_{jk} \cup \mathbf{H}'_{ijk})$ *has no holes.* From claim 2 $\forall\ r, s, t \in \{i, j, k\}$ such that $r \neq s \neq t$, $\mathbf{G}'_{rs} \cup \mathbf{G}'_{rt}$ has no holes and, since by construction $\partial\mathbf{N}'$ is convex and from claim 1 $\partial\mathbf{N}' \subset (\mathbf{G}'_{ij} \cup \mathbf{G}'_{ik} \cup \mathbf{G}'_{jk})$, then $(\mathbf{G}'_{rs} \cup \mathbf{G}'_{rt} \cup \mathbf{H}'_{ijk})$ has no holes. As this is satisfied $\forall\ r, s, t \in \{i, j, k\}$ then $(\mathbf{G}'_{ij} \cup \mathbf{G}'_{ik} \cup \mathbf{G}'_{jk} \cup \mathbf{H}'_{ijk})$ has no holes.

Claim 4: $\mathbf{G}'_{ijk} \subset (\mathbf{G}'_{ij} \cup \mathbf{G}'_{ik} \cup \mathbf{G}'_{jk} \cup \mathbf{H}'_{ijk})$. From claims 1 and 3 $\mathbf{N}' \subset (\mathbf{G}'_{ij} \cup \mathbf{G}'_{ik} \cup \mathbf{G}'_{jk} \cup \mathbf{H}'_{ijk})$, $\forall F'_{ijk} \in \mathbf{G}'_{ijk}$.

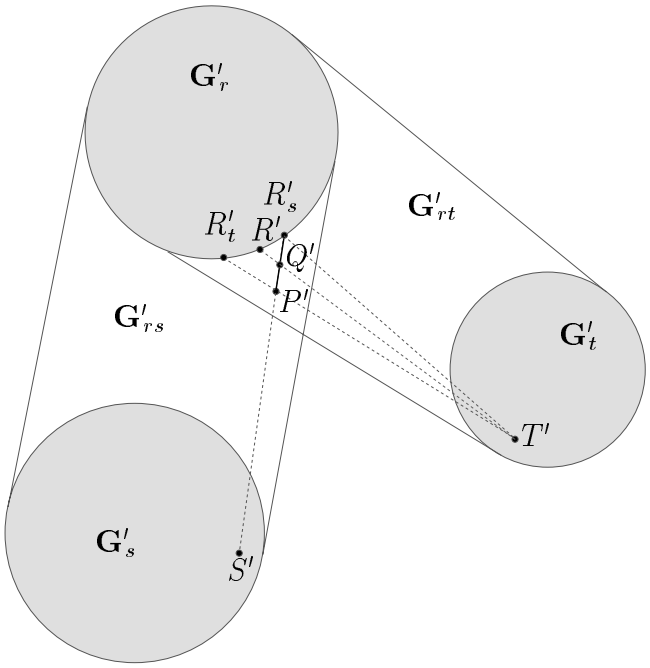

Figure 3.40: $\mathbf{G}'_{rs} \cap \mathbf{G}'_{rt}$ *is a connected region* $\forall\, r, s, t \in \{i, j, k\}$.

Claim 5: $(\mathbf{G}'_{ij} \cup \mathbf{G}'_{ik} \cup \mathbf{G}'_{jk} \cup \mathbf{H}'_{ijk}) \subset \mathbf{G}'_{ijk}$. By definition $\mathbf{G}'_{ij} \subset \mathbf{G}'_{ijk}$, $\mathbf{G}'_{ik} \subset \mathbf{G}'_{ijk}$, $\mathbf{G}'_{jk} \subset \mathbf{G}'_{ijk}$ and $\mathbf{H}'_{ijk} \subset \mathbf{G}'_{ijk}$.

From claims 4 and 5 $\mathbf{G}'_{ijk} = \mathbf{G}'_{ij} \cup \mathbf{G}'_{ik} \cup \mathbf{G}'_{jk} \cup \mathbf{H}'_{ijk}$. ◇

Proposition 18: For a contact situation with $n > 3$ basic contacts $\mathbf{H}'_S = \emptyset$.

Proof: Since planar movements have only three degrees of freedom $\bigcup_{\forall s \subset S} \mathbf{G}'_s$ cover all the possible non-negative linear combinations spanned by the n basic contacts. ◇

3.6.3 Contact identification from force information

An observed generalized reaction force $\vec{g}_o$ is compatible with the contact situation determined by a set S of n basic contacts iff [7]:

$$U_g \cap \mathbf{G}_S \neq \emptyset \tag{3.167}$$

where U_g is the uncertainty force parallelepiped centered at $\vec{g}_o$ (Section 3.1.2). Figure 3.41 shows U_g together with its dual representation U'_g.

Condition (3.167) is expressed in the dual plane as:

$$U'_g \cap \mathbf{G}'_S \neq \emptyset \tag{3.168}$$

From equation (3.166), this condition is satisfied if and only if at least one of the following two conditions is satisfied:

$$U'_g \cap [\bigcup \mathbf{G}'_s] \neq \emptyset \tag{3.169}$$

$$U'_g \cap \mathbf{H}'_S \neq \emptyset \tag{3.170}$$

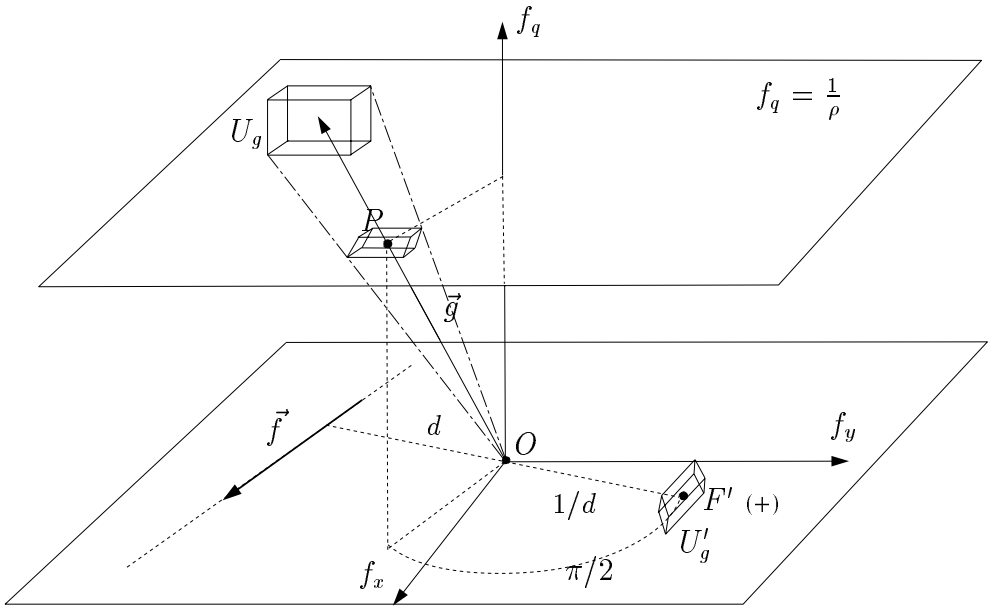

Figure 3.41: Generalized force uncertainty U_g and its representation U'_g.

Given an observed reaction force $\vec{g}_o$ and the domain $\mathbf{G}'_S$ of a contact situation, the following algorithm evaluates the above conditions. The algorithm returns "compatible" when $\vec{g}_o$ is compatible with $\mathbf{G}'_S$ and "incompatible" otherwise; this result is stored in a global variable R_S that is used to speed up further evaluations of condition (3.169) for other contact situations. The function test($\mathbf{H}'_S$, $\vec{g}_o$) directly evaluates condition (3.170) for a given observed reaction force $\vec{g}_o$; it returns "true" when the condition is satisfied and "false" otherwise.

classify($\mathbf{G}'_S$, $\vec{g}_o$)

FOR each $s \in S$
  IF $\mathbf{G}'_s$ has not been yet classified THEN R_s = classify($\mathbf{G}'_s, \vec{g}_o$)
  IF R_s = "compatible" THEN
    R_S = "compatible"
    RETURN R_S

cond. (3.169)

IF test($\mathbf{H}'_S, \vec{g}_o$) = "true" THEN R_S = "compatible"
ELSE R_S = "incompatible"
RETURN R_S

cond. (3.170)

END

For a given observed force $\vec{g}_o$, let define:

V'_q: the dual point representing the generalized force with head on vertex q of U_g, with $q \in \{1, ..., 8\}$.

e'_q: the straight segment containing the dual points representing the generalized forces with heads on the edge q of U_g, with $q \in \{1, ..., 12\}$.

$\mathbf{P}'_q$: the polygon containing the dual points representing the generalized forces with heads on the face q of U_g, with $q \in \{1, ..., 6\}$.

E_q: the dual point of the line that contains e'_q.

The function test evaluates condition (3.170) by sequentially testing the following three conditions and returning "true", as soon as one of them is satisfied, or "false" otherwise:

$$V'_q \in \mathbf{H}'_S, \quad \text{for any} \quad q \in \{1, ..., 8\} \tag{3.171}$$

$$e'_q \cap \mathbf{H}'_S \neq \emptyset, \quad \text{for any} \quad q \in \{1, ..., 12\} \tag{3.172}$$

$$\mathbf{P}'_q \supset \mathbf{H}'_S, \quad \text{for any} \quad q \in \{1, ..., 6\} \tag{3.173}$$

The evaluation of any of the conditions (3.171) to (3.173) assumes that the previous ones are not satisfied and it is performed in a different way depending on the number of the basic contacts involved, as it is specified below.

One Basic Contact i

From proposition 15 and equation (3.163):

- *Condition* (3.171) is satisfied if V'_q belongs to both $\widehat{m'n'}$ and $\widehat{a'b'}$:

$$[V'_q \in \widehat{m'n'}] \text{ AND } [V'_q \in \widehat{a'b'}] \tag{3.174}$$

  Figure 3.42a shows a case in which the dual representations of two vertices of U_g are inside $\mathbf{G}'_i$.

- *Condition* (3.172) is satisfied if a segment e'_q crosses either $\widehat{m'n'}$ being inside $\widehat{a'b'}$, or $\widehat{a'b'}$ being inside $\widehat{m'n'}$, or both regions being its supporting line the dual line of a point of $\mathbf{W}$:

$$\begin{gathered}[(e'_q \subset \widehat{m'n'}) \text{ AND } (e'_q \cap \widehat{a'b'} \neq \emptyset)] \text{ OR} \\ [(e'_q \cap \widehat{m'n'} \neq \emptyset) \text{ AND } (e'_q \subset \widehat{a'b'})] \text{ OR} \\ [(e'_q \cap \widehat{m'n'} \neq \emptyset) \text{ AND } (e'_q \cap \widehat{a'b'} \neq \emptyset) \text{ AND } (E_q \in \mathbf{W})]\end{gathered} \tag{3.175}$$

  Figures 3.42b and 3.42c show two situations in which an edge e'_q intersects $\mathbf{G}'_i$.

- *Condition* (3.173) is satisfied if any arbitrary point (e.g. vertex A') of $\mathbf{G}'_i$ belongs to $\mathbf{P}'$, since the edges of $\mathbf{P}'$ do not cross $\mathbf{H}'_i$:

$$A' \in \mathbf{P}'_q \tag{3.176}$$

  Figure 3.42d shows a case in which a face $\mathbf{P}'_q$ contains $\mathbf{G}'$.

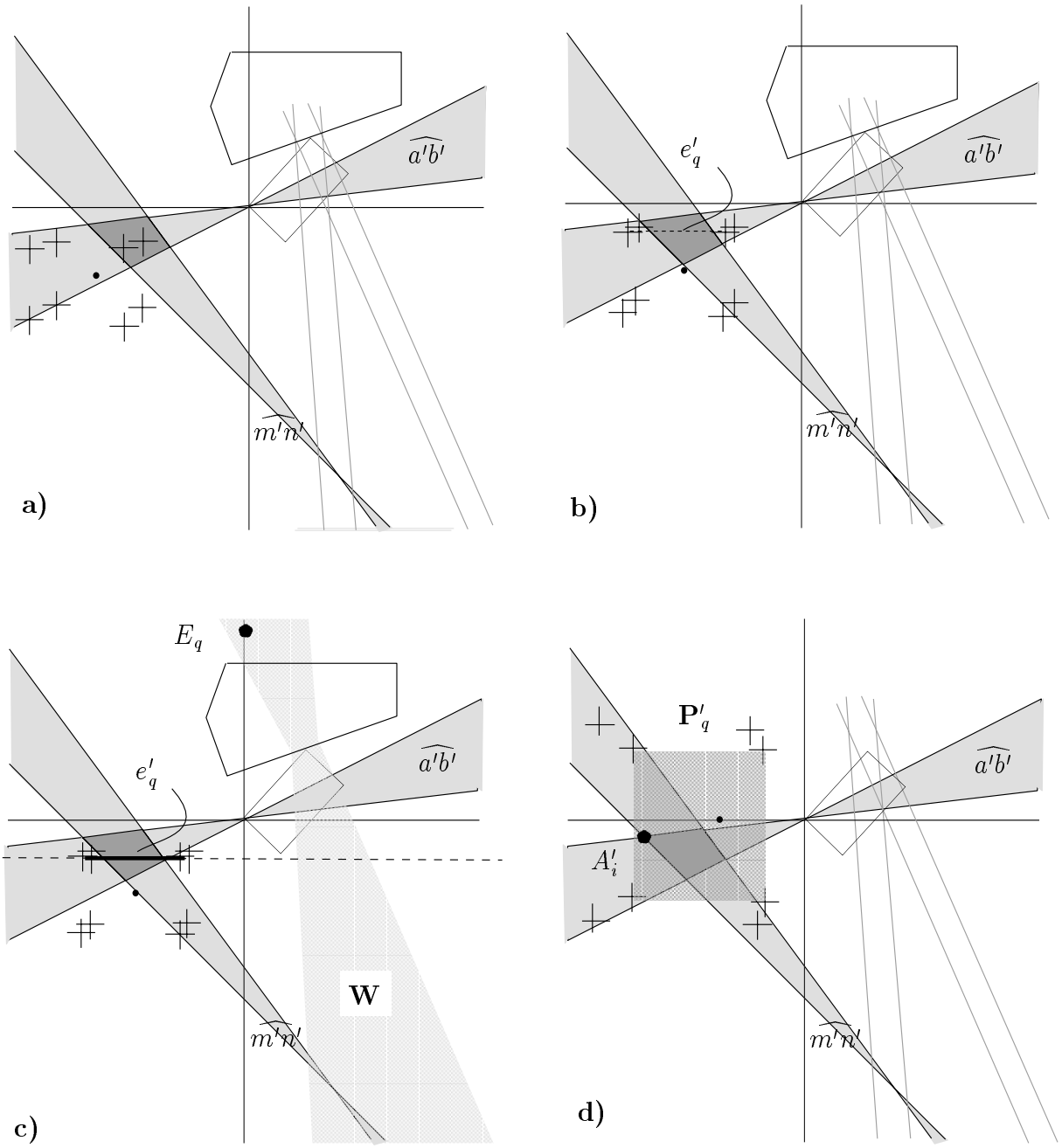

Figure 3.42: Examples of the classification conditions for one basic contact: a) $[V'_q \in \widehat{m'n'}]$ AND $[V'_q \in \widehat{a'b'}]$ b) $[(e'_q \cap \widehat{m'n'} \neq \emptyset)$ AND $(e'_q \subset \widehat{a'b'})]$ c) $[(e'_q \cap \widehat{m'n'} \neq \emptyset)$ AND $(e'_q \cap \widehat{a'b'} \neq \emptyset)$ AND $(E_q \in \mathbf{W})]$ d) $A' \in \mathbf{P}'_q$

Two Basic Contacts i and j

From proposition 16:

- *Condition* (3.171) is satisfied if V'_q belongs to any of the four polygons that compose $\mathbf{H}'_{ij}$:

$$[V'_q \in \mathcal{H}(A'_i, B'_i, A'_j, B'_j)] \text{ OR } [V'_q \in \mathcal{H}(A'_i, B'_i, C'_j, D'_j)] \text{ OR}$$
$$[V'_q \in \mathcal{H}(C'_i, D'_i, A'_j, B'_j)] \text{ OR } [V'_q \in \mathcal{H}(C'_i, D'_i, C'_j, D'_j)] \tag{3.177}$$

  Figure 3.39 shows a case in which an observed reaction force is compatible with a domain $\mathbf{G}'_{ij}$ because the dual representations of three vertices of U_g lies inside $\mathbf{H}'_{ij}$.

- *Condition* (3.172) is satisfied if e'_q intersects any arbitrary polygon of those composing $\mathbf{H}'_{ij}$, since it is already known that the vertices of e'_q are not inside $\mathbf{H}'_{ij}$. Selecting one of these polygons the condition is tested as:

$$e'_q \cap \mathcal{H}(A'_i, B'_i, A'_j, B'_j) \neq \emptyset \tag{3.178}$$

- *Condition* (3.173) is never satisfied since, $\mathbf{P}'_q \not\supset \mathbf{G}'_i$, $\mathbf{P}'_q \not\supset \mathbf{G}'_j$ $\forall q \in \{1, ..., 6\}$ and $e'_q \cap \mathbf{H}'_{ij} = 0$ $\forall q \in \{1, ..., 12\}$.

Three basic contacts i, j and k

From proposition 17 the border of $\mathbf{H}'_{ijk}$ satisfies $\partial\mathbf{H}'_{ijk} \subset (\mathbf{G}'_{ij} \cup \mathbf{G}'_{ik} \cup \mathbf{G}'_{jk})$. Since the function test is only called when condition (3.169) is not satisfied it is already known that $U'_g \cap \mathbf{G}'_{ij} = \emptyset$, $U'_g \cap \mathbf{G}'_{ik} = \emptyset$ and $U'_g \cap \mathbf{G}'_{jk} = \emptyset$; therefore, U'_g is either completely inside $\mathbf{H}'_{ijk}$ or completely outside. As a consequence, it is only necessary to test if a point of U'_g is inside $\mathbf{H}'_{ijk}$; then:

- *Condition* (3.171) is satisfied if

$$V'_q \in \mathcal{H}(F'_i, F'_j, F'_k) \quad \text{for any given } q \tag{3.179}$$

- *Conditions* (3.172) and (3.173) are never satisfied.

More than three basic contacts

From proposition 18 the function test$(\mathbf{H}'_S, \vec{g}_o)$ always returns "false".